

**Design and Stability Analysis of DC-DC Unidirectional,
Bidirectional and Interleaved SEPIC Converters with Swarm
Intelligence Algorithms Based Optimized PID Controller**

by

Al Jaber Mahmud – 170021113

Mehedi Hasan Mithun – 170021119

Md. Ashik Khan – 170021127

A Thesis Submitted to the Academic Faculty in Partial Fulfillment of the Requirements
for the Degree of

**BACHELOR OF SCIENCE IN ELECTRICAL AND ELECTRONIC
ENGINEERING**



Department of Electrical and Electronic Engineering

Islamic University of Technology (IUT)

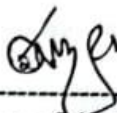
The Organization of Islamic Cooperation (OIC)
Board Bazar, Gazipur-1704, Bangladesh

May 2022

CERTIFICATE OF APPROVAL

The thesis titled "Design and Stability Analysis of DC-DC Unidirectional, Bidirectional and Interleaved SEPIC Converters with Swarm Intelligence Algorithms Based Optimized PID Controller" submitted by Al Jaber Mahmud (170021113), Mehedi Hasan Mithun (170021119), and Md. Ashik Khan (170021127) has been found as satisfactory and accepted as partial fulfillment of the requirement for the degree of Bachelor of Science in Electrical and Electronic Engineering on 10th May, 2022.

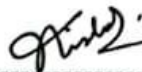
Approved by:



(Signature of the Supervisor)

Dr. Md. Ashraful Hoque
Professor

Department of Electrical and Electronic Engineering
Islamic University of Technology



(Signature of the Co-Supervisor)

Mirza Muntasir Nishat
Assistant Professor

Department of Electrical and Electronic Engineering
Islamic University of Technology



(Signature of the Co-Supervisor)

Fahim Faisal
Assistant Professor

Department of Electrical and Electronic Engineering
Islamic University of Technology

DECLARATION OF CANDIDATES

It is hereby declared that this thesis or any part of it has not been submitted elsewhere for award of any degree or diploma.

Al Mahmud

(Signature of the Candidate)

Al Jaber Mahmud
Student ID: 170021113

Mehedi Hasan Mithun

(Signature of the Candidate)

Mehedi Hasan Mithun
Student ID: 170021119

Ashik

(Signature of the Candidate)

Md. Ashik Khan
Student ID: 170021127

DEDICATION

We would like to dedicate this thesis to our family members and everyone who have given us unwearied support throughout the entirety of our existence and every situation of our life. They have always been a source of motivation for us. They pushed us ahead and showed us how to make the correct decisions. They never fail to inspire us to work hard and move forward to overcome life's difficulties. They have provided us with the protection, wisdom, and fortitude we need to face difficult situations.

ACKNOWLEDGEMENTS

First, we would want to express our heartfelt gratitude to Almighty Allah, our Creator, for creating and instilling in us the intellect to educate ourselves with worldly knowledge and, therefore, complete our thesis research. **Prof. Dr. Md. Ashraful Hoque**, Professor, Department of EEE, IUT, is our respected supervisor. We owe him a debt of gratitude for his continuous advice, care, and support in our pursuit of a career in electrical and electronic engineering. He has always encouraged us to learn new things and broaden our horizons to keep our minds sharp. We would not be exploring the power electronics area if it were not for his motivation. He has encouraged us to learn the fundamentals of the specific field and shown us how to proceed in the right direction

Mr. Mirza Muntasir Nishat, Assistant Professor, Department of EEE, IUT, is our co-supervisor, and we are grateful for his constant mentoring and genuine efforts in our thesis research. He devoted his considerable time guiding and motivating us to finish the work. We conducted a study and collected numerous informative analyses under his leadership to get positive results. Moreover, he gave us the most efficient technique to better understand our research. Without his help, we would become lost and unable to pick the best course of action.

Mr. Fahim Faisal, Assistant Professor, Department of EEE, IUT, served as our co-supervisor and mentored us throughout the research process. He has always been encouraging and motivating us to complete our work correctly. In addition, he has motivated us to study the primary goal of our project, which has given us greater confidence in our ability to build skills while working on the thesis.

We would also like to express our gratitude to **Prof. Dr. Mohammad Rakibul Islam**, Head, Department of EEE, and all the faculty members of the EEE Department, IUT, for their unwavering support, encouragement, and assistance.

Finally, we owe a debt of gratitude to our family for encouraging and assisting us in overcoming life's challenges, as well as enchanting us with their wonderful words. Last but not least, we would like to express our gratitude to our friends for their unconditional support and for keeping our spirits upbeat throughout this journey.

ABSTRACT

This thesis represents an investigative analysis of the closed-loop stability of the Unidirectional SEPIC (Single-Ended Primary Inductor Converter) converter, Bidirectional SEPIC converter, and Interleaved SEPIC Converter by implementing Swarm Intelligence Algorithms (SIA) for designing an optimized PID controller. The applicability and compatibility of three Swarm Intelligence Algorithms, which are Firefly Algorithm (FA), Particle Swarm Optimization (PSO), and Ant Colony Optimization for continuous domain (ACO_R), are analyzed in optimizing the control mechanism of the power converters. The improvement of performance parameters is observed, such as Percentage of Overshoot (%OS), Rise Time (T_r), Settling Time (T_s), and Peak Amplitude. The outcomes are compared with the help of various fitness functions. The thesis focuses on higher-order SEPIC Converters and its variants (fourth-order). Higher-order converters benefit from smaller ripple currents, easier EMC filtering, and avoiding current spikes owing to resistive losses. The converters were developed using State Space Averaging (SSA), and the transfer function of the converter's open-loop system was determined using MATLAB's system identification toolbox. By using the PID controller, the closed-loop system of the converter is introduced. For the tuning purposes of the PID Controller, the PID Tuner App of MATLAB has been used. Nevertheless, for the better performance of the controller, the algorithms are evaluated in the system through different fitness functions: IAE, ITAE, ISE, and ITSE. MATLAB is used to carry out all the simulations. After analyzing the performances for the case of the Unidirectional SEPIC converter, ACO_R -PID (ITSE) is the most optimized controller among all the algorithms based PID controllers in terms of performance parameters. In this case, values of overshoot (1.8603%), settling time (2.3414 sec), and peak amplitude (1.0186) are lower than FA-PID and PSO-PID for each of the error functions. For rise time, the value of ACO_R -PID (ITAE) is better (0.3798 sec). Again, for the case of the Bidirectional SEPIC converter, PSO-PID (ITSE) is the most optimized controller among all the algorithms based PID controllers in terms of performance parameters. In this case, values of overshoot (0.2674%) and peak amplitude (1.0027) are lower than FA-PID and ACO_R -PID for each of the error functions. For rise time, the value of ACO_R -PID (ITAE) is better (0.3798 sec), and for settling time, the value of ACO_R -PID (IAE) is better (0.1134 sec). Furthermore, for the case of the Interleaved SEPIC converter, PSO-PID (ITSE) is the most optimized controller among all the algorithms based PID controllers in terms of performance parameters. In this case, values of overshoot (5.2104%) and peak amplitude (1.0521) are lower than FA-PID and ACO_R -PID for each of the error functions. For rise time and settling time, the values of PSO-PID (ITAE) are better (0.1471 sec and 1.3354 sec, respectively). Hence, Swarm Intelligence Algorithm based optimized PID controller provides more optimized results and performs far better than Conventional PID controller for SEPIC converter and its variants.

TABLE OF CONTENTS

	Page No.
Certificate of Approval	i
Declaration of Candidates	ii
Dedication	iii
Acknowledgements	iv
Abstract	v
Table of contents	vi
List of Tables	ix
List of Figures	xi
List of Acronyms	xvi
CHAPTER – 1: INTRODUCTION AND BACKGROUND STUDY	1
1.1 Introduction	1
1.2 Literature Review	3
1.3 Problem Statement	4
1.4 Thesis Objectives	5
1.5 Thesis Organization	5
CHAPTER – 2: DC-DC CONVERTERS	7
2.1 Working principle of a dc-dc converter	7
2.2 Converter circuit topologies	9
2.2.1 Non-isolated converters	9
2.2.1.1 Buck converter	10
2.2.1.2 Boost converter	12
2.2.1.3 Buck-boost converter	14
2.2.1.4 Cuk converter	15
2.3.1.5 SEPIC converter	17
CHAPTER – 3: DC-DC SEPIC CONVERTER	19
3.1 Conventional SEPIC Converter	19
3.2 State Space Modeling of Unidirectional and Bidirectional SEPIC	21
3.3 State Space Modeling of Interleaved SEPIC	23
3.4 Gain Equation of SEPIC Converter	30
CHAPTER – 4: STUDY OF SWARM INTELLIGENCE ALGORITHM	32
4.1. Survey of Particle Swarm Optimization	32
4.1.1 Identification of PSO	32
4.1.2 Objectives of PSO	32
4.1.3 Advantages and Disadvantages of PSO	33

4.1.4 Features of PSO	33
4.1.5 Methodology PSO	34
4.1.6 Exploitation and Exploration in PSO	35
4.1.7 Mathematical Model of PSO	35
4.1.8 Flowchart of PSO	36
4.2 Survey of Firefly Algorithm	37
4.2.1 Identification of FA	38
4.2.2 Features of FA	38
4.2.3 Exploitation and Exploration in FA	39
4.2.4 Methodology FA	39
4.2.5 Mathematical Model of FA	39
4.2.6 Flowchart of FA	40
4.3 Survey of Ant Colony Optimization for Continuous Domain	41
4.3.1 Identification of ACO _R	42
4.3.2 Advantages and Disadvantages of ACO _R	42
4.3.3 Features of ACO _R	42
4.3.4 Methodology ACO _R	43
4.3.5 Mathematical Model of ACO _R	43
4.3.6 Flowchart of ACO _R	44
CHAPTER – 5: IMPLEMENTATION OF SWARM INTELLIGENCE ALGORITHM BASED PID CONTROLLER	46
5.1 PID Controller	46
5.1.1 Outline of PID Controller	47
5.1.2 Tuning of PID Controller	48
5.2 Objective Function	48
5.3 Layout of SIA-PID Controller	49
CHAPTER – 6: SIMULATION RESULTS AND PERFORMANCE ANALYSIS	51
6.1 Performance Parameters	51
6.2 Unidirectional SEPIC Converter	52
6.2.1. Open-Loop Response	52
6.2.2. Closed-Loop Response with PID Controller	54
6.2.3. Swarm Intelligence Algorithms based PID Controller	56
6.2.3.1. FA-PID Controller	56
6.2.3.2. PSO-PID Controller	60
6.2.3.3. ACO _R -PID Controller	65
6.2.3.4. Comparative Analysis	69
6.3 Bidirectional SEPIC Converter	71

6.3.1. Open-Loop Response	71
6.3.2. Closed-Loop Response with PID Controller	73
6.2.3. Swarm Intelligence Algorithms based PID Controller	74
6.3.3.1. FA-PID Controller	75
6.3.3.2. PSO-PID Controller	79
6.3.3.3. ACO _R -PID Controller	83
6.3.3.4. Comparative Analysis	87
6.4 Interleaved SEPIC Converter	88
6.4.1. Open-Loop Response	88
6.4.2. Closed-Loop Response with PID Controller	90
6.4.3. Swarm Intelligence Algorithms based PID Controller	92
6.4.3.1. FA-PID Controller	92
6.4.3.2. PSO-PID Controller	96
6.4.3.3. ACO _R -PID Controller	100
6.4.3.4. Comparative Analysis	105
CHAPTER – 7: CONCLUSION AND FUTURE WORKS	107
7.1 Synopsis	107
7.2 Future Work	108
REFERENCES	109

LIST OF TABLES

No.	Title	Page No.
1.1	Components and Output of Different Studies	3
6.1	Parameters of Unidirectional SEPIC Converter	52
6.2	Performance Analysis of Open-Loop and Closed-Loop Response [Unidirectional SEPIC]	55
6.3	Parameters of Firefly Algorithm	56
6.4	Gain Values of FA-PID Controller [Unidirectional SEPIC]	56
6.5	Performance Parameters of Conventional and FA-PID Controller [Unidirectional SEPIC]	59
6.6	Parameters of Particle Swarm Optimization Algorithm	60
6.7	Gain Values of PSO-PID Controller [Unidirectional SEPIC]	61
6.8	Performance Parameters of Conventional and PSO-PID Controller [Unidirectional SEPIC]	64
6.9	Parameters of Ant Colony Optimization Algorithm for Continuous Domain	65
6.10	Gain Values of ACO _R -PID Controller [Unidirectional SEPIC]	65
6.11	Performance Parameters of Conventional and ACO _R -PID Controller [Unidirectional SEPIC]	68
6.12	Comparative Performance Parameters of PID Controller (Unidirectional SEPIC Converter)	69
6.13	Parameters of Bidirectional SEPIC Converter	71
6.14	Performance Analysis of Open-Loop and Closed-Loop Response [Bidirectional SEPIC]	74
6.15	Gain Values of FA-PID Controller for Bidirectional SEPIC	75
6.16	Performance Parameters of Conventional and FA-PID Controller for Bidirectional SEPIC	78
6.17	Gain Values of PSO-PID Controller [Bidirectional SEPIC]	79
6.18	Performance Parameters of Conventional and PSO-PID Controller [Bidirectional SEPIC]	82

6.19	Gain Values of ACO_R -PID Controller [Bidirectional SEPIC]	83
6.20	Performance Parameters of Conventional and ACO_R -PID Controller [Bidirectional SEPIC]	86
6.21	Comparative Performance Parameters of PID Controller [Bidirectional SEPIC]	87
6.22	Parameters of Interleaved SEPIC Converter	89
6.23	Performance Analysis of Open-Loop and Closed-Loop Response [Interleaved SEPIC]	92
6.24	Gain Values of FA-PID Controller for Interleaved SEPIC	92
6.25	Performance Parameters of Conventional and FA-PID Controller for Interleaved SEPIC	95
6.26	Gain Values of PSO-PID Controller for Interleaved SEPIC	96
6.27	Performance Parameters of Conventional and PSO-PID Controller [Interleaved SEPIC]	99
6.28	Gain Values of ACO_R -PID Controller for interleaved SEPIC	101
6.29	Performance Parameters of Conventional and ACO_R -PID Controller [Interleaved SEPIC]	104
6.30	Comparative Performance Parameters of PID Controller (Interleaved SEPIC Converter)	105

LIST OF FIGURES

No.	Title	Page No.
2.1	Basic DC-DC boost converter operating modes (a) CCM, (b) DCM	8
2.2	(a) Basic configuration, (b) typical waveforms of Buck Converter, and (c) Voltage gain (G) versus duty cycle (D) of buck converter	10
2.3	(a) Basic configuration, (b) typical waveforms of Buck Converter, and (c) Voltage gain (G) versus duty cycle (D) of boost converter	12
2.4	(a) Basic configuration, (b) typical waveforms of Buck Converter, and (c) Voltage gain (G) versus duty cycle (D) of buck-boost converter	14
2.5	(a) Basic configuration and (b) Voltage gain (G) versus duty cycle (D) of Cuk converter	16
2.6	(a) Basic configuration and (b) Voltage gain versus duty cycle of SEPIC converter	17
3.1	Conventional SEPIC Converter	19
3.2	Traditional SEPIC converter's modes of operation (a) Switch is ON condition and (b) Switch is OFF condition	20
3.3	Interleaved SEPIC : Mode-1	23
3.4	Interleaved SEPIC : Mode-2	25
3.5	Interleaved SEPIC : Mode-3	26
3.6	Interleaved SEPIC : Mode-4	28
3.7	Voltage Gain vs. duty cycle with variable load	30
3.8	Voltage Gain vs. duty cycle with variable load	31
4.1	Flowchart of PSO	37
4.2	Flowchart of FA	41
4.3	Flowchart of ACO _R	45
5.1	Simulink Model of PID Controller	47
5.2	Layout of Optimized PID Controller	50
6.1	Model of Open-Loop Unidirectional SEPIC by Simulink	53
6.2	Step Response of Open-Loop System of Unidirectional SEPIC	53
6.3	Step Response of Closed-Loop System with PID Controller of	54

	Unidirectional SEPIC	
6.4	Step Response of Closed-Loop System with Conventional PID of Unidirectional SEPIC	55
6.5	Step Response of IAE for FA-PID (Unidirectional SEPIC Converter)	57
6.6	Step Response of ISE for FA-PID (Unidirectional SEPIC Converter)	57
6.7	Step Response of ITSE for FA-PID (Unidirectional SEPIC Converter)	58
6.8	Step Response of ITAE for FA-PID (Unidirectional SEPIC Converter)	58
6.9	Comparative Analysis of Step Responses for FA-PID (Unidirectional SEPIC Converter)	59
6.10	Comparative Chart of Performance Parameters for FA-PID (Unidirectional SEPIC Converter)	60
6.11	Step Response of IAE for PSO-PID (Unidirectional SEPIC Converter)	61
6.12	Step Response of ISE for PSO-PID (Unidirectional SEPIC Converter)	62
6.13	Step Response of ITSE for PSO-PID (Unidirectional SEPIC Converter)	62
6.14	Step Response of ITAE for PSO-PID (Unidirectional SEPIC Converter)	63
6.15	Comparative Analysis of Step Responses for PSO-PID (Unidirectional SEPIC Converter)	63
6.16	Comparative Chart of Performance Parameters for PSO-PID (Unidirectional SEPIC Converter)	64
6.17	Step Response of IAE for ACO _R -PID (Unidirectional SEPIC Converter)	66
6.18	Step Response of ISE for ACO _R -PID (Unidirectional SEPIC Converter)	66
6.19	Step Response of ITSE for ACO _R -PID (Unidirectional SEPIC Converter)	67
6.20	Step Response of ITAE for ACO _R -PID (Unidirectional SEPIC Converter)	67
6.21	Comparative Analysis of Step Responses for ACO _R -PID (Unidirectional SEPIC Converter)	68
6.22	Comparative Chart of Performance Parameters for ACO _R -PID (Unidirectional SEPIC Converter)	69
6.23	Overall Comparative Step Response Analysis of PID Controller (Unidirectional SEPIC Converter)	70
6.24	Overall Comparative Chart of Optimum PID Controller (Unidirectional	71

	SEPIC Converter)	
6.25	Model of Open-Loop Bidirectional SEPIC by Simulink	72
6.26	Step Response of Open-Loop System of Bidirectional SEPIC	72
6.27	Step Response of Closed-Loop System with PID Controller of Bidirectional SEPIC	73
6.28	Step Response of Closed-Loop System with Conventional PID of Bidirectional SEPIC	74
6.29	Step Response of IAE for FA-PID (Bidirectional SEPIC Converter)	75
6.30	Step Response of ISE for FA-PID (Bidirectional SEPIC Converter)	76
6.31	Step Response of ITSE for FA-PID (Bidirectional SEPIC Converter)	76
6.32	Step Response of ITAE for FA-PID (Bidirectional SEPIC Converter)	77
6.33	Comparative Analysis of Step Responses for FA-PID (Bidirectional SEPIC Converter)	77
6.34	Comparative Chart of Performance Parameters for FA-PID (Bidirectional SEPIC Converter)	78
6.35	Step Response of IAE for PSO-PID (Bidirectional SEPIC Converter)	79
6.36	Step Response of ISE for PSO-PID (Bidirectional SEPIC Converter)	80
6.37	Step Response of ITSE for PSO-PID (Bidirectional SEPIC Converter)	80
6.38	Step Response of ITAE for PSO-PID (Bidirectional SEPIC Converter)	81
6.39	Comparative Analysis of Step Responses for PSO-PID (Bidirectional SEPIC Converter)	81
6.40	Comparative Chart of Performance Parameters for PSO-PID (Bidirectional SEPIC Converter)	82
6.41	Step Response of IAE for ACO _R -PID (Bidirectional SEPIC Converter)	83
6.42	Step Response of ISE for ACO _R -PID (Bidirectional SEPIC Converter)	84
6.43	Step Response of ITSE for ACO _R -PID (Bidirectional SEPIC Converter)	84
6.44	Step Response of ITAE for ACO _R -PID (Bidirectional SEPIC Converter)	85
6.45	Comparative Analysis of Step Responses for ACO _R -PID (Unidirectional SEPIC Converter)	85
6.46	Comparative Chart of Performance Parameters for ACO _R -PID (Bidirectional SEPIC Converter)	86

6.47	Overall Comparative Step Response Analysis of PID Controller (Bidirectional SEPIC Converter)	87
6.48	Overall Comparative Chart of Optimum PID Controller (Bidirectional SEPIC Converter)	88
6.49	Model of Open-Loop Interleaved SEPIC by Simulink	89
6.50	Step Response of Open-Loop Interleaved Converter	90
6.51	Step Response of Closed-Loop Interleaved Converter with PID Controller	91
6.52	Step Response of Closed-Loop System with Conventional PID of Bidirectional SEPIC	91
6.53	Step Response of IAE for FA-PID (Interleaved SEPIC Converter)	93
6.54	Step Response of ISE for FA-PID (Interleaved SEPIC Converter)	93
6.55	Step Response of ITSE for FA-PID (Interleaved SEPIC Converter)	94
6.56	Step Response of ITAE for FA-PID (Interleaved SEPIC Converter)	94
6.57	Comparative Analysis of Step Responses for FA-PID (Interleaved SEPIC Converter)	95
6.58	Comparative Chart of Performance Parameters for FA-PID (Interleaved SEPIC Converter)	96
6.59	Step Response of IAE for PSO-PID (Interleaved SEPIC Converter)	97
6.60	Step Response of ISE for PSO-PID (Interleaved SEPIC Converter)	97
6.61	Step Response of ITSE for PSO-PID (Interleaved SEPIC Converter)	98
6.62	Step Response of ITAE for PSO-PID (Interleaved SEPIC Converter)	98
6.63	Comparative Analysis of Step Responses for PSO-PID (Interleaved SEPIC Converter)	99
6.64	Comparative Chart of Performance Parameters for PSO-PID (Interleaved SEPIC Converter)	100
6.65	Step Response of IAE for ACO _R -PID (Interleaved SEPIC Converter)	101
6.66	Step Response of ISE for ACO _R -PID (Interleaved SEPIC Converter)	102
6.67	Step Response of ITSE for ACO _R -PID (Interleaved SEPIC Converter)	102
6.68	Step Response of ITAE for ACO _R -PID (Interleaved SEPIC Converter)	103
6.69	Comparative Analysis of Step Responses for ACO _R -PID (Interleaved SEPIC Converter)	103

6.70	Comparative Chart of Performance Parameters for ACO_R -PID (Interleaved SEPIC Converter)	104
6.71	Overall Comparative Step Response Analysis of PID Controller (Interleaved SEPIC Converter)	105
6.72	Overall Comparative Chart of Optimum PID Controller (Interleaved SEPIC Converter)	106

LIST OF ACRONYMS

Abbreviated Form	Description
FET	Field-Effect Transistor
SSA	State Space Averaging
PID	Proportional Integral Derivative
SIA	Swarm Intelligence Algorithm
PSO	Particle Swarm Optimization
FA	Firefly Algorithm
ACO	Ant Colony Optimization
IAE	Integral Absolute Error
ISE	Integral Squared Error
ITSE	Integral Time Squared Error
ITAE	Integral Time Absolute Error
DCM	Discontinuous Conduction Mode
CCM	Continuous Conduction Mode
QPSO	Quantum-behaved PSO
DFOPID	Discrete Fractional Order PID
SA	Simulated Annealing
SMPS	Switch Mode Power Supplies
EMI	Electromagnet Interference
LED	Light Emitting Diode
HID	High Intensity Discharge
PDF	Probability Density Function
SEPIC	Single Ended Primary Inductance Converter
FFNN	Feed-Forward Neural Networks
MOSFET	Metal Oxide Semiconductor Field Effect Transistor
FPGA	Field Programmable Gate Array

CHAPTER 1

INTRODUCTION AND BACKGROUND STUDY

Power electronics is one of the most advanced branches of engineering in recent years, with researchers praising the system's efficacy, stability, performance, etc. [1]. Power electronics play an essential role in our daily lives, with a wide range of applications. DC-DC converters are a type of power electronics that has had an enormous impact on the world today. It may change a DC voltage level to the desired level, which can be stepped up, down, or kept constant. Cell phone chargers [2], LED drivers [3], flashlights, hybrid and electric cars, UPS, PV cells [4], dc micro-grids [5], fuel cells, wind turbines, telecommunication industries, high-intensity discharge (HID) lamp ballasts used in automotive headlamps, and so on are only a few of the applications for DC-DC converters [6-9]. However, due to the action of the switches, these devices exhibit nonlinear features such as higher overshoot, greater ripples in output voltage, and instability [10]. This thesis study addresses the concerns mentioned above and gives better control over the converter system to maximize their applications' effectiveness. Furthermore, in order to improve the controller's performance and produce optimum system output with steady performance parameters, Swarm Intelligence Algorithms were infused with the PID controller in an investigative method.

1.1 Introduction

Power electronics have become vital in practically every element of life as the modern age progresses. Peter Cooper Hewitt created power electronics in 1902. In Power Electronics, DC-DC converters are critical for increasing energy conversion efficiency. The DC-DC conversion was first presented in the 1920s, and since then, the development of DC-DC converters has accelerated significantly.

Several types of DC-DC converters are available, depending on the needs of the consumers. DC-DC converters are divided into two types: isolated and non-isolated. In contrast to isolated converters, non-isolated converters cannot generate isolation between input and output voltages [11]. Non-isolated converters include buck-boost, buck, boost, SEPIC, CUK, and others [12]. Like everything else in this period, these converters have benefits and limitations.

Among many converters, the boost converter has a high input ripple current, and the buck converter has a high output ripple voltage compared to many DC-DC converters. However, these can be reduced by applying a switched capacitor and an inductor [13-14]. High harmonics are created in buck-boost converters, which can be reduced by adding a large capacitor or an LC filter and has an inverted input voltage in output [15]. In the CUK converter, hysteresis produces an enhanced voltage regulation. The perception of hysteresis is very similar to that of the snubber circuit in a power rectifier circuit. An additional capacitor and inductor are prerequisites in the CUK converter to report the complications of unnecessary ripple voltage, ripple current, and harmonics which cause the system to become bulky and expensive [16]. Furthermore, Buck-

boost and CUK converters produce the inverted output voltage, which may not be desired in some applications. Moreover, because of the properties of having discontinuity in input current, buck and buck-boost converters have significant power loss in input switching [17]. Although there are drawbacks to SEPIC converters, including the boundaries of inductor size and high over-voltage at start-up, SEPIC is the only converter able to output a non-inverted form of input voltage and higher flexibility in output voltage. Despite this, SEPIC has a lower input ripple current [18]. Thus, the SEPIC converter manifests better performance in terms of these problems and is brought into play in different power electronics sectors [19].

SEPIC's open-loop system might be unstable or have low-performance parameters. As a result, controllers can make the system a closed-loop system to govern the system. By integrating the open-loop system into the closed-loop control system, SEPIC can advance its total performance. The stability of the plant can be increased, and the discrepancy of the performance parameters will be minor. In today's engineering world, the PID controller is one of the most extensively utilized and effective controllers. Prior to the previous couple of decades, PID controllers accounted for over 90% of all controllers utilized [20]. A closed-loop system using the PID controller for the SEPIC can improve performance and make it more stable with improved performance characteristics. The inclusion of a PID controller can enhance the SEPIC. When a PID controller is included in a power converter, it can effectively maintain steady-state operation and eliminate unstable operation caused by the nonlinear phenomena in the SEPIC. The gain parameters Proportional (K_P), Integral (K_I), and Derivative (K_D) are referred to as PID. Each gain comes with its own set of responsibilities. Obtaining the gain values for the PID controller, on the other hand, is a complex operation. To date, a large number of PID tuning algorithms have been introduced. For instance, the Cohen-coon technique, the Ziegler-Nichols method, the constant open-loop transfer function method, the internal model controller, and the synthesis method [22-25]. Using the MATLAB PID tuner app via trial and error method, manual tuning might yield a more or less excellent outcome. However, manually tuning PID controller parameters is tedious and time-consuming, especially for systems with complex equations.

For overcoming this problem, Different algorithms, on the other hand, can be used to get more optimal gain values. Various academics have created many metaheuristic algorithms to obtain optimum results from the search space's convergent output. Particle Swarm Optimization (PSO) [26-27], Genetic Algorithm [28-29], Self-organizing Algorithm [30], Harmony Search [31], Ant Colony Optimization Algorithm [32], Firefly algorithm [33], Shuffled Frog Leaping Algorithm [34], Fuzzy Logic [35-36] etc. are said to be metaheuristic algorithms. Metaheuristics are higher-level methods for determining which may produce a satisfactory solution, primarily when computation capability is restricted or incomplete. These are good algorithms for obtaining better solutions when the dimensionality is high. The purpose is to search the search space quickly for a near-optimal solution. More optimum gain values may be determined using the technique, which is then utilized to improve the performance characteristics of the DC-DC SEPIC converter and its variants.

In this work, Firefly Algorithm (FA), Particle Swarm Optimization (PSO), and Ant Colony Optimization Algorithm for continuous domain (ACO_R) will be used for optimization process of PID Controller of the closed-loop system of SEPIC Converter and its variants and comparative analysis will be reported in terms of performance parameters of different fitness functions.

1.2 Literature Review

Many scholars have endorsed the use of various algorithms in power converters, and there is a large body of research on the issue. One of these potential study scenarios is the paper by Nishat et al. [37], in which they used SA in PID to test the stability of the SEPIC converter. Liping Chen et al. [38] employed the QPSO technique in the DFOPID controller to investigate the performance of the SEPIC converter. Amin Alqudah et al. [39] employed the SA optimization technique in a PID controller for adaptive regulation of buck and boost converters. Vahab Haji Haji et al. [40] used ABC, GA, PSO, FA, and DFA for FOPID controller in a chopper converter to regulate DC motor drive with various fitness functions. To investigate the step response of the improved DC-DC buck converter, Yaqoob et al. [41] used FA and GA in the PID controller. Shagor et al. [42] used the Firefly Algorithm (FA) optimization method in a PID controller to analyze the SEPIC converter's performance parameters and stability. Nishat et al. [20] applied the Genetic Algorithm (GA) optimization technique in a PID to investigate the stability of the SEPIC converter. Altinoz et al. [43] used the PSO technique to optimize a PID controller for buck converter by comparing the performance characteristics of eight different fitness functions. Sundareswaran et al. [44] designed a feedback controller for a buck-boost converter utilizing the Genetic Algorithm (GA) and evolutionary search. Sundareswaran et al. [45] applied a Genetic Algorithm (GA) to a feedback controller to enhance the dynamic response of a boost converter at all operation conditions. For high performance on a BLDC motor, Jaber et al. [46] used the firefly algorithm approach in a PID controller to determine the PID parameters. Meher et al. [47] developed a DC-DC bidirectional SEPIC converter that combined a Type-III controller and an IMC controller to regulate the system's transient responses and performance parameters. There was no optimization procedure employed to choose the gain values in the study. Komathi et al. [48] studied about interleaved SEPIC converter with conventional ZN tuned and IMC based PI controller and compared between them with based on different performance parameters. Again, different researchers took different approaches to reducing the impact of RHP. The removal of RHP zeros in boost converters was studied by Leoncini et al. [49] The RHP zeros were shifted to LHP in that study based on the injecting inductor current; however, this resulted in static voltage inaccuracy, which is undesirable in the actual world. Likewise, Hung et al. [50] additionally employed a boost converter to reduce the system's impact from RHP zeros. The components and output of performance parameters of above mentioned studies are enlisted in Table 1.1.

TABLE 1.1. COMPONENTS AND OUTPUT OF DIFFERENT STUDIES

Ref	Converter	Controller	Algorithm	Function	%OS
[37]	SEPIC	PID	SA	IAE	2.2
				ISE	3.04
[38]	SEPIC	DFOPID	QPSO	ITAE	7.3
[39]	Buck	PID	SA	ITAE	15.4
	Boost	PID	SA	ITAE	9.7
[40]	Chopper	FOPID	GA	ITSE	17.14
				ITAE	19.59
			PSO	ITSE	16.34
				ITAE	6.829
			ABC	ITSE	17.31

				ITAE	8.89
			FA	ITSE	17.24
				ITAE	5.044
			DFA	ITSE	16.91
				ITAE	6.32
[41]	Buck	PID	FA	ITSE	10.68
				MSE	11.12
				F	12.23
			GA	ITSE	19.3
				MSE	18.894
				F	42.62
[42]	SEPIC	PID	FA	IAE	2.14
				ISE	2.84
				ITSE	2.95
				ITAE	6.11
[20]	SEPIC	PID	GA	IAE	9.03
				ITAE	17.2
				ISE	10
[43]	Buck	PID	PSO	IAE	7.647
				ISE	7.647
				ITSE	15.663
[44]	Buck-Boost	Feedback	GA	$1/1+F(x)$	1.125
[45]	Boost	Feedback	GA	$1/F(x)$	0
[46]	BLDC Motor	PID	PSO	ITAE	43.5 at 1000 rpm
					19.1 at 2000 rpm
			FA		44.3 at 1000 rpm
					20.4 at 2000 rpm
[47]	Bidirectional SEPIC	Type III	--	--	5.68
		IMC			17.9
[48]	Interleaved SEPIC	Conventional ZN - PI	--	--	38.6
		IMC - PI			3.17

1.3 Problem Statement

The SEPIC converter is one of the most extensively used converters in power electronics applications. However, because nonlinearity is a part of the system, control engineers face a constant struggle in achieving a stable and speedier reaction. In the case of an open-loop response, a stable output can be produced, but there is a lot of overshoot, a higher rise time, and a higher settling time, which is not desirable in modern power converters. In addition, Right Half Plane (RHP) zeros are present in the open-loop system of the Bidirectional SEPIC Converter, which can cause the system to become unstable and is not a good indicator for the percentage of overshoots and undershoots. In addition, Right Half Plane (RHP) zeros are present in the open-

loop system of the Bidirectional SEPIC Converter, which can cause the system to become unstable and is not a good indicator for the percentage of overshoots and undershoots. As a result, it is critical to figure out how to make fast and reliable power converters that can attain stability quickly. In order to obtain a stable output with less overshoot, rise time, settling time, and peak amplitude, a closed-loop system is required. A conventional PID controller is used for this. However, the controller parameters must be fine-tuned using a rigorous trial-and-error process to get steady output. As a result, nonlinear optimization techniques based on swarm intelligence algorithms are used to achieve optimum PID controller settings and improve overall system performance and control. Among various techniques, Firefly Algorithm (FA), Particle Swarm Optimization (PSO), and Ant Colony Optimization Algorithm for continuous domain (ACO_R) are implemented to design and develop optimized PID controller for SEPIC converter and its variants.

1.4 Thesis Objectives

The primary goal of this thesis is to establish swarm intelligence algorithms for PID controllers for SEPIC converter and its variants. The following are some additional goals:

- ✓ To observe and estimate various performance parameters of power electronic converters, particularly DC-DC SEPIC converter and its variants.
- ✓ To investigate the compatibility of various swarm intelligence algorithms for power electronic converter controller design.
- ✓ To optimize the performance parameters of closed-loop SEPIC converter and its variants using nonlinear control approaches.
- ✓ To compare conventional PID controller and optimized PID controller for SEPIC Converters and their variants.
- ✓ To witness the poles and zeros of the SEPIC converter and its variants for the conventional and optimized controller and comprehend the converter's stability.

1.5 Thesis Organization

This thesis focuses on designing and analyzing the swarm intelligence optimization algorithms based PID controller for obtaining better performance parameters and stability of SEPIC converter and its variants.

- ✓ In chapter 2, different widely used dc-dc converters are detailed. In addition, the methodologies and analyses of dc-dc converters are detailed.

- ✓ In Chapter 3, the Unidirectional SEPIC converter, Bidirectional SEPIC converter, and Interleaved SEPIC converter are studied, and State Space Modeling of the converters is demonstrated. The converter is next subjected to open-loop and closed-loop analysis.
- ✓ In chapter 4, a general discussion of the Firefly Algorithm (FA), Particle Swarm Optimization (PSO), and Ant Colony Optimization Algorithm for Continuous Domain (ACO_R) algorithms are described.
- ✓ In Chapter 5, the implementation of the Swarm Intelligence Algorithm of the PID controller is presented in detail, the algorithm's objective function and the architecture of the optimized PID Controller are explained.
- ✓ In Chapter 6, the simulation results of the optimized PID controller for the SEPIC converter and its variants are included. The performance parameters are explored, and quantitative analysis is offered. The poles and zeros are also observed in this section.
- ✓ In Chapter 7, the conclusion of the thesis is included, including a quick review of the findings and some recommendations for further research.

CHAPTER 2

DC-DC CONVERTERS

Several converter topologies have been adopted across a broad array of applications due to decades of active study on AC-DC and DC-DC converters. The necessity for supplying dc power is evidenced by the demand for constant voltage in various appliances. Therefore, DC-DC power converters are utilized in various works and applications, including renewable energy concerned works and discoveries like electric vehicles, LED drives, motor drives, personal computers, laptop computers, spacecraft power systems, office equipment, and telecommunications equipment, inverters, and smart grids [51].

DC-DC converters shift the DC voltage level from one to another. MOSFETs and integrated circuits, for example, have a large operating voltage range, demanding the supply of a voltage to every device. The efficiency, ripple, and load-transient response of a circuit can all be improved using DC-DC Converters. Operational conditions such as input and output criteria usually dictate which external parts and components operate best. As a result, conventional circuits must be adjusted or modified during the manufacturing process to meet the requirements of each specific requirement. Developing a circuit that meets all standards and regulations necessitates a significant amount of industry experience and knowledge.

Switched-mode dc-dc converters have become very widespread in functional appliances. The relevant attribute of these converters is that they conserve input energy before discharging it at a specific voltage to the output. Energy storage elements can be magnetic field storage components such as inductors and transformers and electric field storage components such as capacitors. These power converters' improved efficiency speeds up the cooling process and extends the battery's life. In addition, the introduction of power FETs, which can switch very effectively with lower losses than bipolar junction transistors, has resulted in an increase in efficiency. The voltage rating of dc-dc converters represents the limitation of step-up or step-down voltage transformation. In contrast, the regulation rating represents the departure of the output voltage from the input voltage and load current [52].

2.1 Working Principle of a DC-DC Converter

A typical circuit configuration for dc-dc converters is a boost converter, which works on the step-up concept. As a result, this electronic circuit shows how a low input dc voltage can be converted to a high output dc voltage [53]. The essential components of a dc-dc converter include semiconductor switching devices, as well as electrical and electronic components. The two operating modes of these converters are Continuous Conduction Mode (CCM) and Discontinuous Conduction Mode (DCM).

In Figure 2.1(a), an inductor (L), capacitor (C), diode (D), switching device (MOSFET), and input voltage source (V_{in}) are shown in a dc-dc boost converter operating in CCM mode. One pulse width modulator is attached to the boost converter to control the switch. Energy is stored in the inductor (L) during the period of the ON switching condition, which eventually transfers more energy to the output. The current in the inductor is reduced in the OFF-switching state, and the magnetic field created is low in energy to keep the current flowing to the load.

Figure 2.1 shows the DCM mode operation of the same dc-dc boost circuit (b). Energy will be distributed to the inductor for storage purposes in the ON state, whereas in the OFF state, the inductor current will go to zero if this condition persists for a long time. The capacitor is charged and discharged in a mechanism that is based on the input voltage. DCM mode's output voltage is lower than CCM mode's output voltage.

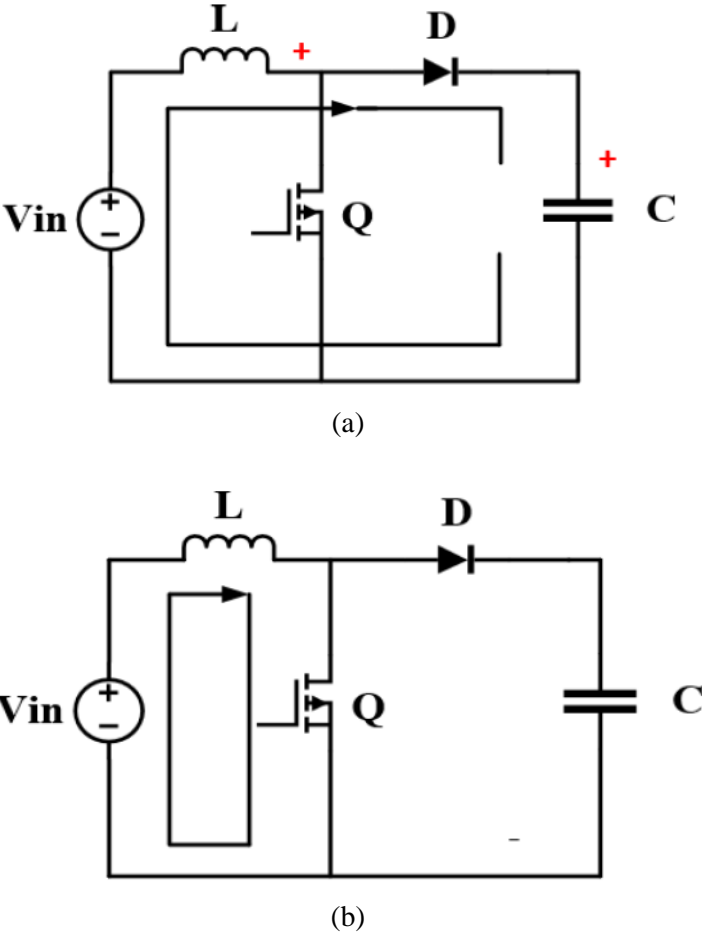


Fig 2.1. Basic DC-DC boost converter operating modes (a) CCM, (b) DCM

The applications of dc-dc converters are seen from several aspects. The main reasons for the popularity of dc-dc converters in power electronics applications are power supply system simplification, load equalization to the power supply, isolation of primary and secondary circuits,

and electromagnetic interference prevention system (EMI). These converters are now being used in a variety of industries. Power supply, voltage regulators, and electronic devices were the primary applications. However, advancements in dc-dc converter technology have led to applications in renewable energy, automobiles, telecommunications, and spacecraft power systems. [54-55]

2.2 Converter circuit topologies

The DC-DC conversion is a challenging aspect of any system, and we must choose the proper regulator topology for our design. The electrical isolation between the input and output of a DC-DC converter is classified into two categories: isolated and non-isolated converters. The goal of an isolated DC-DC converter is to create a new ground potential on the output side of the system. An isolated converter is preferred in high-voltage systems because it ensures operator safety when servicing the systems output side; the operator will be less likely contact with a high-voltage source. Non-isolated converters are briefly discussed in this section.

2.2.1 Non-isolated converters

The inductor is often used in a non-isolated converter, and there is no consistent dc voltage isolation between the input and output. Dc isolation between the input and output voltages is not required in most situations. The non-isolated dc-dc converter has a constant dc route between its input and output. The primary benefits of these converters are listed below [56-57]:

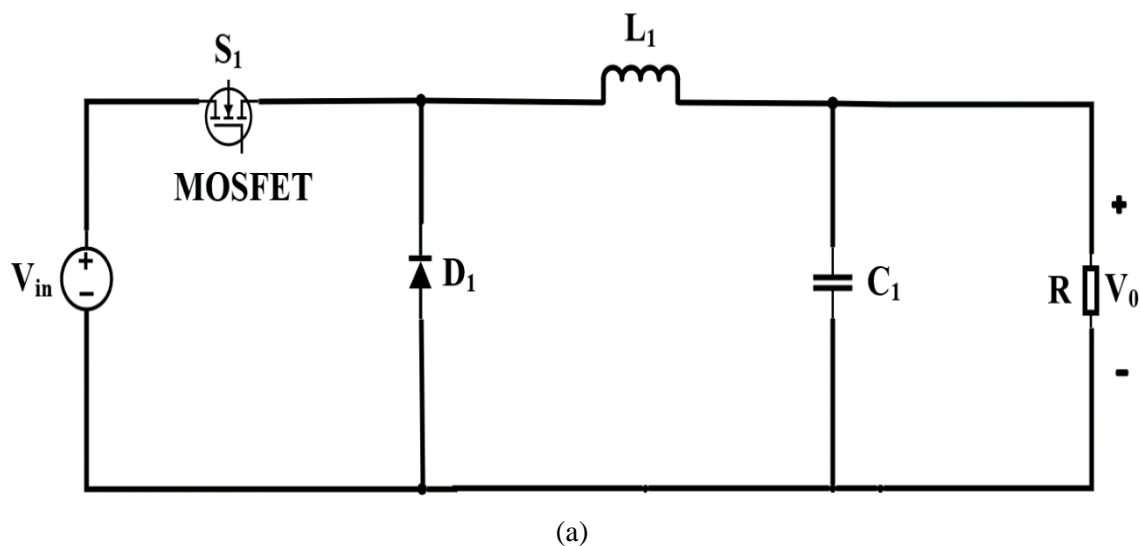
- Isolation may raise the cost of a power supply system by requiring the use of components such as Custom transformers, Opto-couplers, High insulation levels etc. Non-isolated systems are less expensive to construct since they do not need these additional items.
- The power converter increases in size as more components are added. Non-isolated converters are, as a result, smaller in size than their isolated equivalents. They have a proclivity towards greater switching frequencies, reducing the size of other components.
- The non-isolated structure is more efficient since it allows for direct output sensing. It is easy to adjust the output and enhance transient performance without isolation components like transformers.

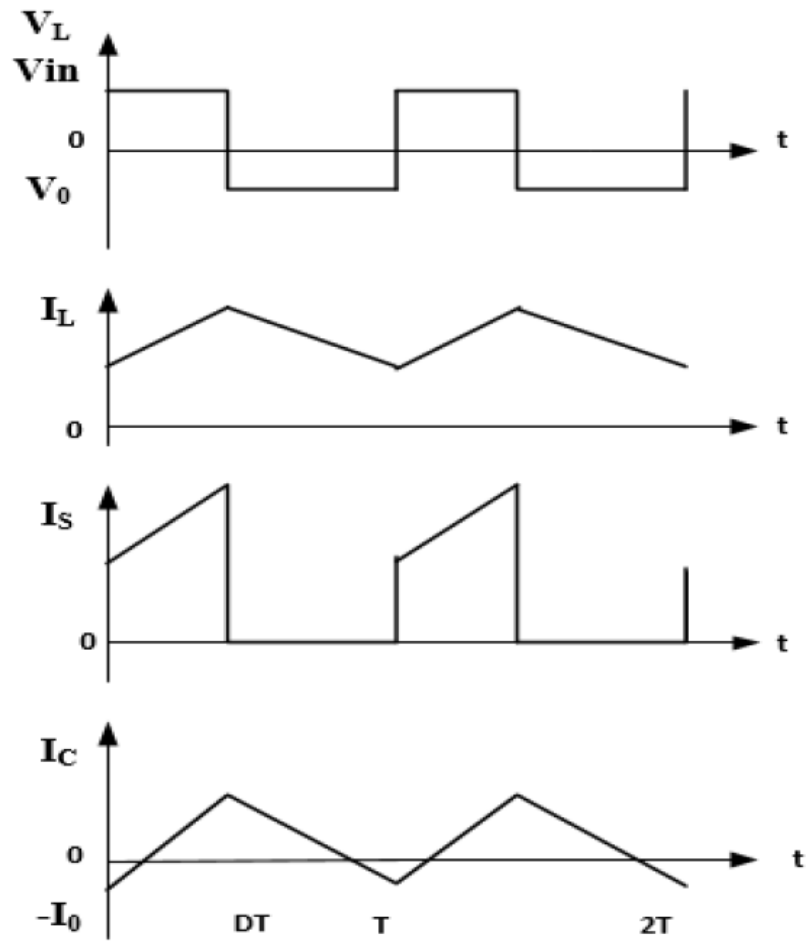
Depending on the conversion technique and circuit design, non-isolated converters can be specified in various ways. The following are widely used non-isolated converters:

- i. Buck converter
- ii. Boost converter
- iii. Buck-boost converter
- iv. Cuk converter
- v. SEPIC converter

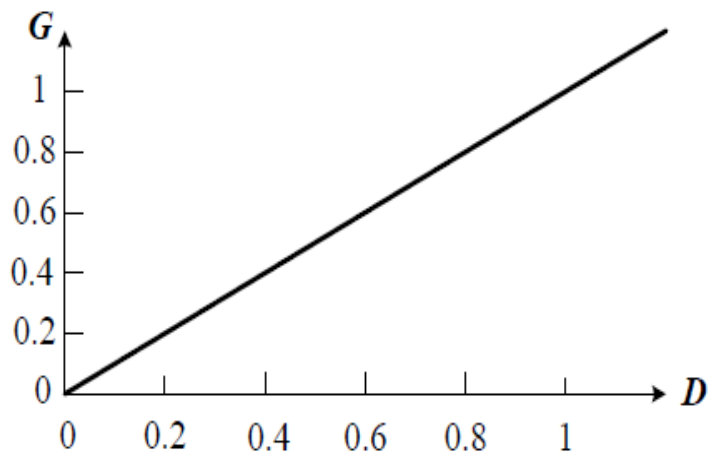
2.2.1.1 Buck converter

The output voltage of the buck converter must be less than or equal to the input voltage, and for this, it is known as a step-down converter. The buck converter is the most commonly used step-down converter between the Switch Mode Power Supplies (SMPS) topologies. A conventional buck converter circuit is displayed in Fig 2.2(a) includes one switching element, a rectifier, and filter elements. The output portion's inductor gives a constant current to the load. Under the premise that the induction current is never negative, the relevant waveforms are given in Fig. 2.2(b). The converter is said to be in continuous conduction mode, meaning the inductor current is never zero. The diode gets reverse biased when the switch is turned on, and the input voltage charges the inductor. When the switch is turned off, the diode is forward biased, and the inductor discharges to the load. It has a voltage gain of $g = D$, as shown in figure 2.2. (c)





(b)

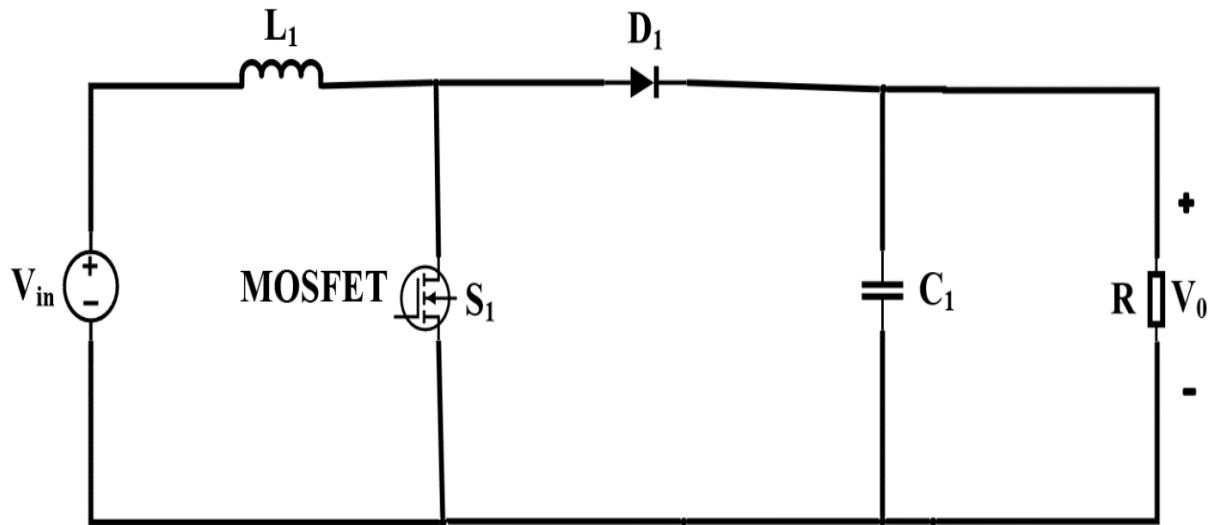


(c)

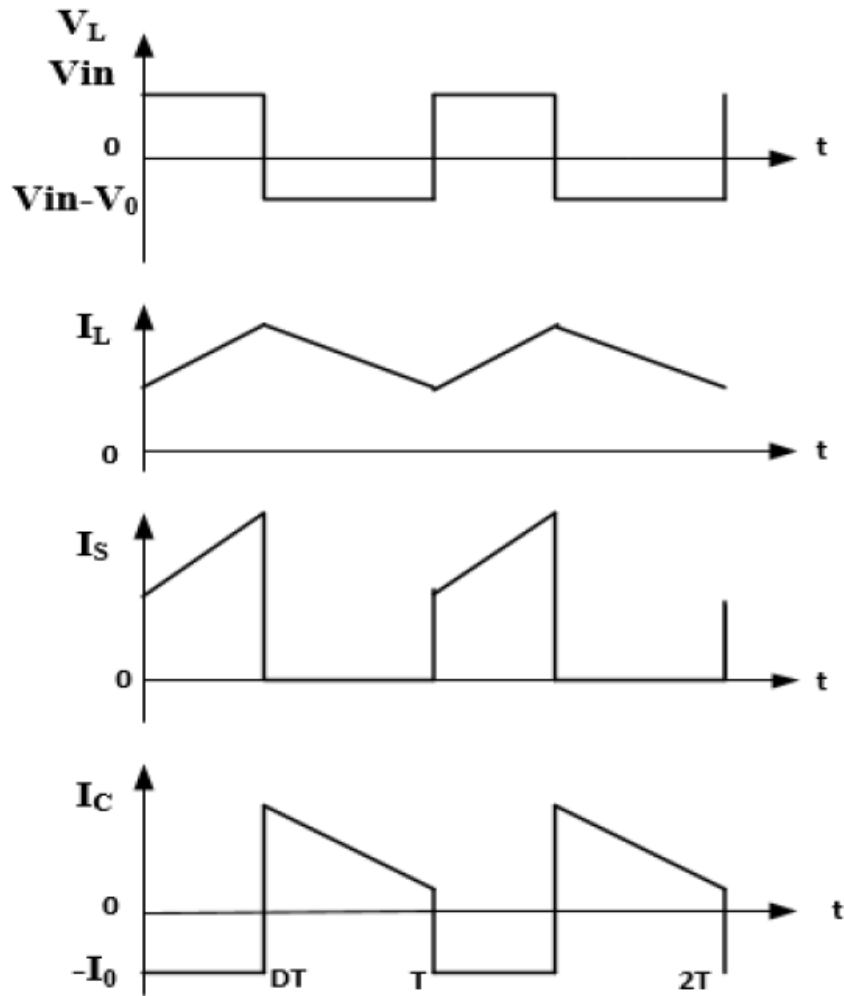
Fig. 2.2. (a) Basic configuration, (b) typical waveforms of Buck Converter, and (c) Voltage gain (G) versus duty cycle (D) of buck converter

2.2.1.2 Boost converter

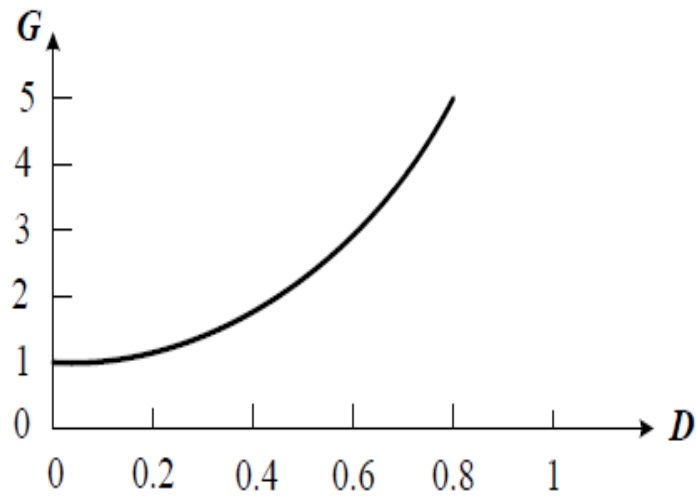
As a "step-up" converter, the voltage output of the boost converter is always greater than or equal to the input voltage. The boost converter's basic circuit configuration is shown in Fig. 2.3(a). A voltage source, an inductor, a switching device, a capacitor, a diode, and a load resistance are all included in the circuit. Figure 2.3(b) shows the waveforms in CCM mode [53]. The diode is reverse biased, and the switch is on in the ON condition. Energy is stored in the inductor as current flows from the voltage source to the switching device. The diode is forward biased, and the switch is off in the OFF state. The inductor transfers the stored energy to the output load while maintaining a constant current flow and raising the output voltage. $G = 1/(1 - D)$ is the converter's gain which is plotted in fig 2.3(c).



(a)



(b)



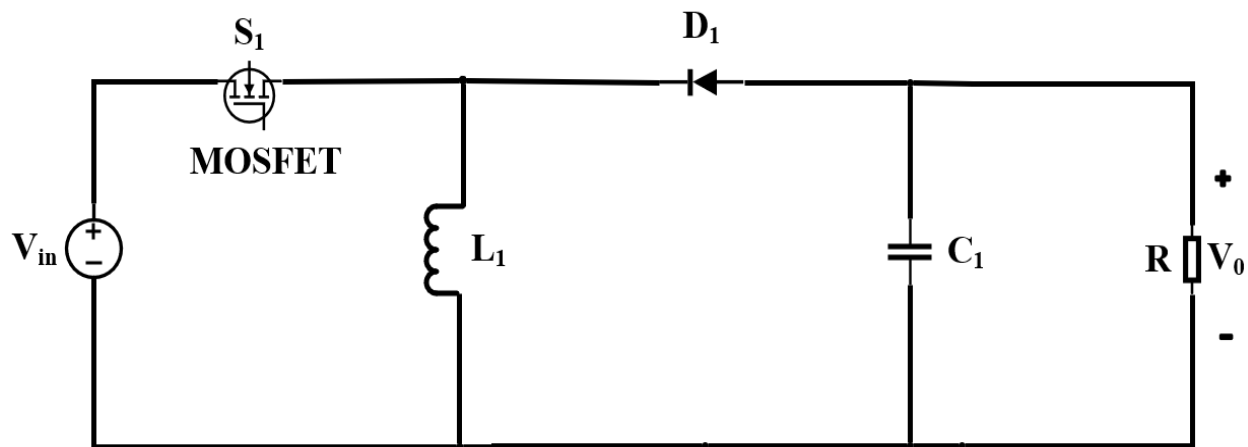
(c)

Fig. 2.3. (a) Basic configuration, (b) typical waveforms of Buck Converter, and (c) Voltage gain (G) versus duty cycle (D) of boost converter

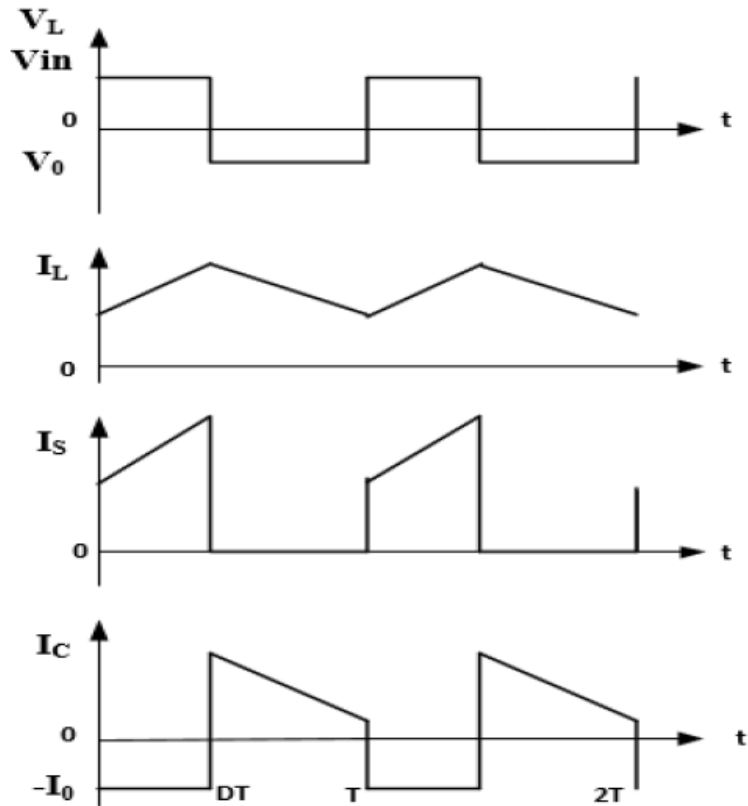
2.2.1.3 Buck-boost converter

A buck-boost converter is an inverting converter that can work as a step-down or step-up converter. As a result, depending on the duty cycle, the output voltage is either higher or lower than the input voltage. Figure 2.4(a) shows the topology of a buck-boost converter. Dc input voltage source, controlled switch, inductor, capacitor, diode, and load resistance are the components of the converter. Figure 2.4(b) shows the waveforms of this converter in CCM mode [58-59].

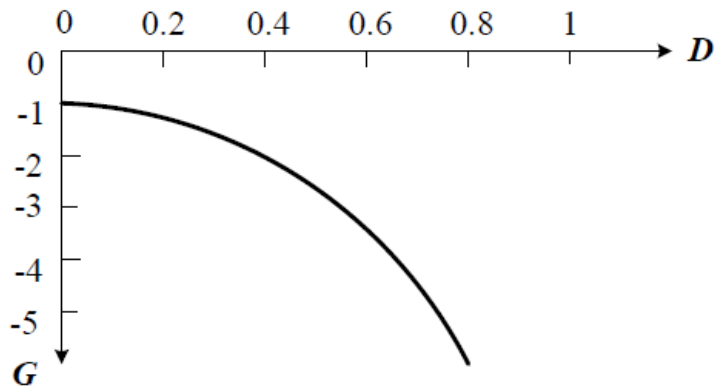
When the switch is turned on, the diode is turned off, and the inductor is charged. The voltage, the switch, and the inductor will all enhance the current flow. When the switch is turned off, the diode is forward biased, and the inductor sends the stored energy to the capacitor and load resistance. As a result, the buck-boost circuit's voltage gain is $g = -D/(1 - D)$. The switches will be faced with a lot of voltage stress. It is characterized by a non-pulsating current [60-61].



(a)



(b)



(c)

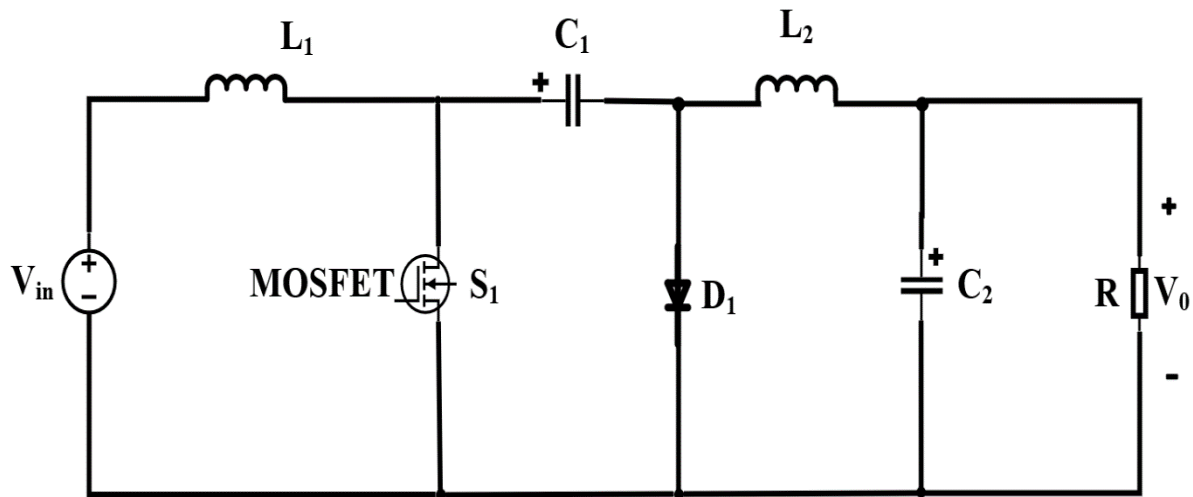
Fig. 2.4. (a) Basic configuration, (b) typical waveforms of Buck Converter, and (c) Voltage gain (G) versus duty cycle (D) of buck-boost converter

2.2.1.4 Cuk converter

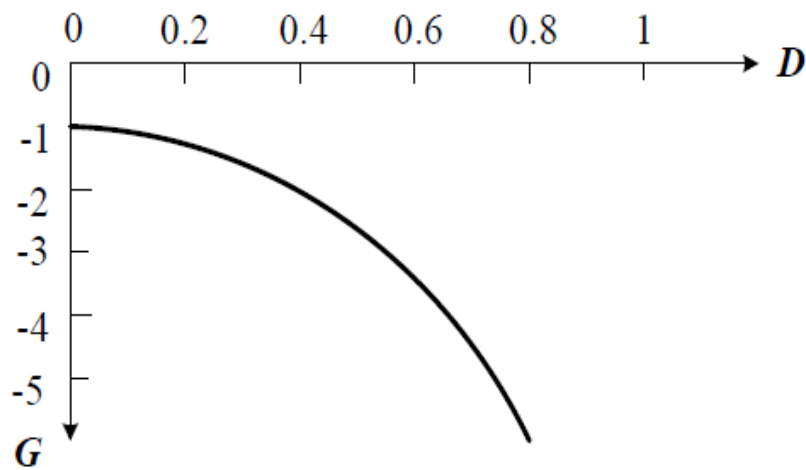
The Cuk converter is a DC-DC power electronic converter named after its inventor, Slobodan Cuk. The invention's primary goal was to minimize the effects of pulsing current. The Cuk converter emulates the behavior of an ideal transformer by producing ripple-free dc input and

output currents. After analyzing the Cuk converter, the concept of coupling inductances in dc-dc converters received much attention. The Cuk converter provides two notable benefits: practical applications for managing the consequences of multifunctional converter configurations and theoretical examples dealing with some new switching compositional concepts [62].

Cuk converter has more components compared to boost, buck, and buck-boost converters. Two inductors, two capacitors, one switch, and one diode are the significant components of a typical Cuk converter. Cuk converter is a hybrid of buck and boost converters. The input side looks like a boost converter, and the output side looks like a buck converter in a disconnected inverting way by a capacitor between them, as seen in fig 1. Compared to the input voltage, the Cuk converter's output voltage is reversed. Figures 2.5(a) and 2.5(b) illustrate the circuit diagram and also the voltage gain as a function of the duty cycle. The Cuk converter has been the most efficient and lowest switching losses. Because of the inductor on the output stage, it can provide excellent output current characteristics [63-65].



(a)

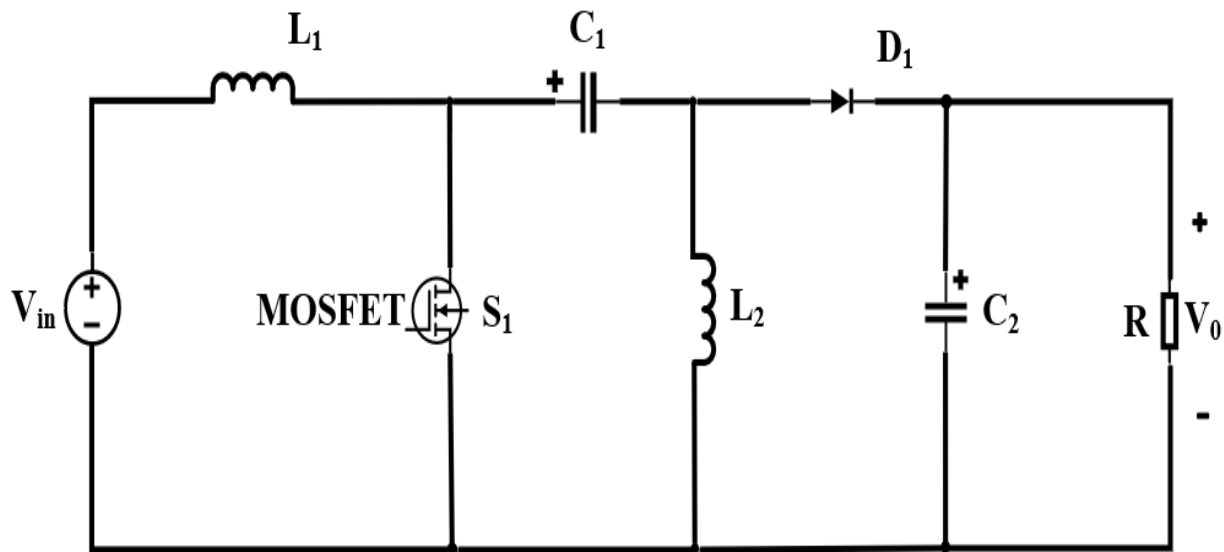


(b)

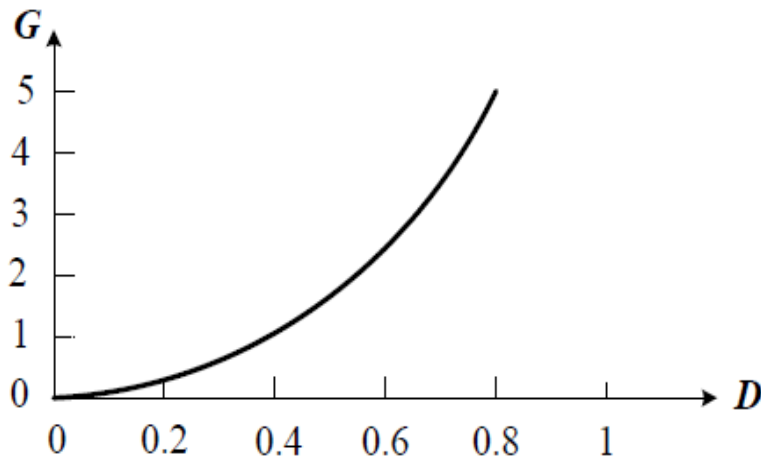
Fig. 2.5. (a) Basic configuration and (b) Voltage gain (G) versus duty cycle (D) of Cuk converter

2.3.1.5 SEPIC converter

The single-ended primary-inductor converter (SEPIC) is a DC-DC converter that permits the output voltage can be larger than, less than, or equal to the input voltage. The duty cycle of the control switch (S1) regulates the SEPIC's output. The output voltage's polarity is not reversed. The conventional circuit diagram of SEPIC is shown in figure 2.6(a). The voltage gain of SEPIC converter is $G = D/(1 - D)$, which is illustrated in 2.6(b).



(a)



(b)

Fig. 2.6. (a) Basic configuration and (b) Voltage gain versus duty cycle of SEPIC converter

The Unidirectional SEPIC converter is the most essential and commonly used of all the converters. It can change the duty cycle to step up and step down the input voltage without changing the polarity. Furthermore, this converter has a minimal input ripple current and can be extended to several outputs [66]. Moreover, the Bidirectional SEPIC converter can provide power flow in both forward and backward directions. Again, the Interleaved SEPIC converter uses the current splitting mechanism to reduce the conduction losses of the switch to increase the efficiency, and thus, the output ripple current will be reduced. As a result, the SEPIC converter and its variants were chosen as the thesis' processing facility. In the following chapters, mathematical modeling, open loop, and closed-loop response, implementation of an optimized PID controller using nonlinear approaches, simulation results, and a comparison study will be described.

CHAPTER 3

DC-DC SEPIC CONVERTER

The single-ended primary inductor converter is a standard DC-DC converter that is a fourth-order system, finding it challenging to operate and only appropriate for applications with prolonged variations. The duty cycle of the control transistor is used to control the SEPIC's output. As a result of the power converter's switching nature, the SEPIC exhibits high nonlinear behavior in both static and dynamic settings. For both power electronic engineers and control engineers, designing high-performance control for SEPIC is a great challenge. In general, good DC-DC converter regulation enables stability under all operating conditions. A small-signal state-space equation of the converter system could be constructed using various state-space averaging approaches. PI and PID control are viable solutions for optimizing the stability of SEPIC converter dynamics while maintaining accurate operation in any working state. These control systems have several benefits, including stability, even for substantial line and load variations, reduced steady error, robustness, good dynamic response, and ease of implementation. The fundamental benefit of PI control schemes is their resistance to changes in plant/system parameters, which results in invariant dynamic and static responses in the ideal scenario.

3.1 Conventional SEPIC Converter

A SEPIC is an essential converter that is widely used in power electronics that allows the duty cycle of the switching device to control the output voltage. Two inductors (L_1 , L_2), two capacitors (C_1 , C_2), one diode (D_1), one switch (S_1) with duty cycle (D), and a resistive load (R) construct the SEPIC converter.

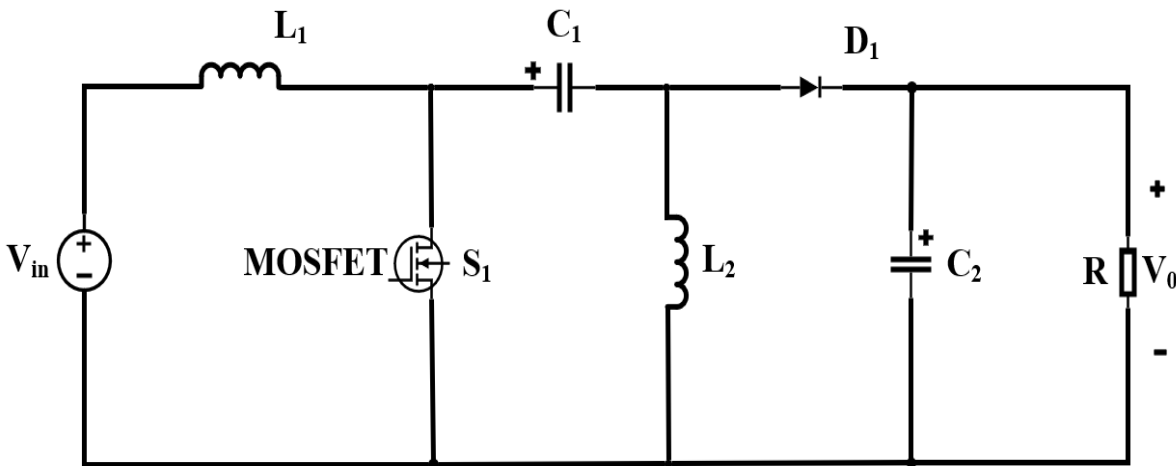


Fig. 3.1. Conventional SEPIC Converter [67]

Figure 3.1 shows the circuit schematic of a traditional SEPIC converter, whereas Figure 3.2 shows the corresponding circuits in ON and OFF states (a and b). At first, the switch is open in a SEPIC converter, and KVL can be applied in this situation. Moreover, KVL can also be applied in the inner loop while the switch is closed, the inner loop is produced. In this scenario, capacitor C_2 is providing the load power. The current flowing through inductors L_1 and L_2 is increasing while the capacitors (C_1 and C_2) are discharging. The capacitors are charged, and the inductor currents are discharged when the switch is opened again. In this situation, KVL demonstrates that $V_{L1} = -V_0$. It has a zero average voltage across the first inductor L_1 .

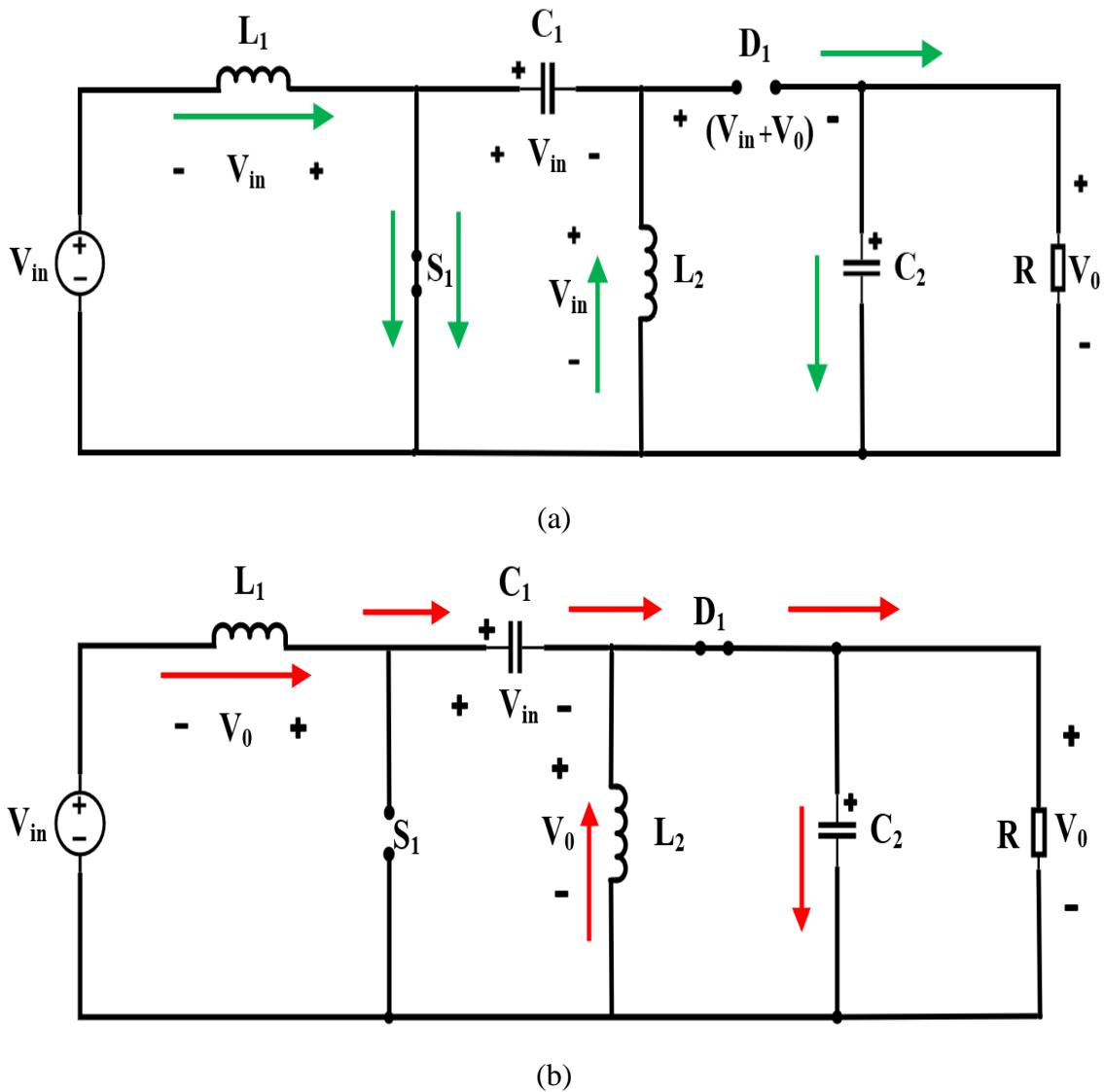


Fig. 3.2. Traditional SEPIC converter's modes of operation (a) Switch is ON condition and (b) Switch is OFF condition

3.2 State Space Modeling of Unidirectional and Bidirectional SEPIC

The state space average technique depicts the SEPIC converter using a first-order differential equation since this mathematical model is best suited to explain any nonlinear dynamic system in a simple form. The matrix is created after collecting input, output, and state variables are represented in first-order differential form. As a result, the state space form makes modeling and analyzing a system with various inputs and outputs compact and straightforward. Unlike the frequency domain technique, the state space representation uses linear components and zero beginning conditions to demonstrate the system, making it a valuable tool for modeling power converters.

$$V_{C1} = 0 ; 0 \leq t \leq dT \quad (3.1)$$

$$I_{L2} = I_{D1} + I_0 \quad (3.2)$$

$$\frac{dI_{L1}}{dt} = \frac{V_{in}}{L_1} ; 0 \leq t \leq dT \quad (3.3)$$

$$\frac{dI_{L1}}{dt} = -\frac{V_0}{L_1} ; dT \leq t \leq T \quad (3.4)$$

$$\frac{V_0}{V_{in}} = \frac{D}{1-D} \quad (3.5)$$

Mode-1: S₁ is ON and D₁ is OFF

$$\frac{dI_{L1}}{dt} = \frac{V_{in}}{L_1} \quad (3.6)$$

$$\frac{dI_{L2}}{dt} = \frac{V_{C1}}{L_2} \quad (3.7)$$

$$\frac{dV_{C1}}{dt} = -\frac{I_{L1}}{C_1} \quad (3.8)$$

$$\frac{dV_{C2}}{dt} = \frac{1}{C_2} \left(\frac{V_{C2}}{R} \right) \quad (3.9)$$

$$x_1(t) = M_1x(t) + N_1u(t) \quad (3.10)$$

$$y_1(t) = P_1x(t) + Qu(t) \quad (3.11)$$

$$\begin{bmatrix} \frac{dI_{L1}}{dt} \\ \frac{dI_{L2}}{dt} \\ \frac{dV_{C1}}{dt} \\ \frac{dV_{C2}}{dt} \end{bmatrix} = \begin{bmatrix} 0 & 0 & 0 & 0 \\ 0 & 0 & \frac{1}{L_2} & 0 \\ 0 & -\frac{1}{C_2} & 0 & 0 \\ 0 & 0 & 0 & \frac{1}{RC_2} \end{bmatrix} \begin{bmatrix} I_{L1} \\ I_{L2} \\ V_{C1} \\ V_{C2} \end{bmatrix} + \begin{bmatrix} \frac{1}{L_2} \\ 0 \\ 0 \\ 0 \end{bmatrix} V_{in} \quad (3.12)$$

$$y(t) = [0 \ 0 \ 0 \ 1] \begin{bmatrix} I_{L1} \\ I_{L2} \\ V_{C1} \\ V_{C2} \end{bmatrix} \quad (3.13)$$

Mode-2: S₁ is OFF and D₁ is ON

$$\frac{dI_{L1}}{dt} = \frac{1}{L_1} (V_{in} - V_{C1} - V_{C2}) \quad (3.14)$$

$$\frac{dI_{L2}}{dt} = \frac{1}{L_2} (-V_{C2}) \quad (3.15)$$

$$\frac{dV_{C1}}{dt} = \frac{1}{C_1} (I_{L1}) \quad (3.16)$$

$$\frac{dV_{C2}}{dt} = \frac{1}{C_2} \left(I_{L1} + I_{L2} - \frac{V_{C2}}{R} \right) \quad (3.17)$$

$$x_2(t) = M_2x(t) + N_2u(t) \quad (3.18)$$

$$y_2(t) = P_2x(t) + Qu(t) \quad (3.19)$$

$$\begin{bmatrix} \frac{dI_{L1}}{dt} \\ \frac{dI_{L2}}{dt} \\ \frac{dV_{C1}}{dt} \\ \frac{dV_{C2}}{dt} \end{bmatrix} = \begin{bmatrix} 0 & 0 & -\frac{1}{L_1} & -\frac{1}{L_1} \\ 0 & 0 & 0 & -\frac{1}{L_2} \\ \frac{1}{C_1} & 0 & 0 & 0 \\ \frac{1}{C_2} & \frac{1}{C_2} & 0 & -\frac{1}{RC_2} \end{bmatrix} \begin{bmatrix} I_{L1} \\ I_{L2} \\ V_{C1} \\ V_{C2} \end{bmatrix} + \begin{bmatrix} \frac{1}{L_1} \\ 0 \\ 0 \\ 0 \end{bmatrix} V_{in} \quad (3.20)$$

$$y(t) = [0 \quad 0 \quad 0 \quad 1] \begin{bmatrix} I_{L1} \\ I_{L2} \\ V_{C1} \\ V_{C2} \end{bmatrix} \quad (3.21)$$

3.3 State Space Modeling of Interleaved SEPIC

Mode-1: S₁ is ON, S₂ is OFF, D₁ is OFF, and D₂ is ON

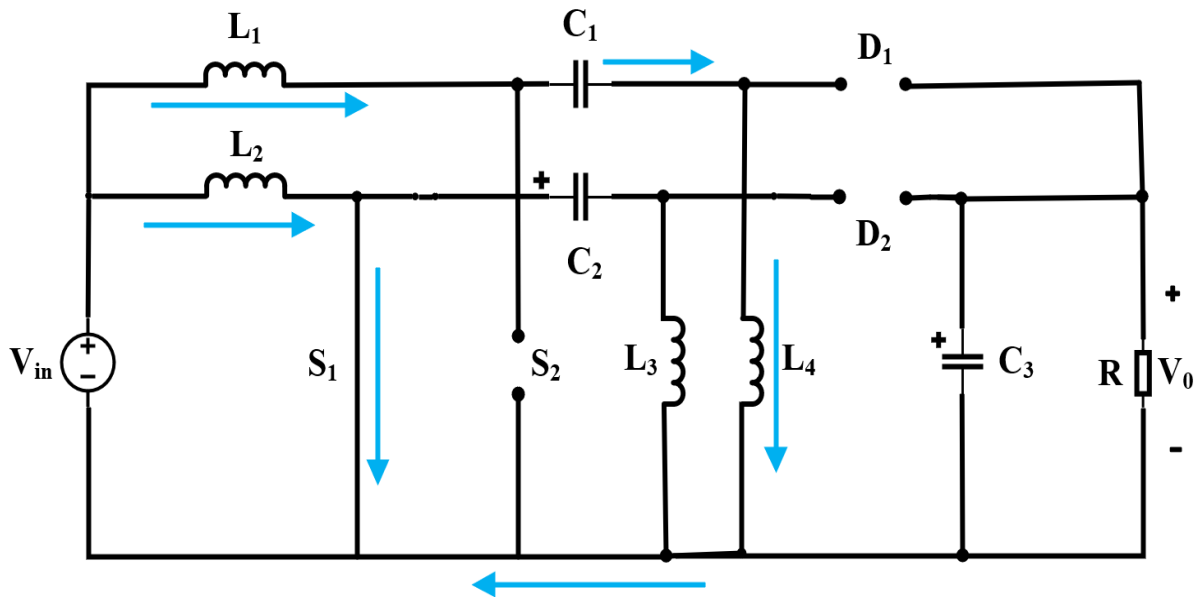


Fig. 3.3. Interleaved SEPIC : Mode-1

$$\begin{bmatrix} \frac{dI_{L2}}{dt} \\ \frac{dI_{L3}}{dt} \\ \frac{dI_{L1}}{dt} \\ \frac{dI_{L4}}{dt} \\ \frac{dV_{C2}}{dt} \\ \frac{dV_{C1}}{dt} \\ \frac{dV_{C3}}{dt} \end{bmatrix} = \begin{bmatrix} 0 & 0 & 0 & 0 & 0 & 0 & 0 \\ 0 & 0 & 0 & 0 & \frac{1}{L_3} & 0 & 0 \\ 0 & 0 & 0 & 0 & 0 & \frac{1}{L_1 + L_4} & 0 \\ 0 & 0 & 0 & 0 & 0 & 0 & 0 \\ 0 & -\frac{1}{C_2} & 0 & 0 & 0 & 0 & 0 \\ 0 & 0 & \frac{1}{C_1} & 0 & 0 & 0 & 0 \\ 0 & 0 & 0 & 0 & 0 & 0 & -\frac{1}{RC_3} \end{bmatrix} \begin{bmatrix} I_{L2} \\ I_{L3} \\ I_{L1} \\ I_{L4} \\ V_{C2} \\ V_{C1} \\ V_{C3} \end{bmatrix} + \begin{bmatrix} \frac{1}{L_2} \\ 0 \\ \frac{1}{L_1 + L_4} \\ 0 \\ 0 \\ 0 \\ 0 \end{bmatrix} V_{in} \quad (3.22)$$

$$k_1 = [0 \ 0 \ 0 \ 0 \ 0 \ 0 \ 1] \begin{bmatrix} I_{L2} \\ I_{L3} \\ I_{L1} \\ I_{L4} \\ V_{C2} \\ V_{C1} \\ V_{C3} \end{bmatrix} \quad (3.23)$$

Mode-2: S_1 is OFF, S_2 is OFF, D_1 is ON, and D_2 is OFF

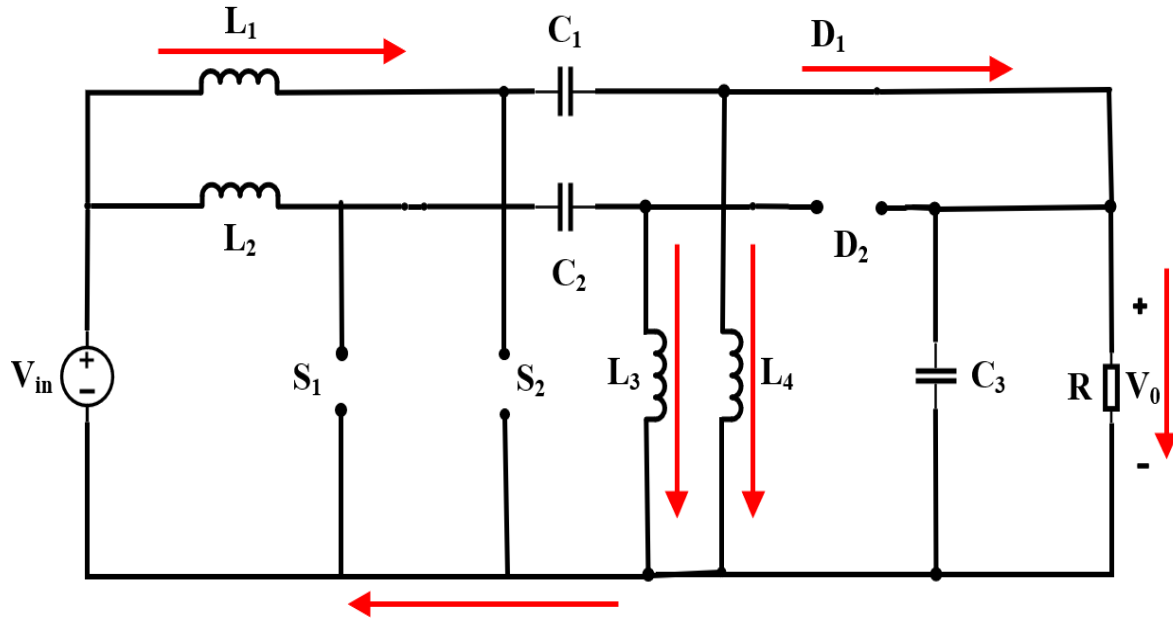


Fig. 3.4. Interleaved SEPIC : Mode-2

$$\begin{bmatrix} \frac{dI_{L_2}}{dt} \\ \frac{dI_{L_3}}{dt} \\ \frac{dI_{L_1}}{dt} \\ \frac{dI_{L_4}}{dt} \\ \frac{dV_{C_2}}{dt} \\ \frac{dV_{C_1}}{dt} \\ \frac{dV_{C_3}}{dt} \end{bmatrix} = \begin{bmatrix} 0 & 0 & 0 & 0 & -\frac{1}{L_2} & 0 & -\frac{1}{L_2} \\ 0 & 0 & 0 & 0 & 0 & 0 & -\frac{1}{L_3} \\ 0 & 0 & 0 & 0 & 0 & \frac{1}{L_1 + L_4} & 0 \\ 0 & 0 & 0 & 0 & 0 & 0 & 0 \\ \frac{1}{C_2} & 0 & 0 & 0 & 0 & 0 & 0 \\ 0 & 0 & \frac{1}{C_1} & 0 & 0 & 0 & 0 \\ \frac{1}{C_3} & \frac{1}{C_3} & 0 & 0 & 0 & 0 & -\frac{1}{RC_3} \end{bmatrix} \begin{bmatrix} I_{L_2} \\ I_{L_3} \\ I_{L_1} \\ I_{L_4} \\ V_{C_2} \\ V_{C_1} \\ V_{C_3} \end{bmatrix} + \begin{bmatrix} \frac{1}{L_2} \\ 0 \\ \frac{1}{L_1 + L_4} \\ 0 \\ 0 \\ 0 \\ 0 \end{bmatrix} V_{in} \quad (3.24)$$

$$k_2 = \begin{bmatrix} 0 & 0 & 0 & 0 & 0 & 0 & 1 \end{bmatrix} \begin{bmatrix} I_{L2} \\ I_{L3} \\ I_{L1} \\ I_{L4} \\ V_{C2} \\ V_{C1} \\ V_{C3} \end{bmatrix} \quad (3.25)$$

Mode-3: S_1 is OFF, S_2 is ON, D_1 is OFF, and D_2 is OFF

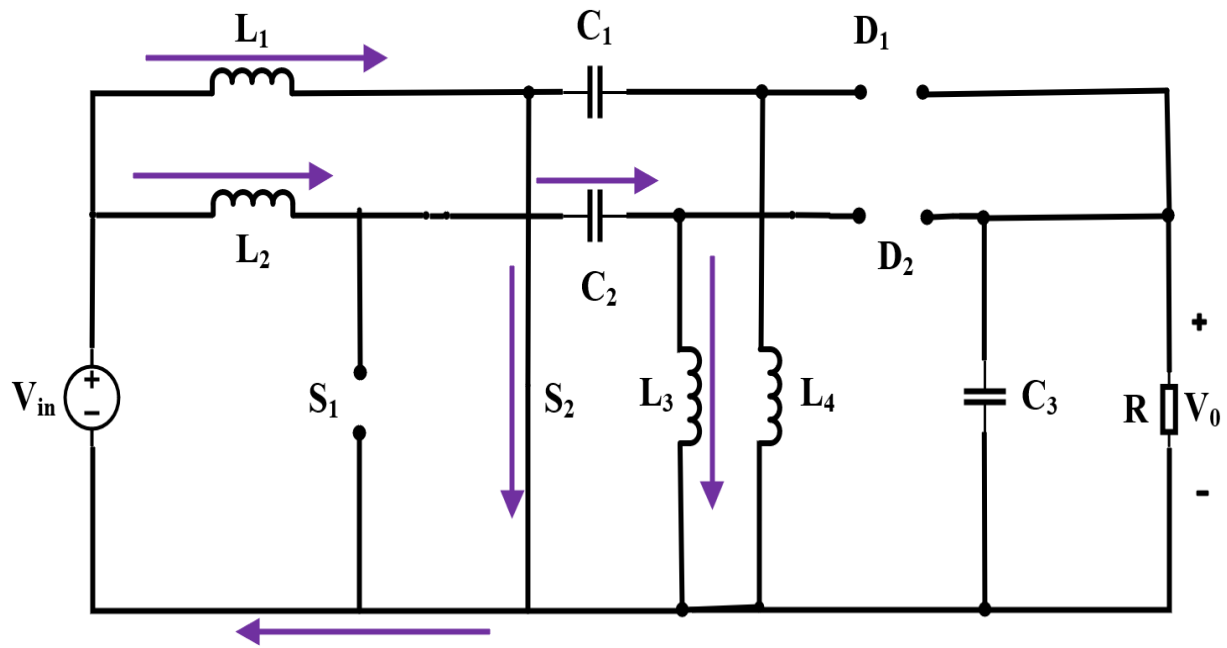


Fig. 3.5. Interleaved SEPIC : Mode-3

$$\begin{bmatrix} \frac{dI_{L2}}{dt} \\ \frac{dI_{L3}}{dt} \\ \frac{dI_{L1}}{dt} \\ \frac{dI_{L4}}{dt} \\ \frac{dV_{C2}}{dt} \\ \frac{dV_{C1}}{dt} \\ \frac{dV_{C3}}{dt} \end{bmatrix} = \begin{bmatrix} 0 & 0 & 0 & 0 & -\frac{1}{L_2 + L_3} & 0 & 0 \\ 0 & 0 & 0 & 0 & 0 & 0 & 0 \\ 0 & 0 & 0 & 0 & 0 & 0 & 0 \\ 0 & 0 & 0 & 0 & 0 & \frac{1}{L_4} & 0 \\ \frac{1}{C_2} & 0 & 0 & 0 & 0 & 0 & 0 \\ 0 & 0 & -\frac{1}{C_1} & 0 & 0 & 0 & 0 \\ 0 & 0 & 0 & 0 & 0 & 0 & -\frac{1}{RC_3} \end{bmatrix} \begin{bmatrix} I_{L2} \\ I_{L3} \\ I_{L1} \\ I_{L4} \\ V_{C2} \\ V_{C1} \\ V_{C3} \end{bmatrix} + \begin{bmatrix} \frac{1}{L_2 + L_3} \\ 0 \\ \frac{1}{L_1} \\ 0 \\ 0 \\ 0 \\ 0 \end{bmatrix} V_{in} \quad (3.26)$$

$$k_3 = [0 \ 0 \ 0 \ 0 \ 0 \ 0 \ 1] \begin{bmatrix} I_{L2} \\ I_{L3} \\ I_{L1} \\ I_{L4} \\ V_{C2} \\ V_{C1} \\ V_{C3} \end{bmatrix} \quad (3.27)$$

Mode-4: S₁ is OFF, S₂ is OFF, D₁ is OFF, and D₂ is ON

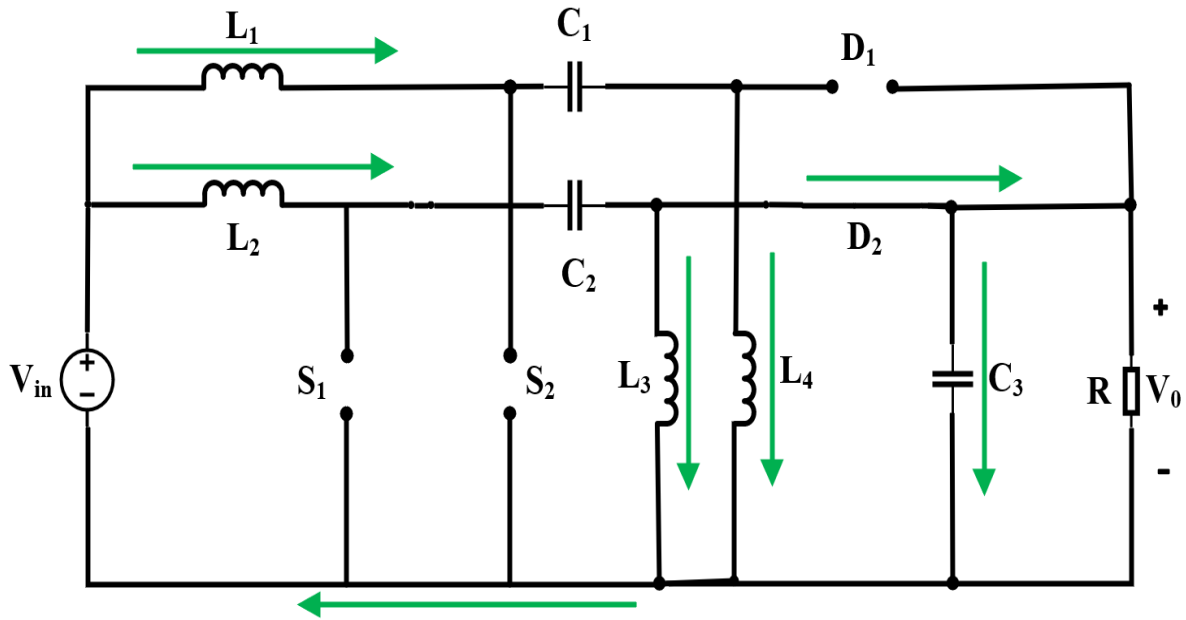


Fig. 3.6. Interleaved SEPIC : Mode-4

$$\begin{bmatrix} \frac{dI_{L2}}{dt} \\ \frac{dI_{L3}}{dt} \\ \frac{dI_{L1}}{dt} \\ \frac{dI_{L4}}{dt} \\ \frac{dV_{C2}}{dt} \\ \frac{dV_{C1}}{dt} \\ \frac{dV_{C3}}{dt} \end{bmatrix} = \begin{bmatrix} 0 & 0 & 0 & 0 & -\frac{1}{L_2 + L_3} & 0 & 0 \\ 0 & 0 & 0 & 0 & 0 & 0 & 0 \\ 0 & 0 & 0 & 0 & 0 & -\frac{1}{L_1} & -\frac{1}{L_1} \\ 0 & 0 & 0 & 0 & 0 & 0 & -\frac{1}{L_4} \\ \frac{1}{C_2} & 0 & 0 & 0 & 0 & 0 & 0 \\ 0 & 0 & \frac{1}{C_1} & 0 & 0 & 0 & 0 \\ 0 & 0 & \frac{1}{C_3} & \frac{1}{C_3} & 0 & 0 & -\frac{1}{RC_3} \end{bmatrix} \begin{bmatrix} I_{L2} \\ I_{L3} \\ I_{L1} \\ I_{L4} \\ V_{C2} \\ V_{C1} \\ V_{C3} \end{bmatrix} + \begin{bmatrix} \frac{1}{L_2 + L_3} \\ 0 \\ \frac{1}{L_1} \\ 0 \\ 0 \\ 0 \\ 0 \end{bmatrix} V_{in} \quad (3.28)$$

$$k_4 = \begin{bmatrix} 0 & 0 & 0 & 0 & 0 & 0 & 0 & 1 \end{bmatrix} \begin{bmatrix} I_{L2} \\ I_{L3} \\ I_{L1} \\ I_{L4} \\ V_{C2} \\ V_{C1} \\ V_{C3} \end{bmatrix} \quad (3.29)$$

$$A = \begin{bmatrix} 0 & 0 & 0 & 0 & -\frac{(1-D)}{L_2} - \frac{1}{L_2+L_3} & 0 & 0 \\ 0 & 0 & 0 & 0 & \frac{D}{L_3} & 0 & -\frac{(1-D)}{L_3} \\ 0 & 0 & 0 & 0 & 0 & -\frac{1}{L_1+L_4} - \frac{D}{L_4} & -\frac{(1-D)}{L_1} \\ 0 & 0 & 0 & 0 & 0 & \frac{D}{L_4} & -\frac{(1-D)}{L_4} \\ \frac{(2-D)}{C_2} & \frac{-D}{C_2} & 0 & 0 & 0 & 0 & 0 \\ 0 & 0 & \frac{(2-D)}{C_1} & \frac{-D}{C_1} & 0 & 0 & 0 \\ -\frac{(1-D)}{C_3} & -\frac{(1-D)}{C_3} & -\frac{(1-D)}{C_3} & -\frac{(1-D)}{C_3} & 0 & 0 & -\frac{2}{RC_3} \end{bmatrix} \quad (3.30)$$

$$B = \begin{bmatrix} \frac{1}{L_2} + \frac{1}{L_2+L_3} \\ 0 \\ \frac{1}{L_1} + \frac{1}{L_1+L_4} \\ 0 \\ 0 \\ 0 \\ 0 \end{bmatrix} \quad (3.31)$$

$$C = [0 \ 0 \ 0 \ 0 \ 0 \ 0 \ 2] \quad (3.32)$$

3.4 Gain Equation of SEPIC Converter

For an ideal SEPIC converter, the converter's output voltage is connected to the input voltage by the duty cycle when there is no series taken into account.

$$\frac{V_o}{V_{in}} = \frac{D}{1-D} \quad (3.33)$$

The output voltage can be controlled by changing the duty cycle ranging from 0 to 1. To convert to voltage gain (V_o/V_{in}), equation 3.1 is rearranged. The graph in Fig. 3.3 shows the relationship between voltage gain and duty cycle. The voltage gain is 0 when the duty cycle is 0. The voltage gain grows as the duty cycle is increased, and at 0.5 duty cycle, the voltage gain is 1. When the duty cycle is less than 0.5, the converter reduces the input voltage works as a buck converter. The output voltage equals the input voltage at 0.5. When the duty cycle exceeds 0.5, the voltage gain exceeds 1 and works as boost converter. Since the derivation is for an ideal converter, the voltage gain is infinity whenever the duty cycle is 1. For a practical SEPIC converter, equation 3.1 is invalid. As a result, the equation is changed to include the inductor and capacitor internal resistances. The output voltage of an ideal converter is independent of load resistance, whereas the output voltage of a practical converter is dependent on both load resistance and equivalent series resistance.

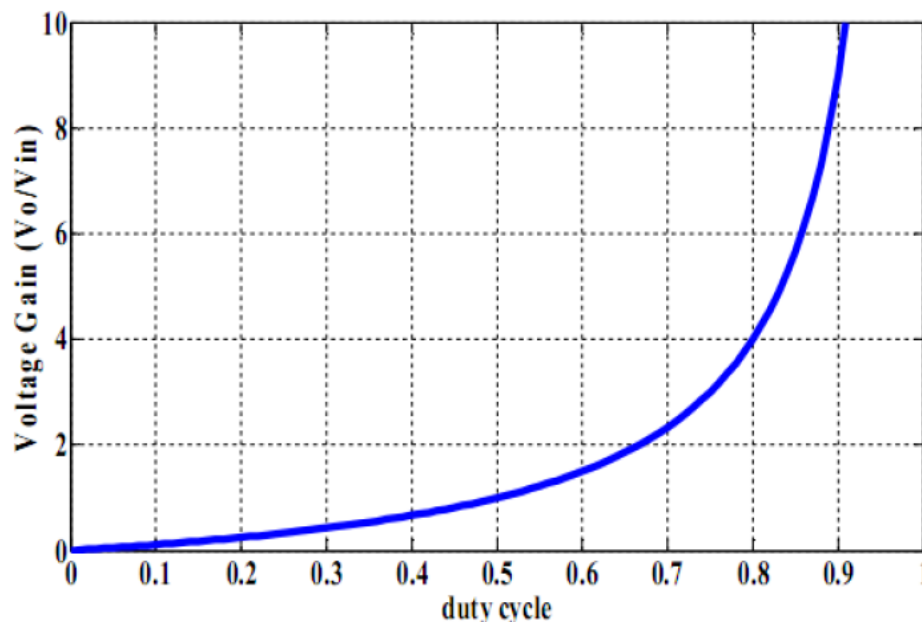


Fig. 3.7. Voltage Gain vs. duty cycle with variable load

The practical converter's output voltage is

$$V_0 = \frac{V_{in}}{\frac{1-D}{D} + \frac{Dr_{L1}}{(1-D)R} - \frac{(1-D)r_{L2}}{DR} + \frac{(2D-1)r_{C1}}{R}} \quad (3.34)$$

The voltage gain is calculated and plotted against the duty cycle by rearranging the equation. The change of voltage gain concerning the duty cycle for various loads is shown in Fig. 3.4. It has been demonstrated that as the load resistance increases, so does the maximum voltage gain. R is varied from 1 to 10 in this figure, and it can be seen that there is no change in voltage gain up to duty cycle 0.8, but once it exceeds 0.8, the voltage gain varies for different values of R, increasing as R is increased.

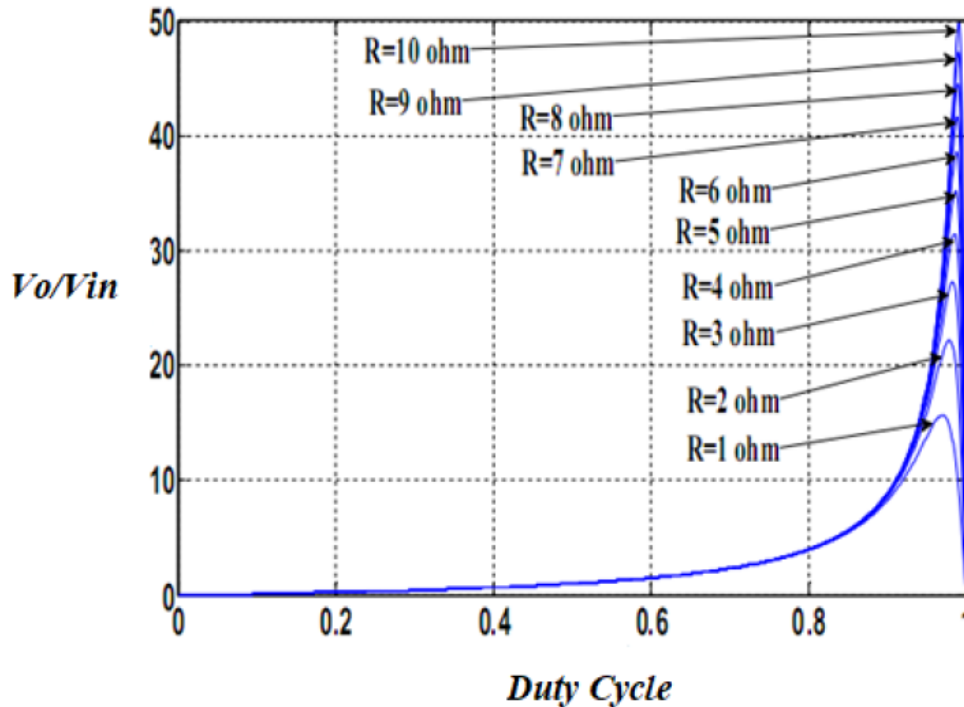


Fig. 3.8. Voltage Gain vs. duty cycle with variable load

CHAPTER 4

STUDY OF SWARM INTELLIGENCE ALGORITHM

In swarm intelligence, almost every algorithm is a meta-heuristic type. Metaheuristics are higher-level processes for determining which may produce a sufficiently good answer, primarily when computation capability is restricted or incomplete. The objective is to explore the search space as quickly as possible to identify a near-optimal solution. These are motivated by the custom and mannerisms witnessed in biological beings or organisms while being in their natural habitat to achieve efficacy in meeting the natural requirements such as acquiring food, preying, surviving from danger, mating, etc. Since nature is unpredictable and changing, the inhabitants living in nature show versatility, dynamic attitude, flexibility, and witty responses. In this thesis, three SIA are used, which are Firefly Algorithm (FA), Particle Swarm Optimization (PSO), and Ant Colony Optimization for continuous domain (ACO_R) algorithm.

4.1.1. Identification of PSO

Particle swarm optimization (PSO) is a heuristic universal optimization solution introduced by Kennedy and Eberhart in 1995 [68]. It was created using swarm intelligence and is focused on bird and fish flock moving behavior models. Kennedy and Eberhart's earliest concepts on swarms of particles focused on developing adaptive calculation through leveraging basic social connection intermediates rather than pure individual analytics solutions [69]. Since it follows the principles followed by social species in nature, PSO falls within the concept of Bio-Inspired Algorithms.

4.1.2 Objectives of PSO

The PSO method contains various goals that essentially allow semi-individuals to use the optimization method to its full potential in order to achieve their aim. The following are the objectives [70]:

1. To generate a detailed analysis of the most frequent PSO factors to get long-term usage from it.
2. To analyze a variety of algorithm operations and outcomes in order to identify the algorithm's functioning and existing rules.

3. To generate a preview of the individual's theoretical background and the impact of the PSO factors on them.
4. To develop other methods to improve the algorithm's performance.

4.1.3 Advantages and Disadvantages of PSO

A Study of the Basic Particle Swarm Optimization Algorithm's Advantages and Drawbacks [71]. Advantages of the basic particle swarm optimization algorithm involve:

1. PSO's intellectual ability is at its core. It can be applied to both scientific and industrial research.
2. In PSO, there are no calculations for overlaps or mutations. Instead, the particle's speed can be used to perform the search. Only the most promising particles are capable of transmitting information to other particles throughout generations, and research is moving at a fast pace.
3. The calculation in PSO is really basic. It has a higher optimization capability and can be completed faster than other development computations.
4. PSO employs a genuine numerical code that is directly determined by the answer. The number of dimensions is the variable in the solution.

Limitations of the basic particle swarm optimization algorithm involve:

1. The approach is sensitive to premature optimism, resulting in less precise speed and direction control.
2. The technique fails to tackle dispersion and optimization difficulties
3. The technique is incapable of controlling difficulties involving non-coordinate systems, such as the equivalent to the areas of production and the objects' movement laws in the energy field.

4.1.4 Features of PSO

Particle Swarm Optimization (PSO) is a self-adaptive and computational method inspired by the swarms' natural behavior. Among the many Artificial Intelligence (AI) systems used to optimize control parameters, PSO is a popular metaheuristic algorithm that deserves special mention for its capability to solve continuous non-linear problems. It has undergone several improvements since its introduction in 1995 by Eberhart and Kennedy [68].

In 1998, Shi and Eberhart introduced a modified PSO to improve the original PSO's performance and added an inertia weight parameter giving a good balance between global and local search capabilities [70]. This technique imitates the problem-solving abilities of some animals, like bird flocking or fish schooling. Interactions among animals contribute to the swarm's collective intelligence. Because of its simplicity, this technique has attracted many researchers, resulting in numerous refinements and modifications to the fundamental PSO [71].

4.1.5 Methodology PSO

The process in the search space begins with a random initiation of a swarm of particles, which further travels around the search space. To begin its iteration process, it does not require an appropriate starting solution [69]. Each particle in the PSO algorithm learns from its own and another particle with a better fitness value. The swarms then discover their individual best solutions, which are referred to as their local best solutions. Finally, the swarms collaborate to find the best global solution. Every particle tries to get into the best possible position for maximal fitness, updating its position and velocity in the process. Multiple iterations are performed to ensure that the delivered solution is optimal. The method starts with a population of particles, each of which has been programmed to discover competent outcomes in the search space. The advantage of having a population of particles is that it reduces calculation time because everyone is looking for the same thing at the same time. Furthermore, the particles can travel to each point and corner of the search region to find various information that is useful in reaching conclusions.

In our thesis, the requirement, also known as the optimization problem, is replicated as the cost function in the algorithm that is programmed to minimize the cost. The particles are now ready to survey the solution space defined by the programmer after defining the objective function. Each particle gains a unique optimal position, indicating the optimum solution. After each particle's motion has been completed, the information is exchanged throughout the population in order to agree on a global optimal location. In each loop, these actions are repeated, and the values are changed accordingly. The velocity of the particle in the current iteration, the particle's personal best position, and the global best solution of the entire population are three parameters that are critical in the algorithm to regulate and determine the movement of the particles.

The three vectors mentioned above are used in the mathematical model to calculate the particle's displacement and velocity in the next iteration. As a result, the computation took both personal and overall experiences into account. The revised forms of the PSO algorithm become more optimized as the number of iterations increases. More parameters are used in the equations for calculating particle movement to improve the algorithm's efficacy. In the equations, random functions are used to ensure that the variables are not locked in the same region. The equation also includes acceleration coefficients, allowing the agents to accelerate toward their personal and global optimal values. However, when choosing the values of the constants, a balance must be maintained because a higher quantity forces the particles to reach towards or beyond the desired locations quickly. In contrast, a lower quantity causes particles to pass the target locations while traveling in the search space without being called back [72]. To bring

equilibrium between the personal and global optimal outcomes, a parameter called inertia weight is applied with the velocity of the particles, which ranges between 0.9 and 0.4. A higher inertia weight value indicates a preference for a worldwide survey, whereas a lower value indicates a preference for a local survey. Finally, when the specified number of iterations is completed, the algorithm is terminated.

4.1.6 Exploitation and Exploration in PSO

Exploitation relates to the algorithm's amplification, while investigation refers to the algorithm's diversity. Both of these characteristics may be seen in this algorithm. The relevant data from the optimal solution is often used for exploitation. To identify the best value, this approach focuses on local inquiries.

On the other hand, Random operations aid in the exploration of the search space. Although the global optimal option is used for evaluation in the acceleration particle swarm optimization, the roles of the personal optimal solution are unclear in the PSO algorithm [68]. Due to the lack of crossover, the PSO algorithm exhibits increased mobility while exerting significant exploration [73].

4.1.7 Mathematical Model of PSO

PSO's mathematical model entails following the movement of the particles. The particles' mobility is determined by their displacement and velocity in the search space. The conventional Particle Swarm Optimization algorithm's equation for determining particle velocity is shown below [74].

$$V_i^{k+1} = W * V_i^k + C_1(P_{best} - X_i^k) + C_2r_2(G_{best} - X_i^k) \quad (4.1)$$

The displacement of the particles is computed using the following equation

$$X_i^{k+1} = X_i^k + V_i^{k+1} \quad (4.2)$$

And the terms denote the following meanings,

W = weight of Inertia

C₁, C₂ = Constants of Acceleration

R₁, R₂ = Random functions

X_i^k = Displacement of the particle in the t^{th} iteration

X_i^{k+1} = Displacement of the n^{th} particle in the $(k+1)^{\text{th}}$ iteration

V_i^k = Velocity of the n^{th} particle in the t^{th} iteration

V_i^{k+1} = Velocity of the particle in the $(k+1)^{\text{th}}$ iteration

P_{best} = value of the n^{th} particle of Personal best

G_{best} = value among the entire population of Global best

4.1.8 Flowchart of PSO

The sequential flow of the operations and the algorithm's execution is described in the parts following,

Step 1. Generate the algorithm by initiate random population of particles.

Step 2. Calculate the fitness function of each particle

Step 3. Compare the present fitness value with previous best value.

Step 4. Compute the updated movement.

Step 5. Compare the personal best solutions of all particles to get the global best value.

Step 6. Update the particle's position and velocity.

Step 7. Execute the algorithm for the number specified number of iterations.

Step 8. If the total number of iterations is not completed, repeat the algorithm from step 3.

Step 9. When the iterations are completed, we get Global best as optimal solution

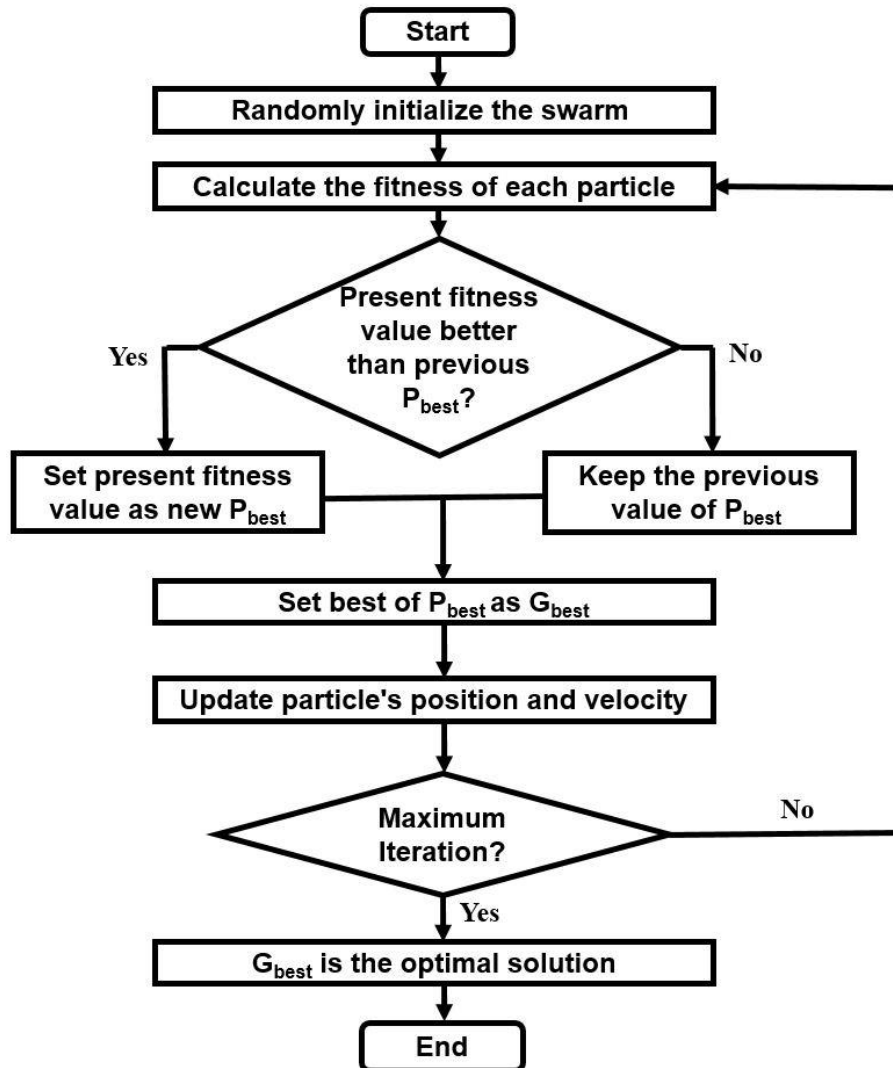


Fig. 4.1. Flowchart of PSO

4.2 Survey of Firefly Algorithm

The Firefly Algorithm is a form of the search algorithm that belongs to the Swarm Intelligence Algorithm (SIA), was proposed in 2008 [33]. The dynamic colony behavior of fireflies inspired the optimization of this technique. Bioluminescence is a biological process that gives fireflies their illuminating abdomens. Their social ritual revolves around their ability to emit light. Fireflies use their glowing anatomy as signals to find food, find shelter, and defend their community from predators.

In this way, the proper use of group information to achieve a common goal is demonstrated. The aforementioned behavior is important in the algorithm used to find the best solutions in a search space.

4.2.1 Identification of FA

Xin She Yang's Firefly Algorithm is a new generation of a meta-heuristic algorithm determined by the social behavior of fireflies in the cloudless sky in the tropical [33]. Fireflies utilize luminescence in diverse lighting rhythms to connect, hunt for food, and attract mates. Several meta-heuristic algorithms can also be developed by emulating nature. Some of the lighting characteristics of fireflies were abstracted to develop a firefly-inspired algorithm. The population size is calculated by the overall number of fireflies in the swarm. FA can address poorly defined problems with imperfect data sets because it is also a stochastic process.

Furthermore, the firefly method powered by swarm intelligence (SI) employs a multi-agent body with a decentralized approach to sweep the search space, implying that individuals move independently of any external coordinator [75]. The SI method also displays strong, versatile, and self-orchestrated qualities while implementing FA in a simple manner [76]. All of these properties, when combined, make the FA a strong candidate for optimization and promising results.

4.2.2 Features of FA

The Firefly Algorithm is an optimization method that uses metaheuristics, stochastics, and artificial intelligence. By its very nature, metaheuristics guide the production of optimum or nearly-optimized solutions through an iterative process [77]. Furthermore, it is non-deterministic and uses an approximation strategy to find answers [78]. FA can address poorly defined problems with imperfect data sets because it is also a stochastic process. Only the following three criteria were applied for the sake of simplification [33].

1. All fireflies are unisex, which means that a firefly would be captivated by some other firefly irrespective of race and gender
2. The attractiveness of fireflies is proportionate to how bright they are. When there are two flashing fireflies, the less bright will move towards the brighter one. The brightness of the firefly is proportional to their attractiveness, which diminishes as the distances among species grow. If there are no light fireflies in the neighborhood, the firefly will move arbitrarily.
3. The luminance of a firefly gets controlled or determined by the objective function's landscape. (As a result, an ideal method's luminance can be proportionate to the scaling factor.)

The modulation of luminance and the creation of desirability are two significant challenges in the FA. For simplification, we can presume that a firefly's desirability is defined by its luminance or light intensity, which is linked to the stored optimal solution [75].

4.2.3 Exploitation and Exploration in FA

The Firefly Algorithm (FA), which is inspired by swarm intelligence, exhibits two distinct behaviors that substantially influence the individual's performance: Exploitation and Exploration. Exploitation refers to the characteristics of a local survey in which data from the optimal solution is used to generate more remedies. In FA, attractiveness is linked to the problem to be solved. Hence the co-efficient of attraction is crucial in exploitation. On the other hand, Exploration is associated with the idea of searching the full search region for various solutions. The randomization factor aids the investigation, and random vectors are associated with the idea of searching the entire search region for various solutions. A balance involving exploitation and exploration must be established to optimize the algorithm's efficient functioning [79].

4.2.4 Methodology FA

The problem to be optimized is translated into an objective function in the algorithm. The objective function is associated with the brightness of the fireflies which is programmed to be minimized for our desired objective. This affirms the acquisition of better solutions as brighter fireflies denote optimal solutions. The generation of possible solutions occurs due to the free movement of the fireflies, which is influenced by the attractive factor of relevant fireflies, distance between them, random functions, and their ability to absorb light [80]. The algorithm starts with a population of fireflies ready to survey the search space that the programmer has specified. Then, to produce a solution, each agent reaches a position in the search region based on the attraction of the other firefly. Both brightness and distance are taken into account when pursuing the alluring firefly. Similarly, the light absorption coefficient and the randomization factor play a role in determining the position. After that, the beautiful firefly's current posture is evaluated in terms of attractiveness. If the new position's attractiveness is higher than the previous one, the related position is used to update the new one. On the other hand, if the attractiveness does not increase, the firefly will remain in the same position. While updating the positions of the fireflies and simultaneously seeking better solutions, the process is halted after the specified number of iterations are completed.

4.2.5 Mathematical Model of FA

The movement of firefly p^{th} is attracted to another more attractive (brighter) firefly q^{th} is determined by

$$x_p^{t+1} = x_p^t + \beta_0 e^{-\gamma r^2} (x_q^t - x_p^t) + \alpha_t \epsilon_p^t \quad (4.3)$$

The totems used in the equations above are described as such:

x_p^{t+1} = Position of Firefly n in the present state.

x_q^t = Position of Firefly b, which is brighter than Firefly n, in the previous state.

x_p^t) = Position of Firefly n in the previous state.

β_0 = Co-efficient of absorption of light.

r = Boundaries of search space signified by a vector of random values following uniform distribution at time t.

4.2.6 Flowchart of FA

The sequential flow of the operations and the algorithm's execution is described in the parts following:

Step 1. Implementation of Parameters

Step 2. Initiate a random population of fireflies to initialize the algorithm.

Step 3. Create a set of random variables for fireflies

Step 4. Compare the desirability of the firefly with respect to its previous position.

Step 5. If desirability enhances, use the corresponding position to update the new position.

Step 6. Determine the luminance based on fitness function

Step 7. Find the most effective firefly

Step 8. Move fireflies according to the desirability.

Step 9. Reach to optimum Solution

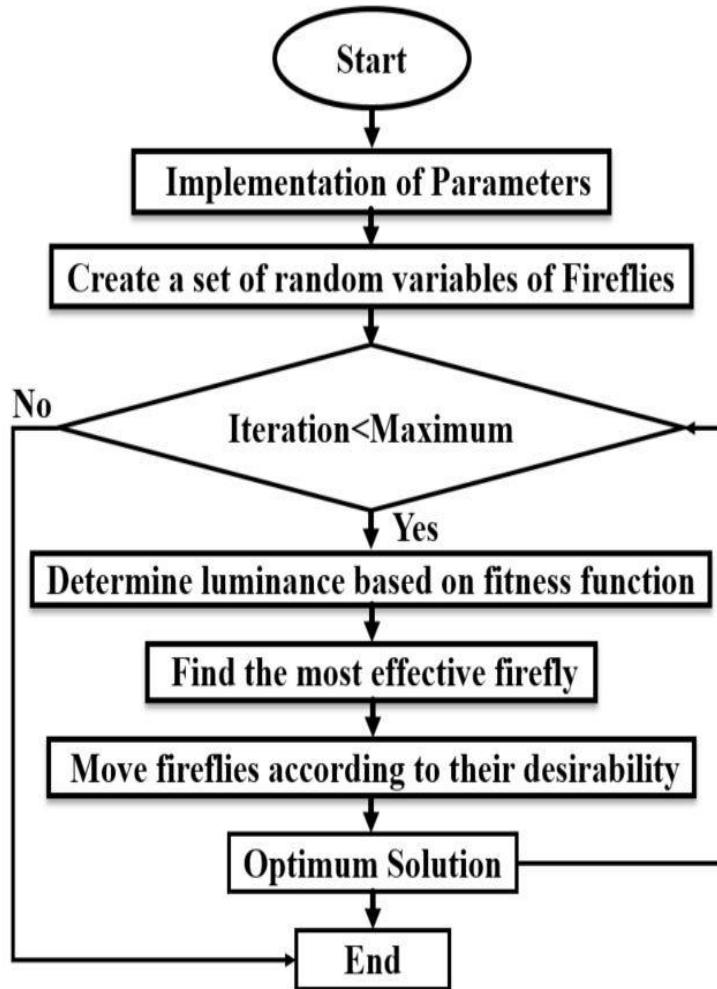


Fig. 4.2. Flowchart of FA

4.3 Survey of Ant Colony Optimization for Continuous Domain

In the recent decade, evolutionary and meta-heuristic algorithms have been frequently used to tackle reservoir operation optimization problems. The Ant Colony Optimization (ACO) approach was initially published in the early 1990s to address combinatorial optimization problems like the traveling salesman and quadratic assignment problems. Real-life ant colonies' foraging behavior inspired it. A new algorithm called ACO_R introduced by Socha and Dorigo, is the most recent approach that still benefits from the core concepts of ACO (2006) [81]. They used traditional benchmark tasks to evaluate the algorithm and discovered that ACO_R beat earlier ant-related algorithms in continuous domains. This research presents the first application of the ACO_R approach to a reservoir operation optimization problem with 60 and 120 operating periods. The current case study shows that ACO_R beats the other ant-based algorithms employed by other academics [81].

4.3.1 Identification of ACO_R

ACO is developed by the ant's browsing behavior which was first used to address discrete optimization problems. The continuous domains were added to the ant colony optimization proposed by Socha and Dorigo [82], called ACO_R. ACO_R changes its pheromone information based on the components of successful solutions obtained during training Feed-Forward Neural Networks (FFNN) just as the normal ACO algorithm. In conventional ACO, however, once the pheromone information has been updated, the actual solutions identified by the ants are discarded. ACO_R, on the other hand, keeps track of a limited number of candidate solutions and keeps the pheromone data structure as a solution archive. Probability density functions replace the discrete probability distributions utilized in the solution formulation by ACO algorithms for combinatorial optimization in ACO_R (PDFs). For the generation of these PDFs over the search space, ACO_R employs a solution archive. ACO_R also generates multimodal PDFs using sums of weighted Gaussian functions [83].

4.3.2 Advantages and Disadvantages of ACO_R

The ACO_R has the following advantages:

1. The ACO_R algorithm aids in the solution of large-scale continuous optimization issues.
2. ACO_R maintains as much variation as feasible in order to examine more parts of the search space before settling on a possible local optimum.
3. The candidate solutions are used to change the probability distribution in a way that is thought to favor high-quality solutions in future sampling.

When dealing with substantial dimensional problems, ACO_R had several limitations.

1. The algorithm's fundamental flaw was a rapid loss of variety, which had a noticeable detrimental influence on the effectiveness of the findings it produced.
2. Unlike most standard ACO algorithms, ACO_R does not really permit heuristic information when training neural networks.

4.3.3 Features of ACO_R

ACO is developed by the ant's browsing behavior which was first used to address discrete optimization problems. The continuous domains were added to the ant colony optimization proposed by Socha and Dorigo [81], called ACO_R. ACO_R is the first method for continuous domains that may be categorized as an ACO algorithm [82]. The ACO_R method is intended to produce a series of probability density functions (PDFs). PDFs supplant the discrete probability distributions utilized in the solution formulation by ACO algorithms for combinatorial optimization in ACO_R.

4.3.4 Methodology ACO_R

ACO is developed by the ant's browsing behavior which was first used to address discrete optimization problems. ACO_R is the first method for continuous domains that may be categorized as an ACO algorithm. The intention of the ACO_R was to produce a series of probability density functions (PDFs). PDFs supplant the discrete probability distributions utilized in the solution formulation by ACO algorithms for combinatorial optimization in ACO_R. For the development of these PDFs over the search space, ACO_R implements a solution archive [82]. ACO_R also develops heterogeneous PDFs using sums of weighted Gaussian functions. To model the multi-promising area of search space, a Gaussian kernel pdf has been proposed. In conventional ACO, however, once the pheromone information has been updated, the actual solutions identified by the ants are discarded. ACO_R, on the other hand, keeps track of a limited number of candidate solutions and keeps the pheromone data structure as a solution archive. The ACO_R algorithm's training procedure can be broken into two parts: solution construction and pheromone production updating. The phase of solution construction is the most important. Each ant in ACO_R generates a proposed solution. Ant is influenced by one when generating its solution in the archive table of solutions. A solution archive named T is used to maintain track of several solutions in ACO_R. The number of kernels that adhere to the Gaussian kernel equals the cardinality of archive T, which is k. As a result, the solutions in T are used to construct probability density functions for Gaussian kernels dynamically. More specifically, the three parameters ω, μ_q, σ_q and must be determined in order to obtain the Gaussian kernel G^{pq} . As a result, the values of the pq^{th} variable of the k solutions in T become elements of vector μ_q for each G_j . Each component of the deviation vector σ_q is considered as follows:

$$\sigma_q = \xi \sum_{e=1}^k \frac{|x_{ep} - x_q|}{k-1} \quad (4.4)$$

This means that the average distance between the chosen solutions x_q and other solutions in the archive is calculated and multiplied by the parameter ξ at each step pq [84]. The parameter $\xi > 0$ behaves similarly to ACO's pheromone evaporation coefficient. The algorithm will be less biased towards locations that have already been explored and kept in the archive if the appropriate selection of ξ is made. The lower the value of ξ , the faster the algorithm will converge.

4.3.5 Mathematical Model of ACO_R

To develop these PDFs over the search space, ACO_R implements a solution archive. ACO_R also develops heterogeneous PDFs using sums of weighted Gaussian functions. $g_q(x)$ as $G^{pq}(x)$.

$$G^{pq}(x) = \sum_{p=1}^k \omega_p g_q(x) = \sum_{p=1}^k w_p \frac{1}{\sigma_q \sqrt{2\pi}} e^{-\frac{(x-\mu_q)^2}{2(\sigma_q)^2}} \quad (4.5)$$

Where k is the number of single pdfs contained in the Gaussian kernel pdf at the pq^{th} building step

μ_q and σ_q are vectors of size k that define the heaviness, and standard deviations associated with the individual Gaussian functions at the building phase.

4.3.6 Flowchart of ACO_R

The sequential flow of the operations and the algorithm's execution is described in the parts following,

Step 1. Initiate population to initialize the algorithm

Step 2. Calculate the new solution and probability

Step 3. Execute the algorithm for the number specified number of iterations.

Step 4. Calculate heaviness and standard deviations

Step 5. Generate the new solution with respect to calculated heaviness and standard deviations

Step 6. Discard the unfit solution from the population

Step 7. Algorithm will give the optimal solution if convergence occur, if doesn't occur repeat the step from 3

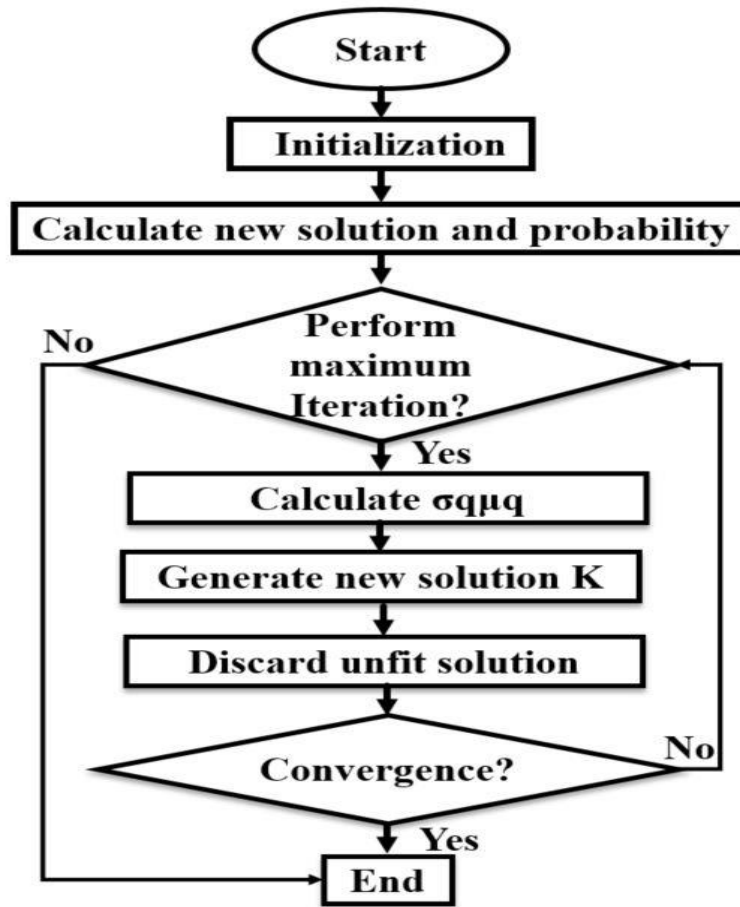


Fig. 4.3. Flowchart of ACO_R

CHAPTER 5

IMPLEMENTATION OF SWARM INTELLIGENCE ALGORITHM BASED PID CONTROLLER

By ushering DC-DC converters through the continuous growth of power regulators from linear to switching stage [85-88], Power Electronics has created a new sort of industrial revolution in the conversion and control of electric power. LED drivers, laptops and computers, electric cars, hydropower plants, solar systems, and many more applications benefit greatly from DC-DC converters [89-92]. However, due to the action of the switches, these converters have nonlinear temperaments, manifesting bigger ripples in output voltage and peak overshoot [93-95]. As a result, several control strategies focused on modulating the output voltage are used in DC-DC converters to achieve improved performance [96]. PID control is the most well-known and widely used of the numerous control approaches for power converters. The usual method, on the other hand, makes determining the precise value of the PID parameters very complex and time-consuming. As a result, SIA is linked to the PID controller in order to obtain optimal values for the PID parameters, which are then used in the closed-loop evaluation of the DC-DC converter's stability.

5.1 PID Controller

Feedback control is a control mechanism that keeps the output value in check by sending the error back to the controller and guiding the input toward a more accurate system. Positive and negative feedback control systems are the two most common forms of feedback control systems. The size of the input is raised in positive feedback by adding the output to the input. In the case of negative feedback, the size of the input is reduced by subtracting the output from the input. As a result, positive feedback enhances the amplifier's gain whereas negative feedback decreases it [97]. Many process controls, such as PI, PD, and PID controllers, are based on this feedback mechanism for safe and productive facilities. In recent years, the notion of PID has become widely applied in industrial process feedback control. The field of automatic steering systems saw the first theoretical analysis and practical application [98]. It was later employed in the manufacturing industry for automatic process control, where it was widely applied in pneumatic and then electronic controllers [99]. The PID principle is now widely employed in applications that require precise and optimal automatic control [100-102].

5.1.1 Outline of PID Controller

The Proportional, Integral, and Derivative components of a PID controller, a control loop feedback mechanism, are made up of three sections. As a result, it's also known as a three-term controller, with terms modified using exploratory approaches such as analytical methods and various optimization techniques including PSO, FA, and ACO_R. Fig. 5.1 depicts the structure of a MATLAB-based PID controller.

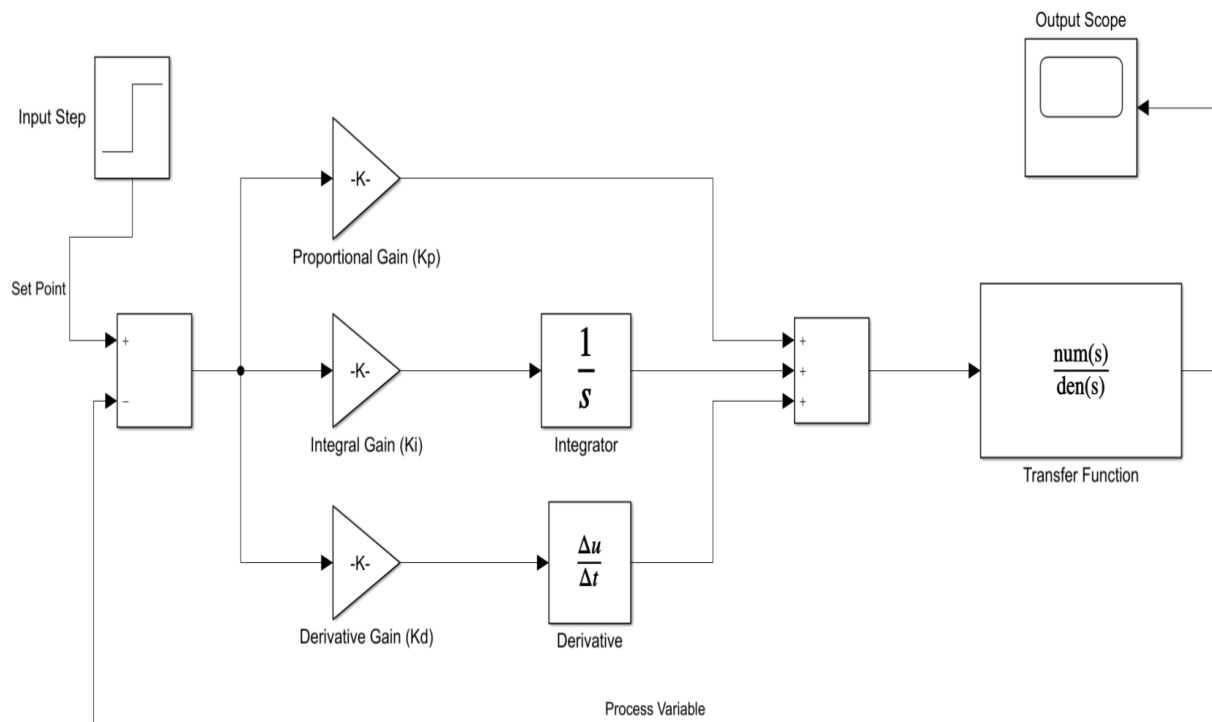


Fig. 5.1. Simulink Model of PID Controller

$e(t) = SP - PV$ defines error value as the difference between a preferred set point (SP) and a computed process variable (PV), as shown in Fig. 5.1. A PID controller uses proportional, integral, and derivative portions to offer a correction based on this error value.

The equation of controller output according to the PID algorithm can be stated as [103],

$$u(t) = K_p e(t) + K_i \int e(t) dt + K_D \frac{d}{dt} e(t) \quad (5.1)$$

Thus, the transfer function of the PID controller is denoted as,

$$\frac{U(s)}{E(s)} = K_p + \frac{K_i}{s} + K_D s \quad (5.2)$$

Here, $u(t)$ represents controller output. Error, $e(t) = r(t) - y(t)$ where $r(t)$ indicates reference variable and $y(t)$ indicates computed process variable. The tuning parameter of controllers are K_P (proportional gain), K_I (integral gain), and K_D (derivative gain).

5.1.2 Tuning of PID Controller

Tuning a PID controller entails adjusting the gain values of proportional, integral, and derivative terms in order to improve the system's response by removing steady-state error, decreasing overshoot, and achieving a short rise and settling time. As a result, the effect of the tuning settings is as follows:

✓ *Proportional term (P):*

P is based on the current error, whereas K_P has an impact on both the rising time and the steady-state error. It can lower both the rising time and the steady-state error, however complete eradication is not attainable. P's mathematical expression is as follows:

$$P = K_P e(t) \quad (5.3)$$

✓ *Integral term (I):*

I rely on the accumulation of previous errors. In return for making the transient reaction slower, K_I can be tuned to eliminate the steady-state inaccuracy. I can be expressed mathematically as follows:

$$I = K_I \int e(t) dt \quad (5.4)$$

✓ *Derivative term (D):*

D is reliant on the forecasting of future errors. The tweaking of k_d can improve the system's stability by lowering overshoot and improving the transient responsiveness. D's mathematical expression is as follows:

$$D = K_D \frac{d}{dt} e(t) \quad (5.5)$$

5.2 Objective Function

The goal function is a real-valued function that is maximized or minimized to improve the response of a system. As a result, in this scenario, several integral performance functions such as IAE, ITAE, ISE, and ITSE are applied to increase system stability while minimizing steady-state error [104].

✓ *Integral Absolute Error (IAE):*

IAE is based on the integration of the absolute error over time in which no weight is added to errors in a system's response. The mathematical expression of IAE is given by,

$$IAE = \int_0^{\tau} |e(t)| dt \quad (5.6)$$

✓ *Integral Squared Error (ISE):*

ISE is based on the integration of the square of the error over time where large errors are prioritized for elimination. The mathematical expression of ISE is given by,

$$ISE = \int_0^{\tau} e(t)^2 dt \quad (5.7)$$

✓ *Integral Time Squared Error (ITSE):*

ITSE is based on the integration of the square of the error that is multiplied by the time over time. The mathematical expression of ITSE is given by,

$$ITSE = \int_0^{\tau} t \cdot e(t)^2 dt \quad (5.8)$$

✓ *Integral Time Absolute Error (ITAE):*

ITAE is based on the integration of the absolute error that is multiplied by the time over time where errors are weighted. The mathematical expression of ITAE is given by,

$$ITAE = \int_0^{\tau} t \cdot |e(t)| dt \quad (5.9)$$

5.3 Layout of SIA-PID Controller

To conduct closed-loop stability study on DC-DC converters, a PID controller is tuned by optimizing values of K_P , K_I , and K_D utilizing the Swarm Intelligence Algorithms (FA, PSO, and ACO_R) mechanism [105-106]. Figure 4.2 shows the general design of this approach. The error is continuously regulated, resulting in a compatible output. For this, SIA uses four error formulas (IAE, ISE, ITAE, and ITSE) to analyze the objective function's performance across a number of repetitions. As a result, the optimal solution obtained through this procedure produces satisfactory outcomes.

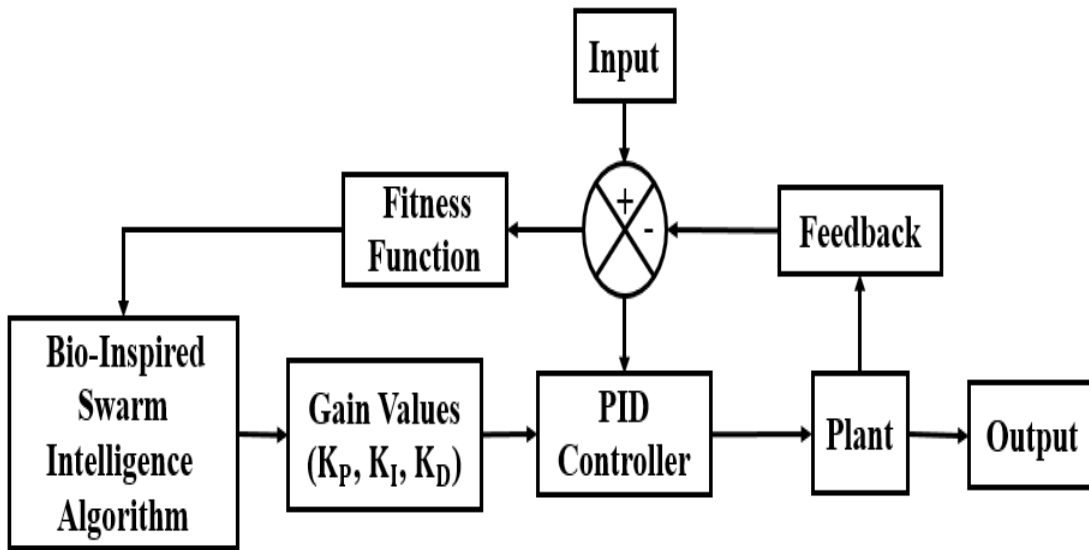


Fig. 5.2. Layout of Optimized PID Controller

CHAPTER 6

RESULTS AND SIMULATION

In this research, the circuit was constructed in Simulink to evaluate the SEPIC converter's performance and its modifications for three distinct optimization algorithms. All simulations and tunings were performed in MATLAB. The response of an open-loop and a conventional closed-loop system is first tested, and the performance characteristics are reported in both tabulated and illustrative form. Next, the system's responses for FA, PSO, and ACO_R-based PID controllers are simulated for different fitness functions in the algorithms to achieve improved performance. After that, the controller values (K_P , K_I , and K_D) and performance parameters are tabulated. As a result, a comparative analysis of algorithms is conducted, and an optimal controller is investigated, ensuring the SEPIC converter and its variants' stability. Later, the transfer function and pole-zero mapping for various optimization techniques' fitness functions are listed and depicted.

6.1 Performance Parameters

The characteristics of step responses for open-loop and closed-loop systems, such as percentage of overshoot, rise time, settling time, and peak amplitude, are considered the system's performance parameters. In addition, it helps in stability analysis of the SEPIC converter and its variants.

✓ **Percentage of overshoot (%OS):**

The occurrence of a signal exceeding its desired output is called the overshoot. The %OS represents the overshoot of the steady-state value at the peak time in percentage. The equation for %OS is given as,

$$\%OS = e^{\frac{\pi\zeta}{\sqrt{1-\zeta^2}}} \times 100 \quad (6.1)$$

Here, ζ represents the damping ratio that prevents oscillation.

✓ **Rise time (T_r):**

The time required for the response to rise from 10% to 90% (0.1 to 0.9) of the steady-state response. The equation for T_r is given as,

$$T_r = \frac{\pi - \phi}{\omega_n \sqrt{1 - \zeta^2}} \times 100 \quad (6.2)$$

✓ **Settling time (T_s):**

The time required for holding the $\pm 2\%$ of the steady-state value. The equation for T_s is given as,

$$T_s = \frac{4}{\zeta\omega_n} \quad (6.3)$$

✓ **Peak Amplitude:**

The peak output value of the response is called as peak amplitude.

6.2 Unidirectional SEPIC Converter

6.2.1. Open-Loop Response

Using Simulink, the circuit for unidirectional SEPIC has been designed, which is depicted in Fig. 6.1. With the help of the system identification toolbox, the transfer function for the open-loop system has been obtained through exploring the input and output data from Simulink, with four poles and three zeros. Table 6.1 presents the parameters of the unidirectional SEPIC converter that have been used in the simulation.

TABLE 6.1. PARAMETERS OF UNIDIRECTIONAL SEPIC CONVERTER

Variable Name	Symbol	Value
Input Voltage	V_{in}	20 V
Output Voltage	V_o	20 V
Duty Cycle	D	50%
Switching Frequency	f_s	100 kHz
Inductor	L_1, L_2	100 μ H
Capacitor	C_1, C_2	0.8 mF, 3mF
Load Resistance	R	1 Ω

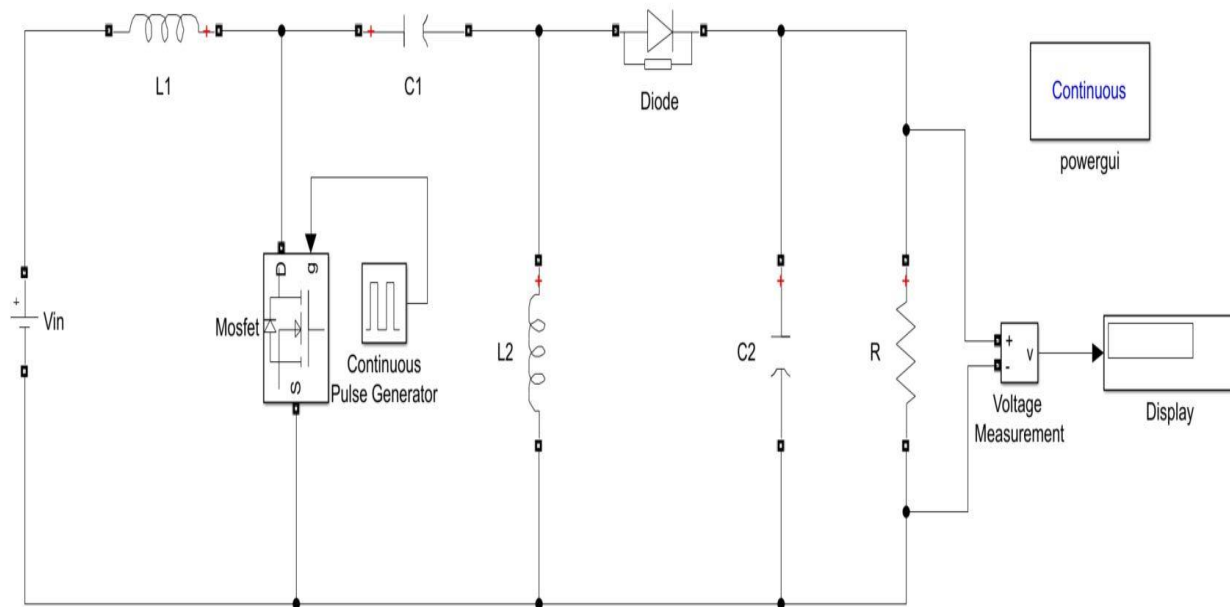


Fig. 6.1. Model of Open-Loop Unidirectional SEPIC by Simulink

The transfer function of the open-loop unidirectional SEPIC converter is as follows:

$$\frac{0.001369s^3 + 1.182 \times 10^{-5}s^2 + 3.972 \times 10^{-8}s + 3.018 \times 10^{-11}}{s^4 + 0.007753s^3 + 2.201 \times 10^{-5}s^2 + 4.588 \times 10^{-8}s + 3.14 \times 10^{-11}}$$

The step response for open-loop system of the unidirectional SEPIC converter is depicted in Fig. 6.2.

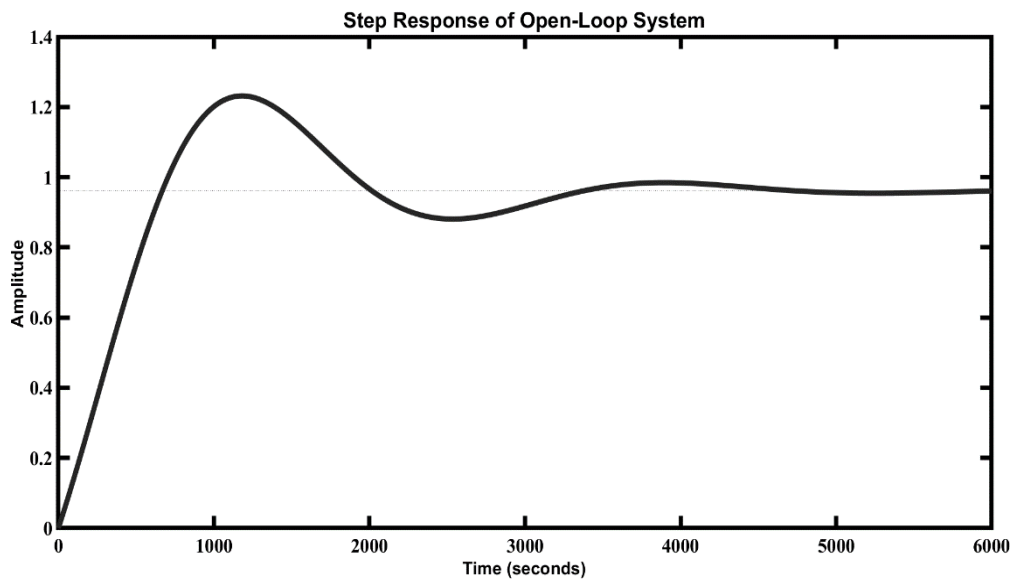


Fig. 6.2. Step Response of Open-Loop System of Unidirectional SEPIC

From the step response shown in Fig. 6.2, it is observed that percentage of overshoot is 28.1341%, rise time is 517.5047 seconds, settling time is 4115.0 seconds, and peak amplitude is 1.2316. So it can be said that overshoot is very high for this open-loop response which must be reduced for having safe application of the converters.

6.2.2. Closed-Loop Response with PID Controller

To improve the system’s performance, closed-loop techniques are used. In our research, we used PID controller for the closed-loop system. The circuit for closed-loop unidirectional SEPIC with conventional PID controller has been designed in Simulink, depicted in Fig. 6.3. Then, the controller was manually tuned using the MATLAB PID Tuner App, and gain values ($K_P=2991.7895$, $K_I=1904.3107$, $K_D=59.9963$) were achieved for the typical PID controller. After then, a step response, as shown in Fig. 6.4, is examined for its many properties in order to assess the system's stability.

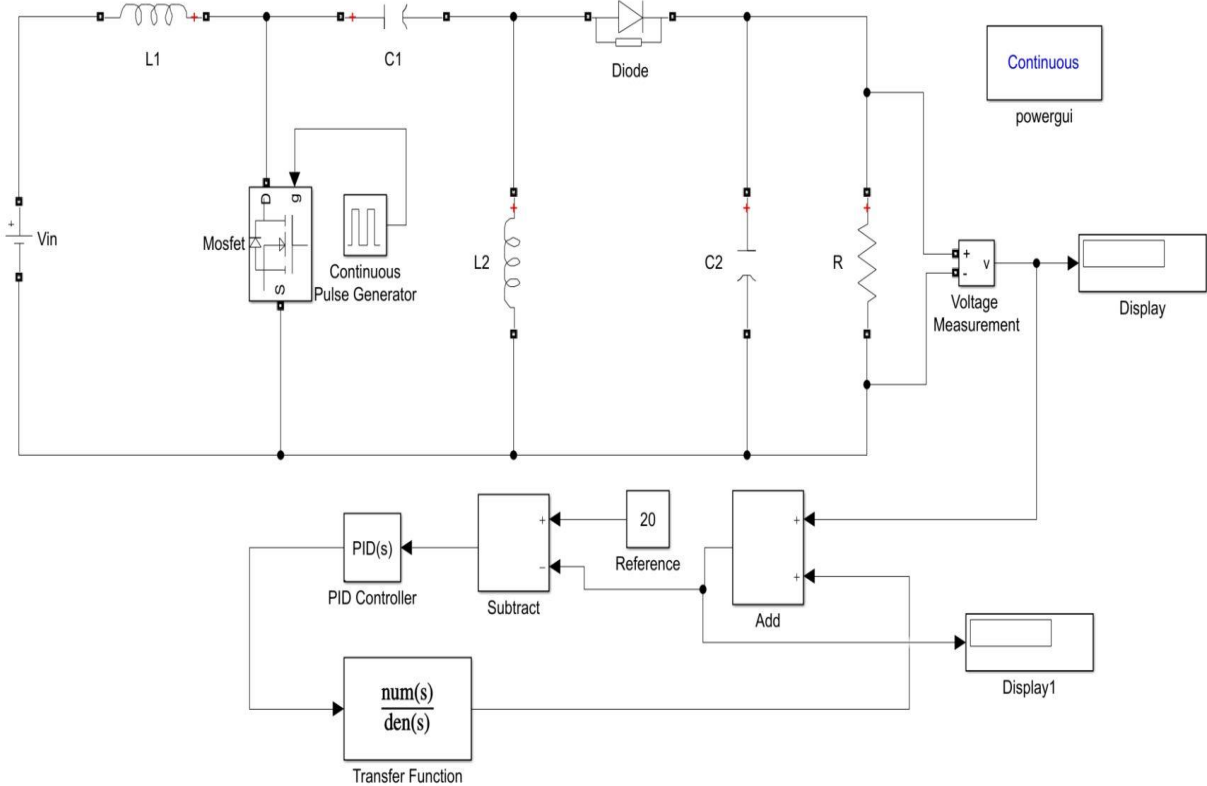


Fig. 6.3. Step Response of Closed-Loop System with PID Controller of Unidirectional SEPIC

The transfer function of the closed-loop unidirectional SEPIC converter is as follows:

$$\frac{0.08213s^5+4.096s^4+2.642s^3+0.02263s^2+7.573\times 10^{-5}s+5.747\times 10^{-8}}{1.082s^5+4.104s^4+2.642s^3+0.02263s^2+7.573\times 10^{-5}s+5.747\times 10^{-8}}$$

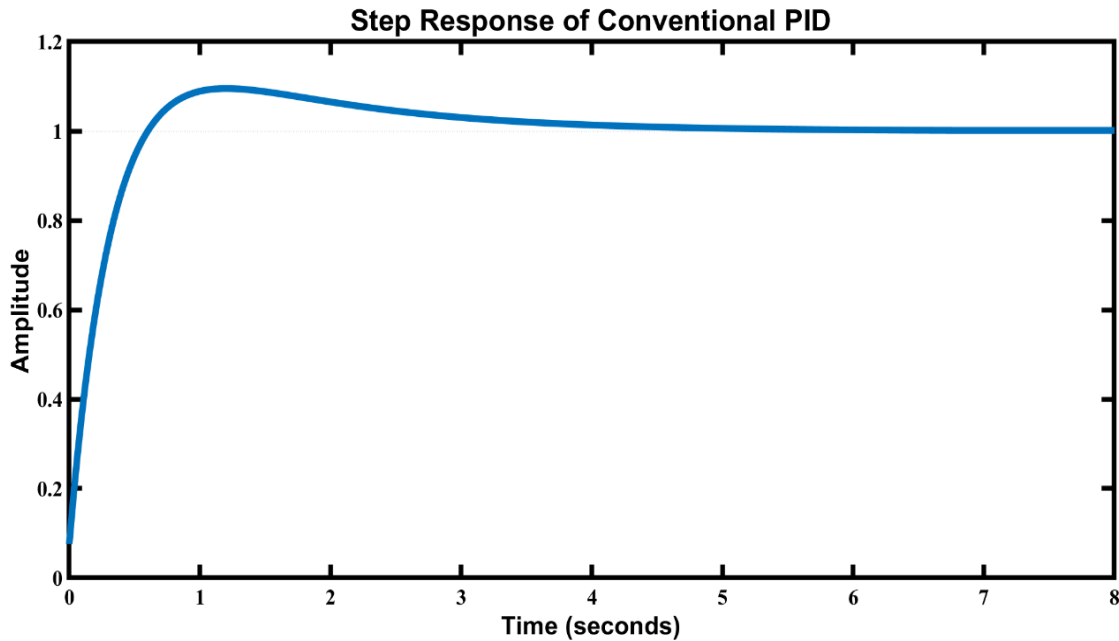


Fig. 6.4. Step Response of Closed-Loop System with Conventional PID of Unidirectional SEPIC

The step response shown in Fig. 6.4, shows that the percentage of overshoot is 9.52%, rise time is 0.423 seconds, settling time is 3.62 seconds, and peak amplitude is 1.0952. These values are less than the open-loop system but not so good as expected. Therefore, the performance parameters; Percentage of Overshoot (%OS), Rise Time (T_r), Settling Time (T_s), and Peak Amplitude are tabulated for both open-loop and closed-loop analysis, which is presented in Table 6.2.

TABLE 6.2. PERFORMANCE ANALYSIS OF OPEN-LOOP AND CLOSED-LOOP RESPONSE [UNIDIRECTIONAL SEPIC]

Performance Parameters	Open-Loop Response	Closed-Loop Response
%OS	28.1341	9.52
T_r (sec)	517.5047	0.423
T_s (sec)	4115.0	3.62
Peak Amplitude	1.2316	1.0952

6.2.3. Swarm Intelligence Algorithms based PID Controller

Though the closed-loop system with conventional PID controller provides better performance than the open-loop system, it is not good enough. So, bio-inspired swarm intelligence optimization algorithms are employed in the controller to reduce overshoot, get faster rise time and settling time. Moreover, step responses are observed, and gain values along with performance parameters are tabulated for FA-PID, PSO-PID, and ACO_R-PID.

6.2.3.1. FA-PID Controller

The firefly algorithm is first applied to have the optimized gain values for the controller. Using the trial and error method, algorithm parameters have been found that are stated in Table 6.3.

TABLE 6.3. PARAMETERS OF FIREFLY ALGORITHM

Mutation Coefficient	α	0.15
Attraction Coefficient	β	0.2
Light Absorption Coefficient	γ	3
Mutation Coefficient Damping Ratio	α_{damp}	0.98
Population Size	40	
No. of Iterations	15	

In comparison to the gain values of the conventional PID controller, improved values of the gain parameters for the four performance indices (IAE, ISE, ITSE, ITAE) of the FA-PID controller have been attained after several simulations in MATLAB, as shown in Table 6.4. The step responses of the FA-PID controller's IAE, ISE, ITSE, and ITAE for the unidirectional SEPIC converter are shown in Figs. 6.5, 6.6, 6.7, and 6.8.

TABLE 6.4. GAIN VALUES OF FA-PID CONTROLLER [UNIDIRECTIONAL SEPIC]

Gains	FA-PID			
	<i>IAE</i>	<i>ISE</i>	<i>ITSE</i>	<i>ITAE</i>
K _p	3276.1	3192.7	3498.7	3635.7
K _i	362.5098	474.6839	591.9918	1566.6
K _d	37.5453	42.7113	11.0828	72.2321

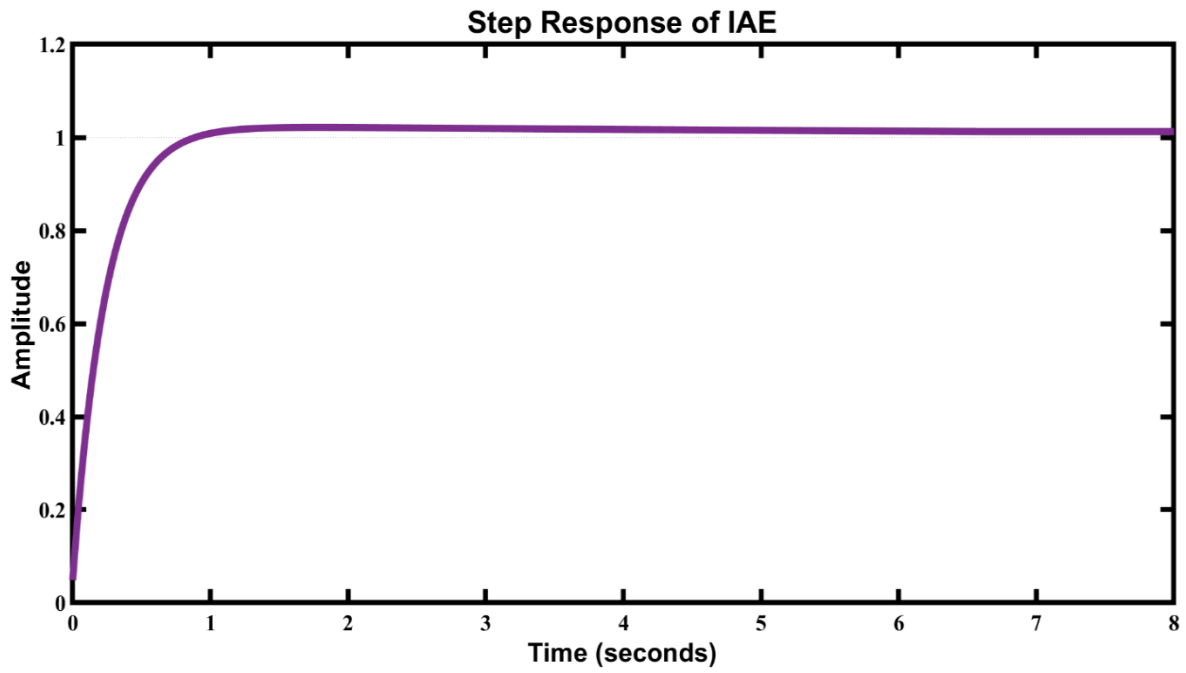


Fig. 6.5. Step Response of IAE for FA-PID (Unidirectional SEPIC Converter)

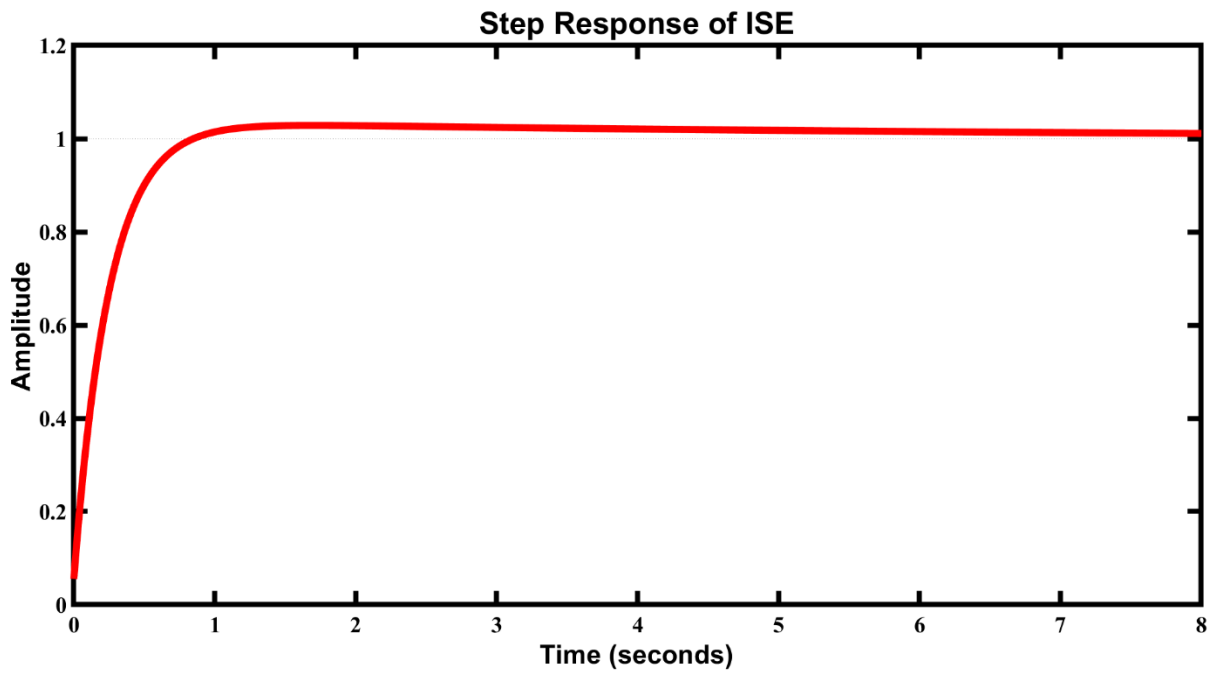


Fig. 6.6. Step Response of ISE for FA-PID (Unidirectional SEPIC Converter)

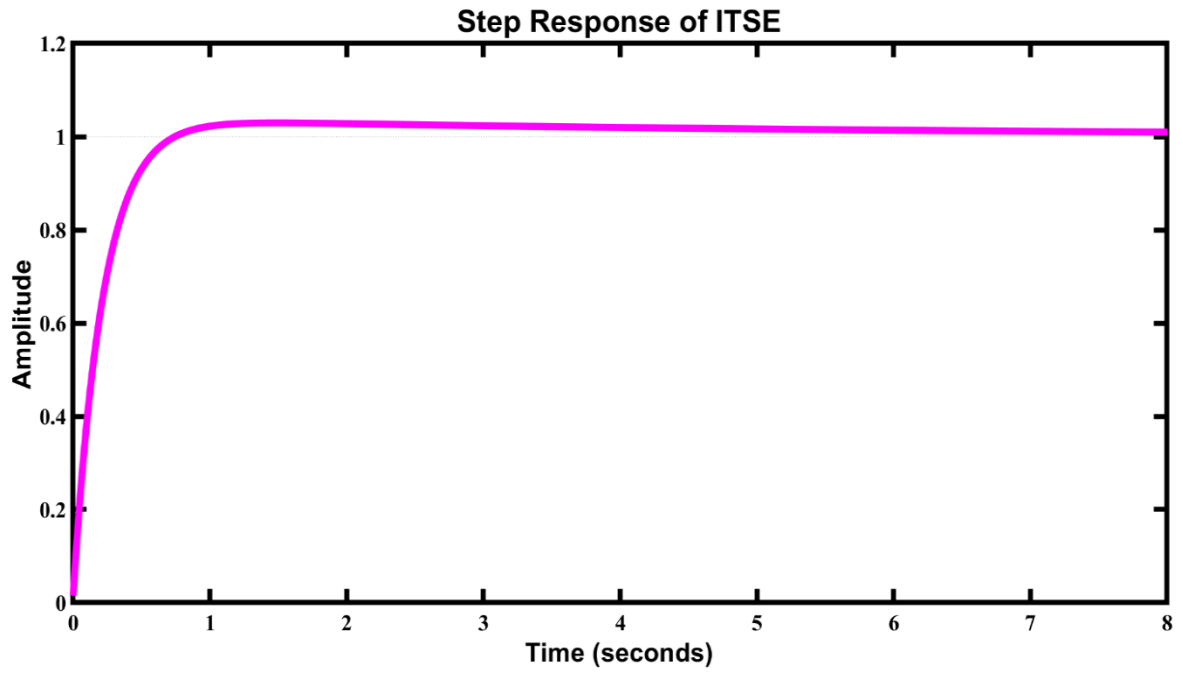


Fig. 6.7. Step Response of ITSE for FA-PID (Unidirectional SEPIC Converter)

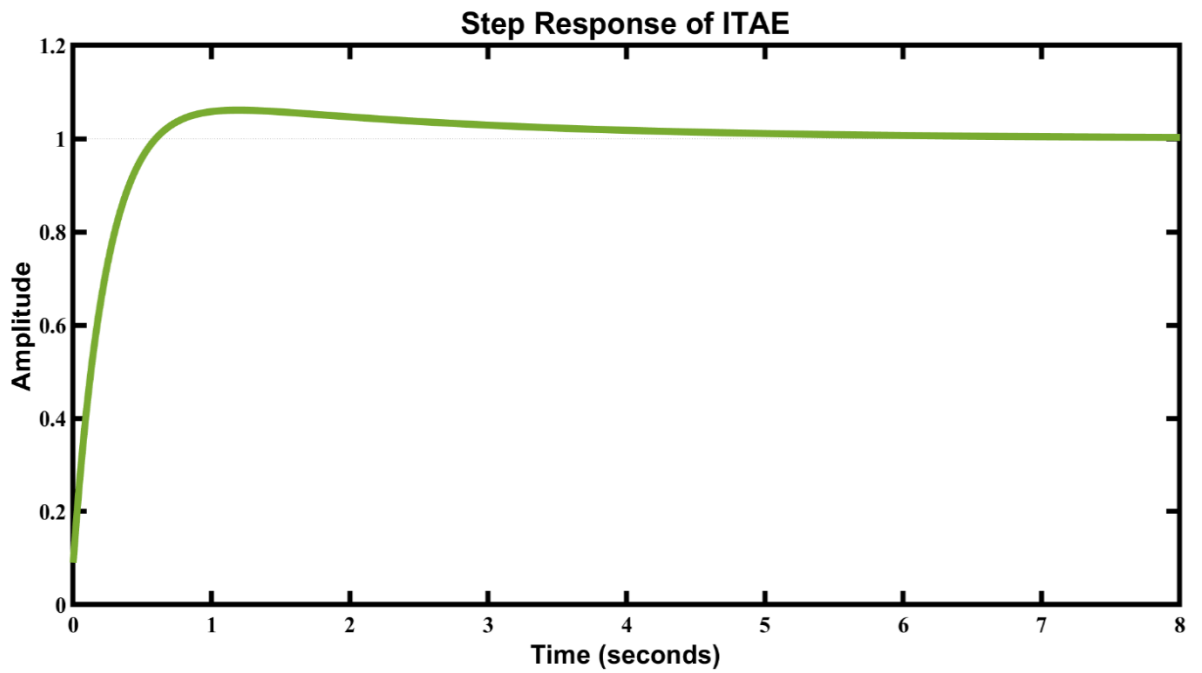


Fig. 6.8. Step Response of ITAE for FA-PID (Unidirectional SEPIC Converter)

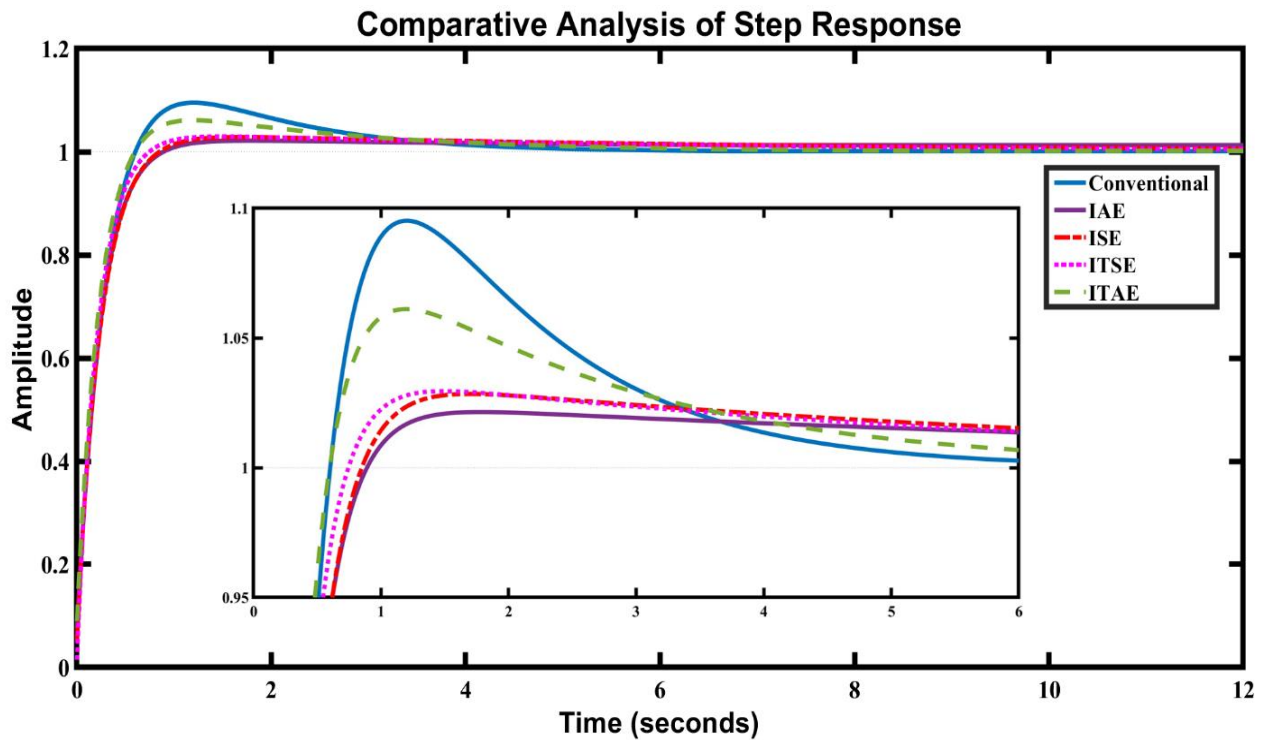


Fig. 6.9. Comparative Analysis of Step Responses for FA-PID (Unidirectional SEPIC Converter)

The performance parameters such as Percentage of Overshoot (%OS), Rise Time (Tr), Settling Time (Ts), and Peak Amplitude are tabulated for FA-PID, which is presented in Table 6.5.

TABLE 6.5. PERFORMANCE PARAMETERS OF CONVENTIONAL AND FA-PID CONTROLLER [UNIDIRECTIONAL SEPIC]

Performance Parameters	Conventional PID	FA-PID			
		<i>IAE</i>	<i>ISE</i>	<i>ITSE</i>	<i>ITAE</i>
%OS	9.52	2.14	2.84	2.95	6.11
Tr (sec)	0.423	0.48	0.484	0.423	0.393
Ts (sec)	3.62	3.08	4.6	4.01	3.97
Peak Amplitude	1.0952	1.0214	1.0284	1.0295	1.0611

By the observation from Fig. 6.9 and Table 6.5, it is visible that FA-PID of IAE performs better than conventional PID and other fitness functions in the percentage of overshoot, settling time, and peak amplitude. In addition, FA-PID of ITAE performs better in terms of rise time. Fig. 6.10 depicts the comparative chart of performance parameters for FA-PID.

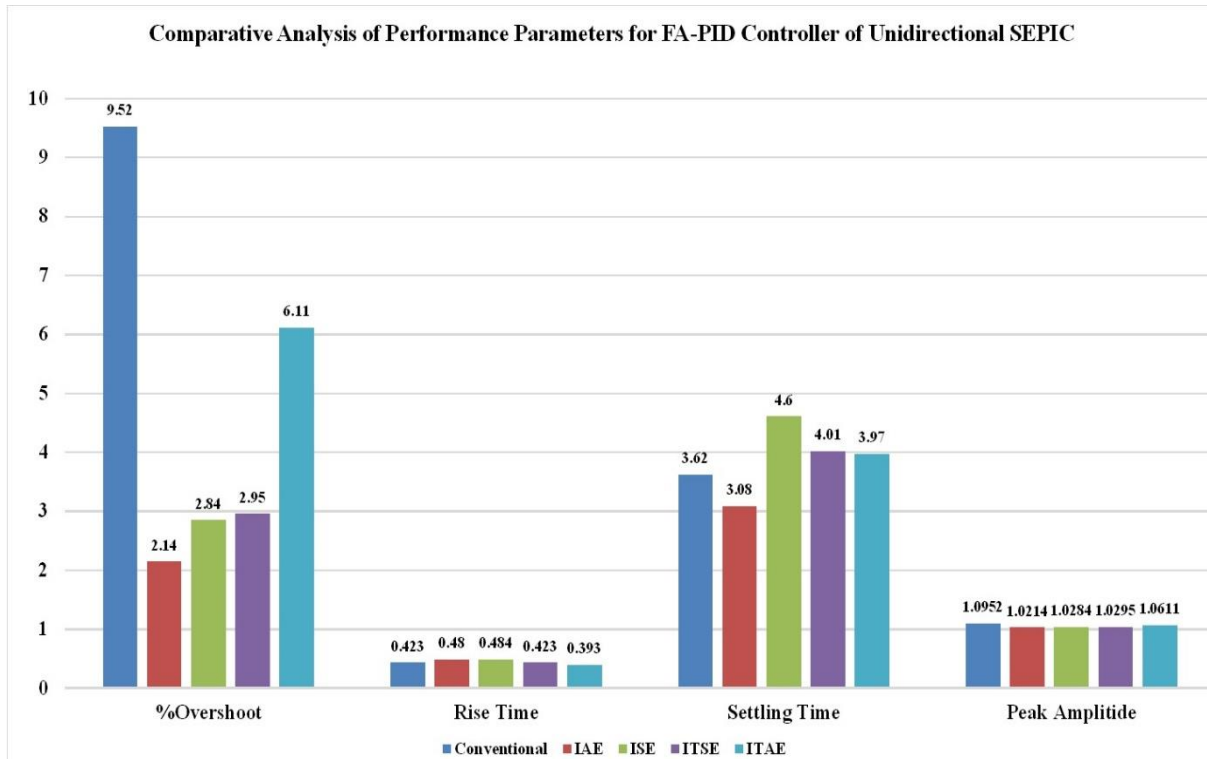


Fig. 6.10. Comparative Chart of Performance Parameters for FA-PID (Unidirectional SEPIC Converter)

6.2.3.2. PSO-PID Controller

The Particle Swarm Optimization (PSO) is applied to have the optimized gain values for the controller. Using the trial and error method, algorithm parameters have been found that are stated in Table 6.6.

TABLE 6.6. PARAMETERS OF PARTICLE SWARM OPTIMIZATION ALGORITHM

Inertia Coefficient	w	0.9
Damping Ratio of Inertia Coefficient	w_{damp}	0.1
Personal Acceleration Coefficient	C_1	0.8
Social Acceleration Coefficient	C_2	0.7
Population Size	40	
No. of Iterations	15	

In comparison to the gain values of the conventional PID controller, improved values of the gain parameters for the four performance indices (IAE, ISE, ITSE, ITAE) of the PSO-PID controller have been attained after several simulations in MATLAB, as shown in Table 6.7. The step

responses of the PSO-PID controller's IAE, ISE, ITSE, and ITAE are shown in Figures 6.11, 6.12, 6.13, and 6.14, respectively.

TABLE 6.7. GAIN VALUES OF PSO-PID CONTROLLER [UNIDIRECTIONAL SEPIC]

Gains	PSO-PID			
	<i>IAE</i>	<i>ISE</i>	<i>ITSE</i>	<i>ITAE</i>
K _p	3612.9	3546.8	3747.1	3656.5
K _i	425.3451	388.7232	480.1782	1468.3
K _d	30.6525	53.2183	69.9648	48.5017

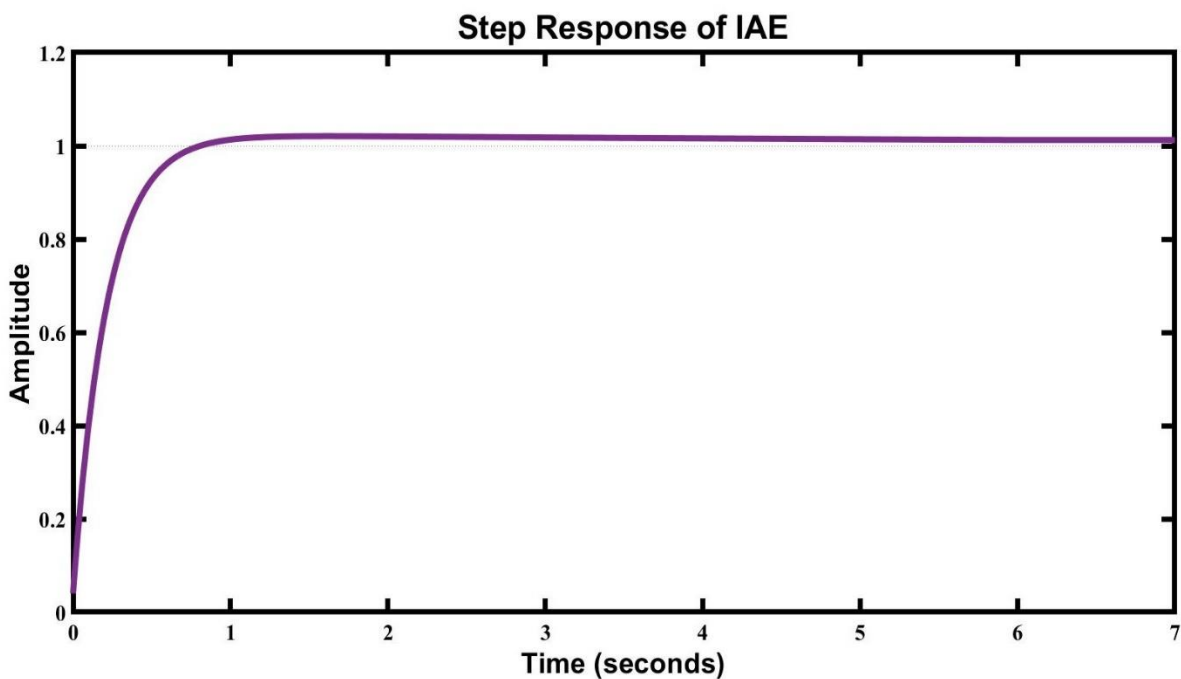


Fig. 6.11. Step Response of IAE for PSO-PID (Unidirectional SEPIC Converter)

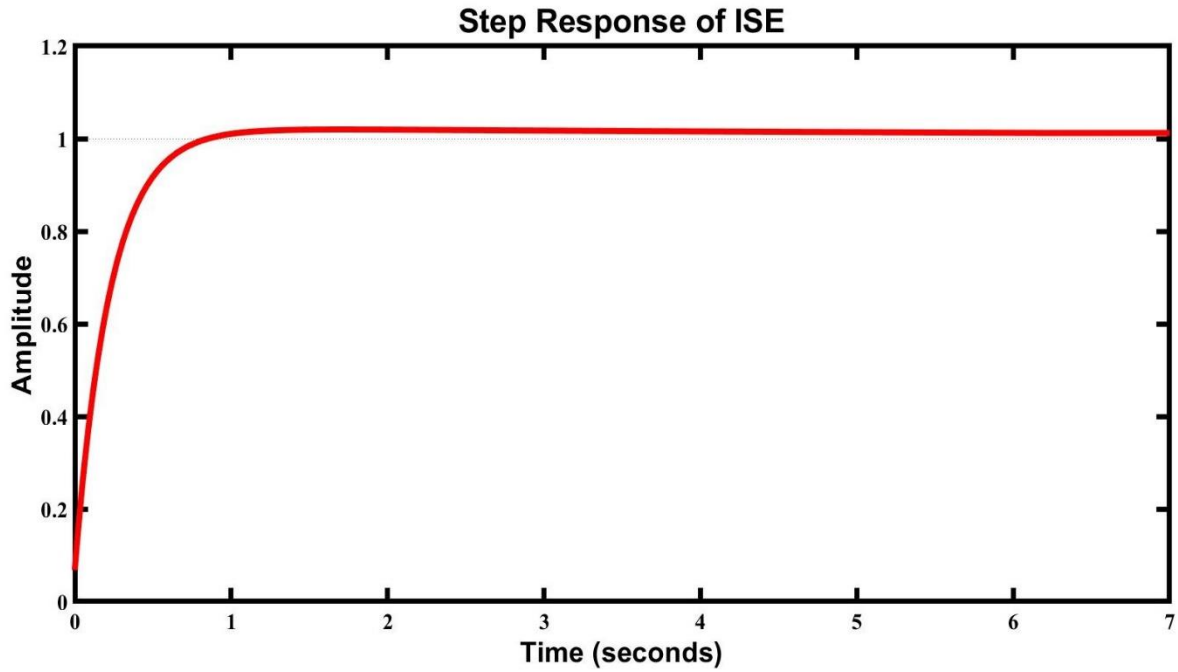


Fig. 6.12. Step Response of ISE for PSO-PID (Unidirectional SEPIC Converter)

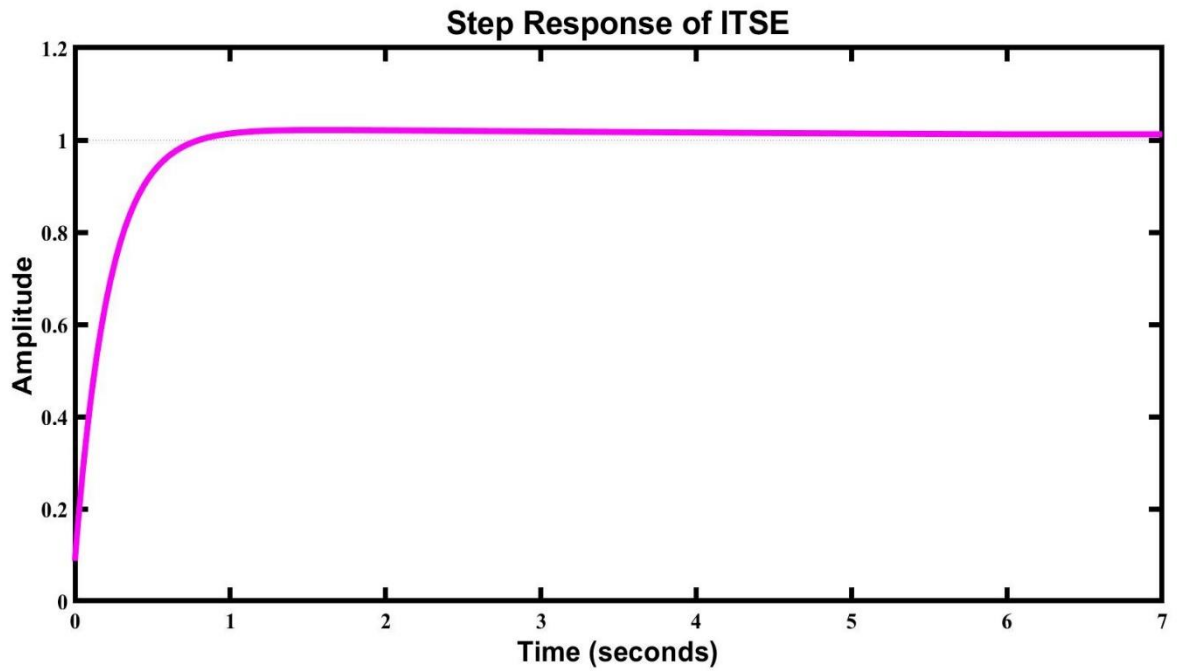


Fig. 6.13. Step Response of ITSE for PSO-PID (Unidirectional SEPIC Converter)

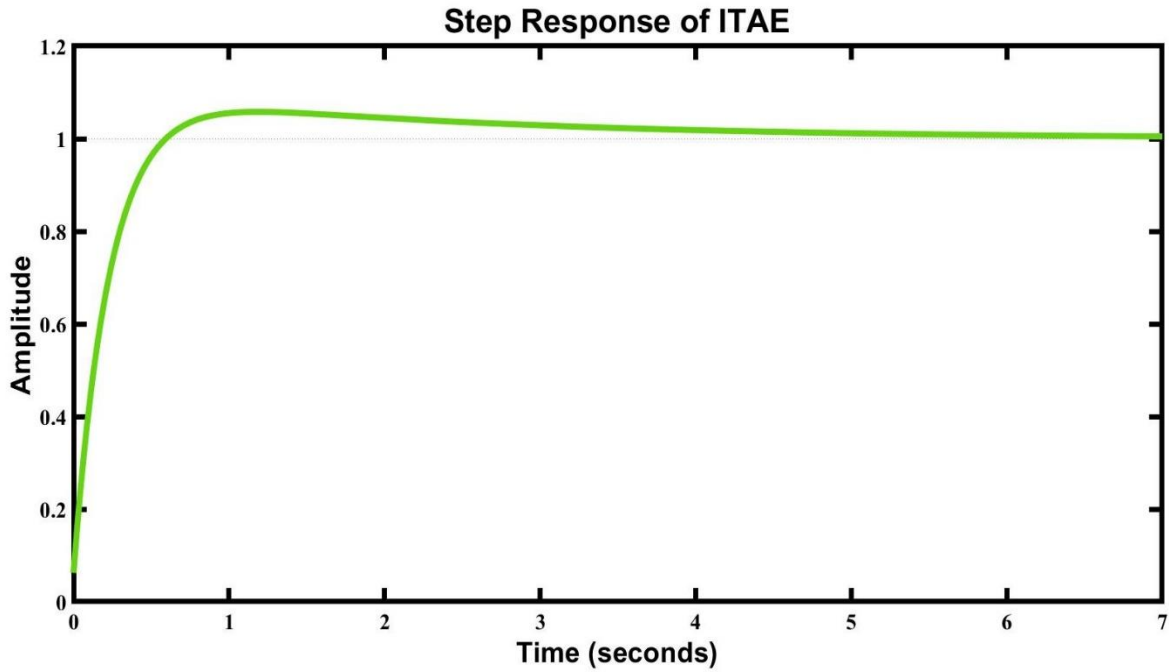


Fig. 6.14. Step Response of ITAE for PSO-PID (Unidirectional SEPIC Converter)

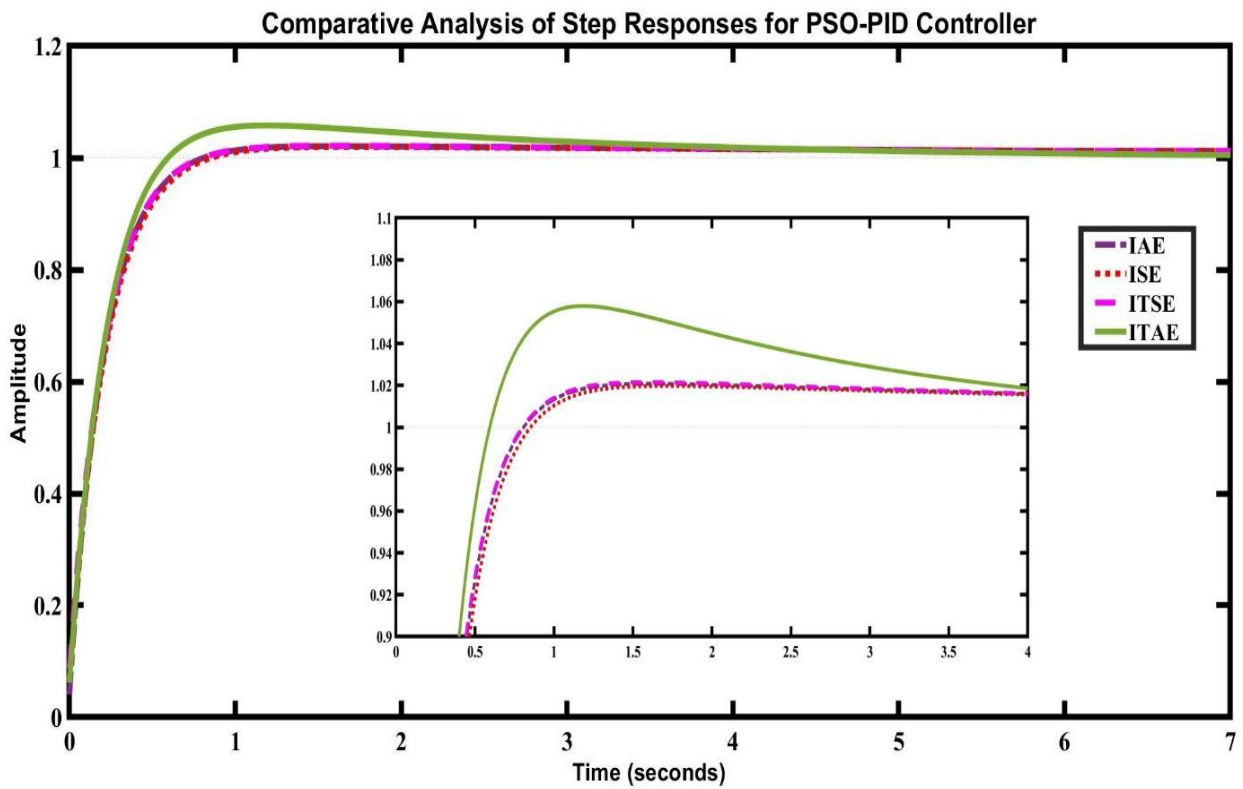


Fig. 6.15. Comparative Analysis of Step Responses for PSO-PID (Unidirectional SEPIC Converter)

The performance parameters such as Percentage of Overshoot (%OS), Rise Time (Tr), Settling Time (Ts), and Peak Amplitude are tabulated for PSO-PID, which is presented in Table 6.8.

TABLE 6.8. PERFORMANCE PARAMETERS OF CONVENTIONAL AND PSO-PID CONTROLLER [UNIDIRECTIONAL SEPIC]

Performance Parameters	Conventional PID	PSO-PID			
		<i>IAE</i>	<i>ISE</i>	<i>ITSE</i>	<i>ITAE</i>
%OS	9.52	2.0773	1.9757	2.1564	5.7925
Tr (sec)	0.423	0.4322	0.4540	0.4355	0.3855
Ts (sec)	3.62	2.4854	2.4418	3.0889	3.9780
Peak Amplitude	1.0952	1.0208	1.0198	1.0216	1.0579

By the observation from Fig. 6.15 and Table 6.8, it is visible that PSO-PID of ISE performs better than conventional PID and other fitness functions in percentage of overshoot, settling time, and peak amplitude. PSO-PID of ITAE performs better in terms of rise time. Fig. 6.16 depicts the comparative chart of performance parameters for PSO-PID.

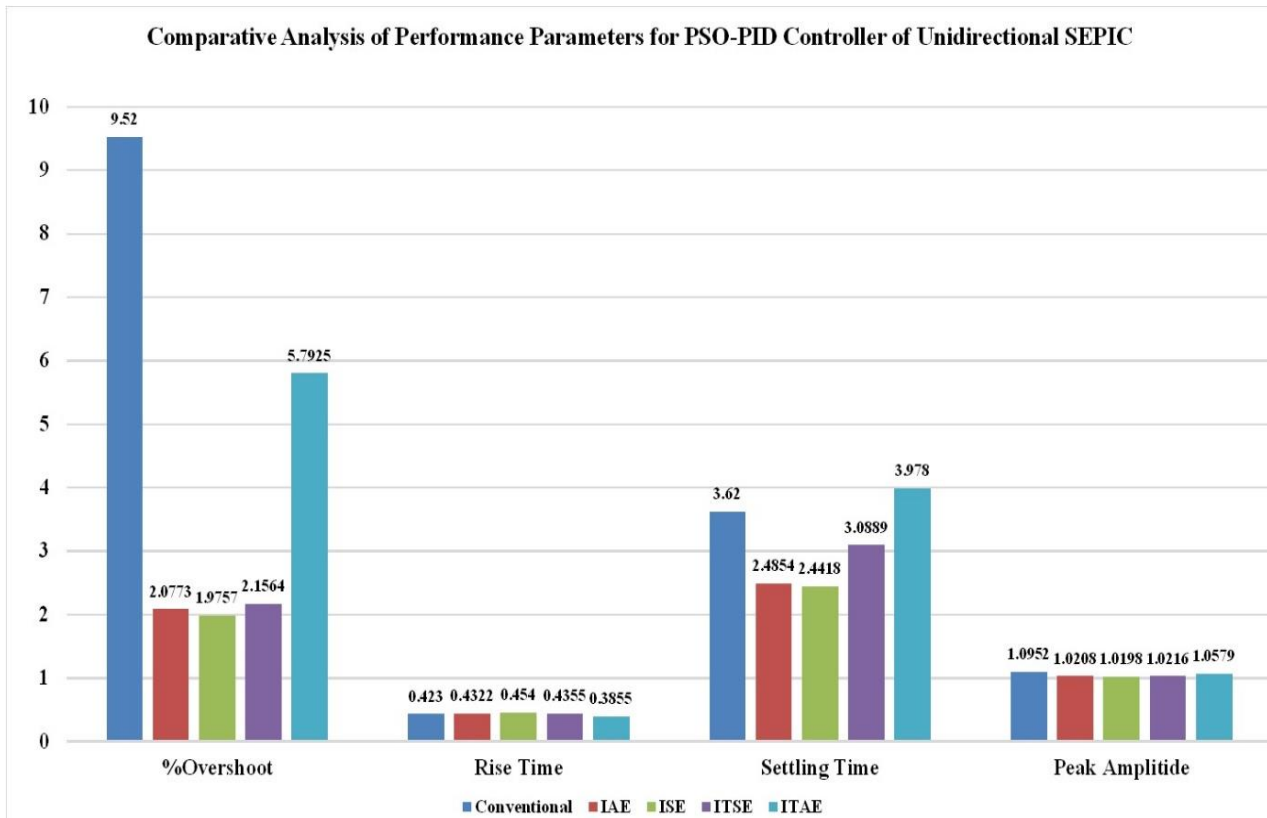


Fig. 6.16. Comparative Chart of Performance Parameters for PSO-PID (Unidirectional SEPIC Converter)

6.2.3.3. ACO_R-PID Controller

The Ant Colony Optimization for continuous domain (ACO_R) is applied to have the optimized gain values for the controller. Using the trial and error method, algorithm parameters have been found that are stated in Table 6.9.

TABLE 6.9. PARAMETERS OF ANT COLONY OPTIMIZATION ALGORITHM FOR CONTINUOUS DOMAIN

Sample Size	nSample	10
Intensification Factor (Selection Pressure)	q	0.01
Deviation-Distance Ratio	ζ	0.016
Archive Size	20	
No. of Iterations	20	

In comparison to the gain values of the conventional PID controller, improved values of the gain parameters for the four performance indices (IAE, ISE, ITSE, ITAE) of the ACO_R-PID controller have been attained after several simulations in MATLAB, as shown in Table 6.10. The step responses of the ACO_R-PID controller's IAE, ISE, ITSE, and ITAE are shown in Figures 6.17, 6.18, 6.19, and 6.20, respectively.

TABLE 6.10. GAIN VALUES OF ACO_R-PID CONTROLLER [UNIDIRECTIONAL SEPIC]

Gains	ACO _R -PID			
	<i>IAE</i>	<i>ISE</i>	<i>ITSE</i>	<i>ITAE</i>
Kp	3419.5	3329.8	3495.1	3491.5
Ki	493.6268	433.8923	354.2103	1903.3
Kd	98.1286	87.4715	81.5848	45.9601

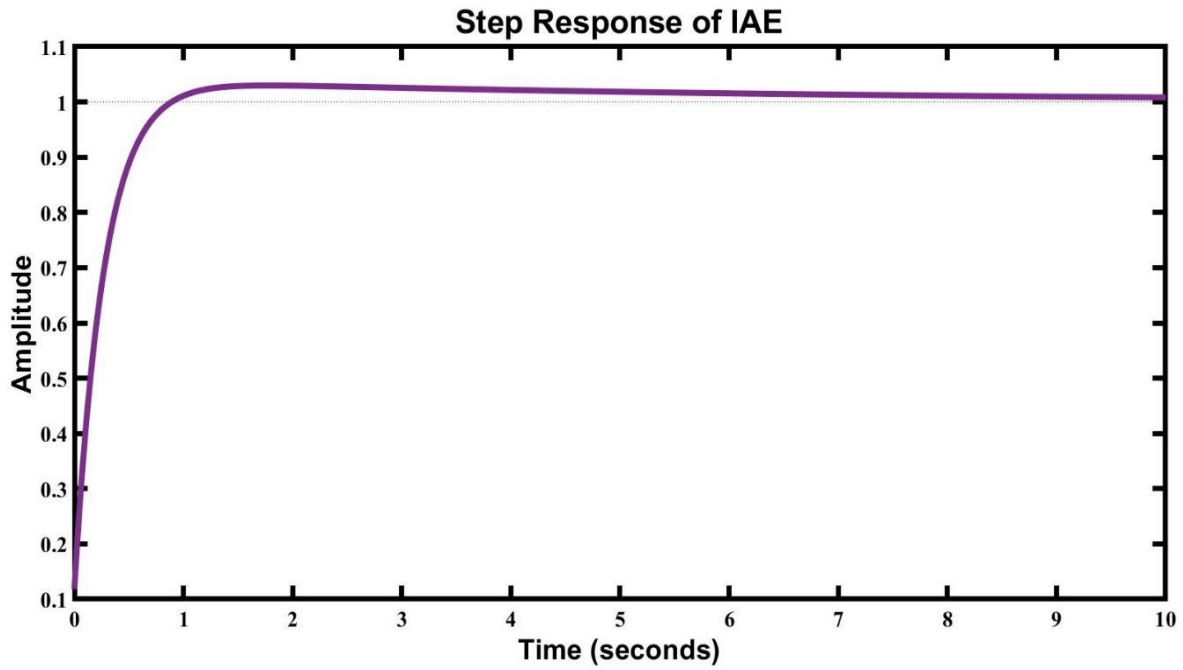


Fig. 6.17. Step Response of IAE for ACO_R -PID (Unidirectional SEPIC Converter)

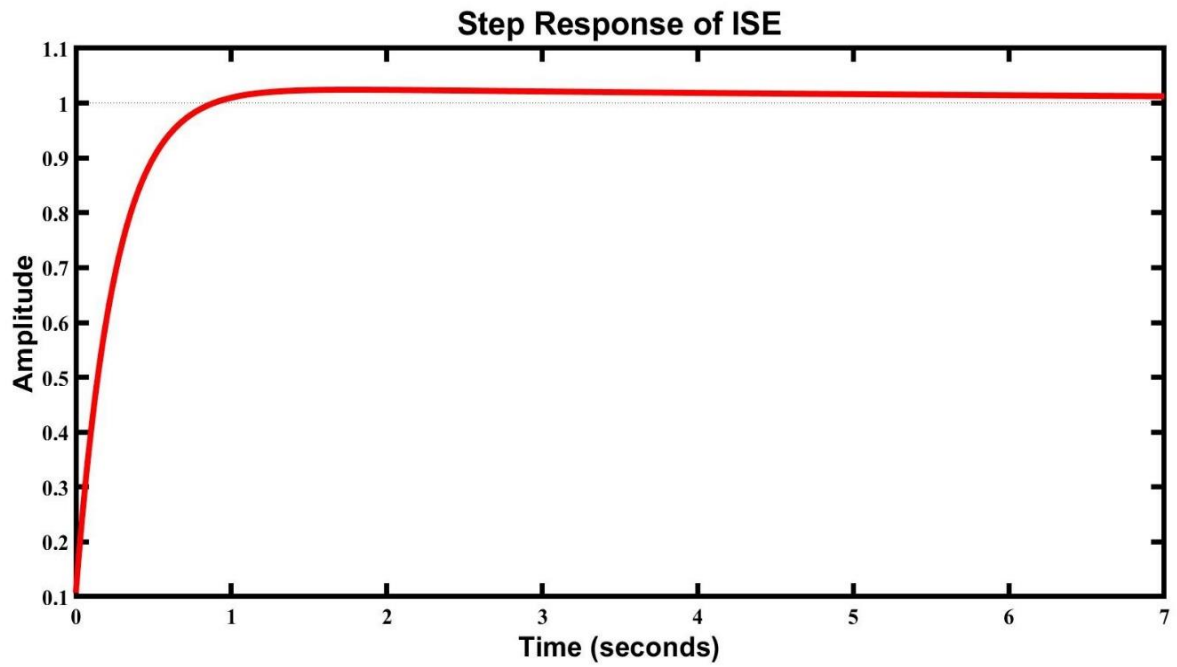


Fig. 6.18. Step Response of ISE for ACO_R -PID (Unidirectional SEPIC Converter)

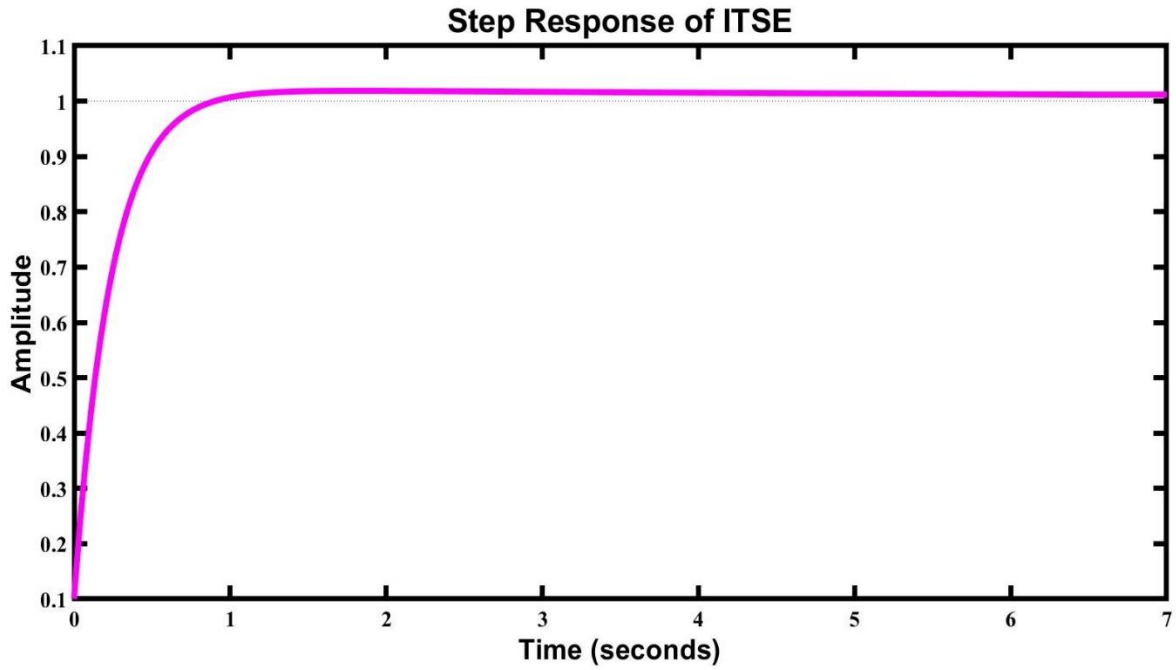


Fig. 6.19. Step Response of ITSE for ACO_R -PID (Unidirectional SEPIC Converter)

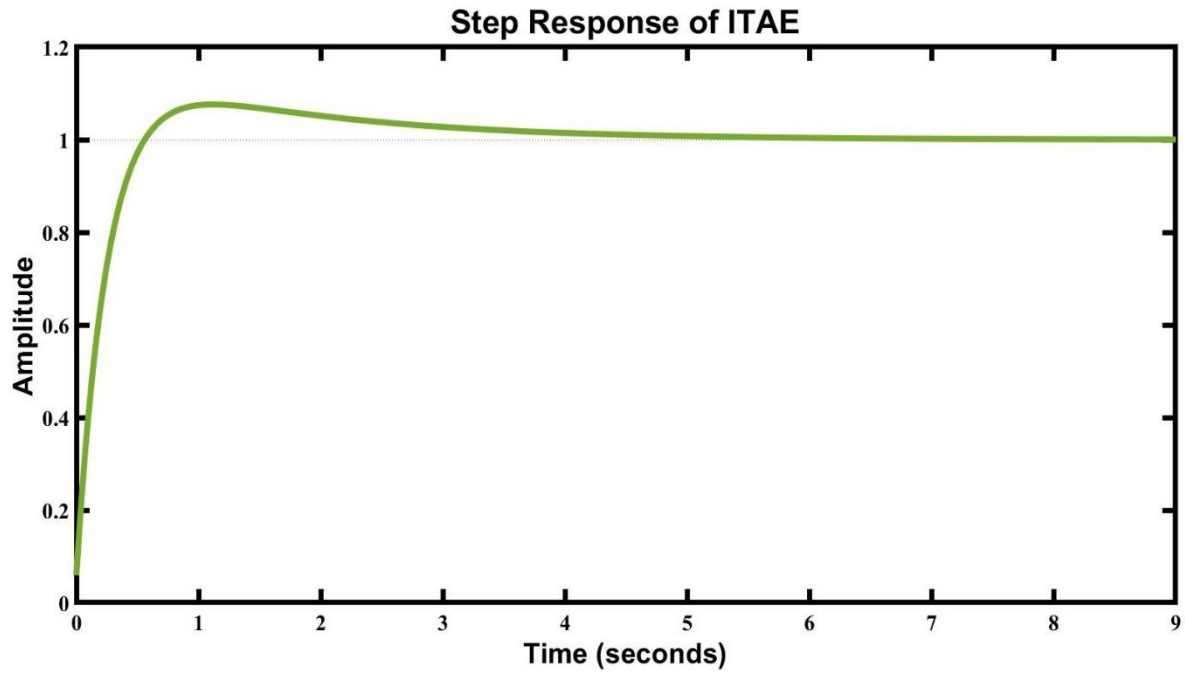


Fig. 6.20. Step Response of ITAE for ACO_R -PID (Unidirectional SEPIC Converter)

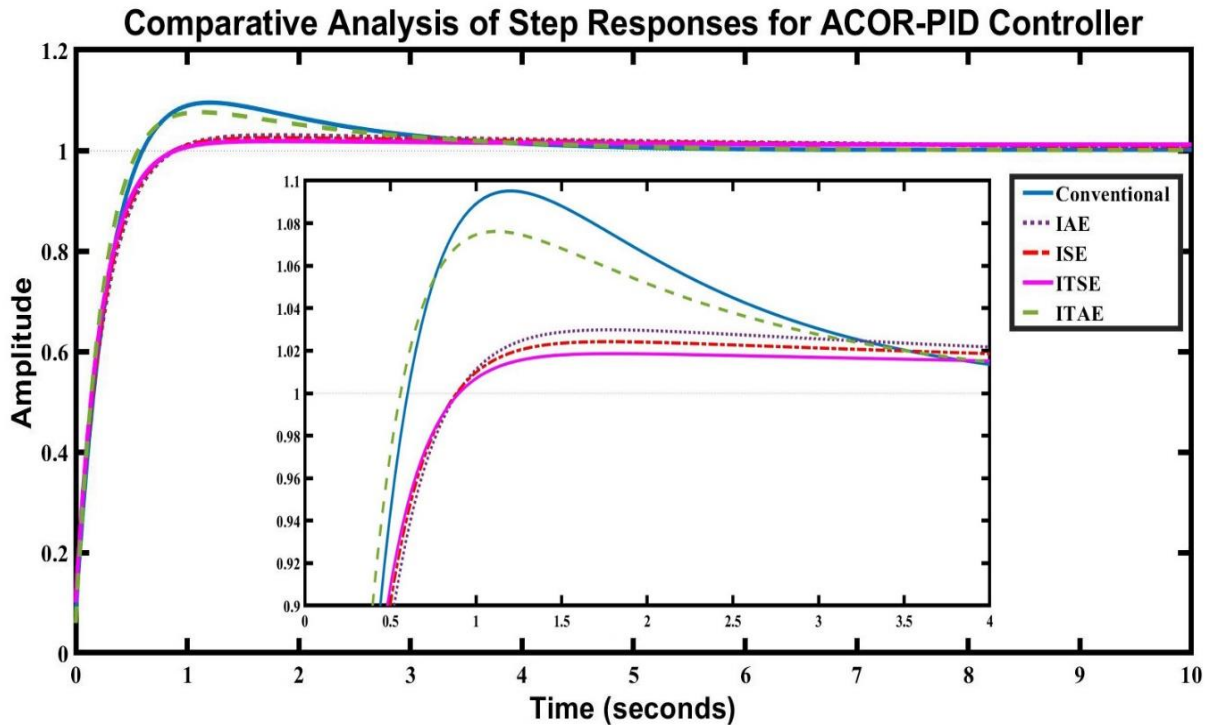


Fig. 6.21. Comparative Analysis of Step Responses for ACOR-PID (Unidirectional SEPIC Converter)

The performance parameters such as Percentage of Overshoot (%OS), Rise Time (Tr), Settling Time (Ts), and Peak Amplitude are tabulated for PSO-PID, which is presented in Table 6.11.

TABLE 6.11. PERFORMANCE PARAMETERS OF CONVENTIONAL AND ACOR-PID CONTROLLER [UNIDIRECTIONAL SEPIC]

Performance Parameters	Conventional PID	ACOR-PID			
		<i>IAE</i>	<i>ISE</i>	<i>ITSE</i>	<i>ITAE</i>
%OS	9.52	2.5852	2.4241	1.8603	7.6137
Tr (sec)	0.423	0.4851	0.4952	0.4781	0.3798
Ts (sec)	3.62	4.5228	4.2980	2.3414	3.6034
Peak Amplitude	1.0952	1.0258	1.0242	1.0186	1.0761

By the observation from Fig. 6.21 and Table 6.11, it is visible that ACOR-PID of ITSE performs better than conventional PID and other fitness functions in percentage of overshoot, settling time, and peak amplitude. ACOR-PID of ITAE performs better in terms of rise time. Fig. 6.22 depicts the comparative chart of performance parameters for ACOR-PID.

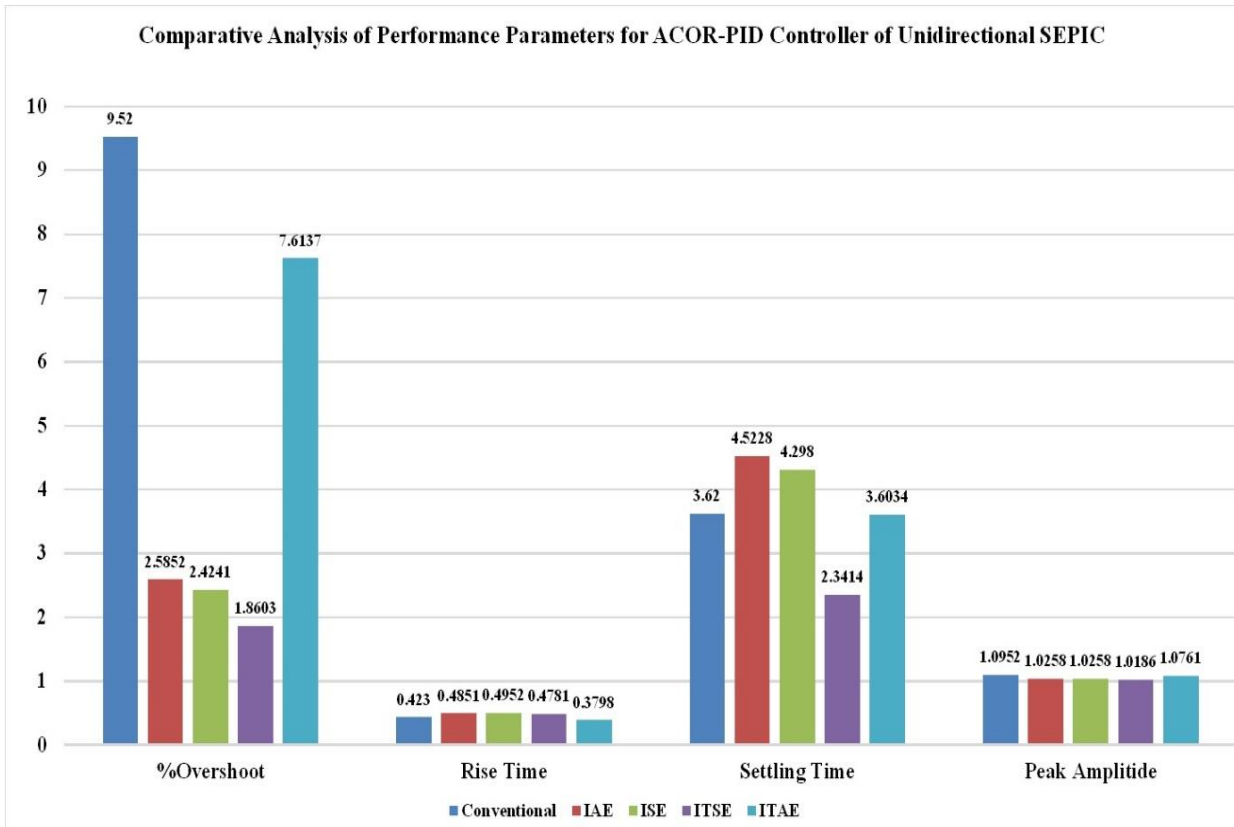


Fig. 6.22. Comparative Chart of Performance Parameters for ACO_R -PID (Unidirectional SEPIC Converter)

6.2.3.4. Comparative Analysis

After implementing all three swarm intelligence optimization algorithms in the unidirectional SEPIC converter, a comparison of performance parameters for optimum PID controller is shown in Table 6.12 based on the better performing fitness function of Table 6.5, 6.8, 6.11. Furthermore, an overall comparative analysis of step responses is shown in Fig. 6.22 based on the best-performing gain values for the unidirectional SEPIC converter.

TABLE 6.12. COMPARATIVE PERFORMANCE PARAMETERS OF PID CONTROLLER (UNIDIRECTIONAL SEPIC CONVERTER)

Attributes	Symbols	PID Controllers			
		Conventional PID	<i>FA-IAE</i>	<i>PSO-ISE</i>	<i>ACO_R-ITSE</i>
Performance Parameters	%OS	9.52	2.14	1.9757	1.8603
	Tr (sec)	0.423	0.48	0.4540	0.4781
	Ts (sec)	3.62	3.08	2.4418	2.3414
	Peak Amplitude	1.0952	1.0214	1.0198	1.0186

Gain Values	Kp	2991.7895	3276.1	3546.8	3495.1
	Ki	1904.3107	362.509 8	388.7232	354.2103
	Kd	59.9963	37.5453	53.2183	81.5848

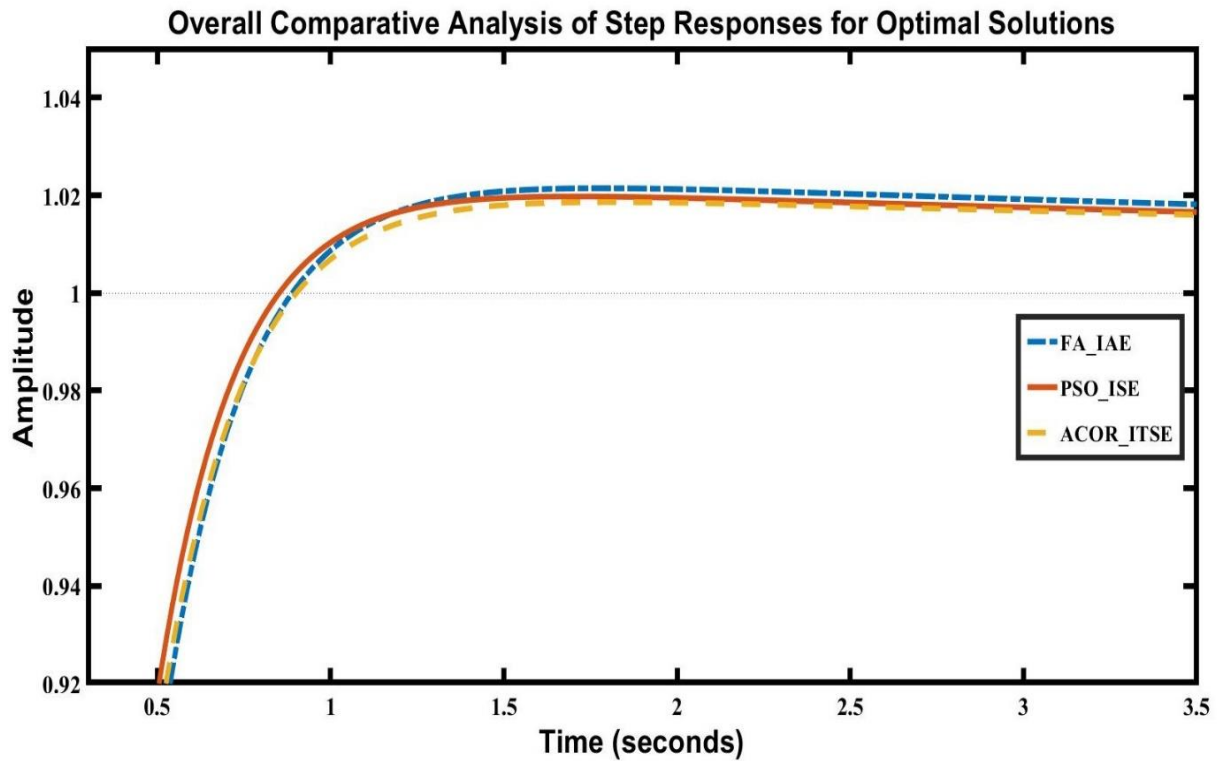


Fig. 6.23. Overall Comparative Step Response Analysis of PID Controller (Unidirectional SEPIC Converter)

By the observation from Table 6.12 and Fig. 6.23, it is evident that ACOR-ITSE performs better in terms of percentage of overshoot (1.8603%), settling time (2.3414 sec), and peak amplitude (1.0186). Fig. 6.24 depicts an overall comparative chart of optimum PID controller for unidirectional SEPIC converter.

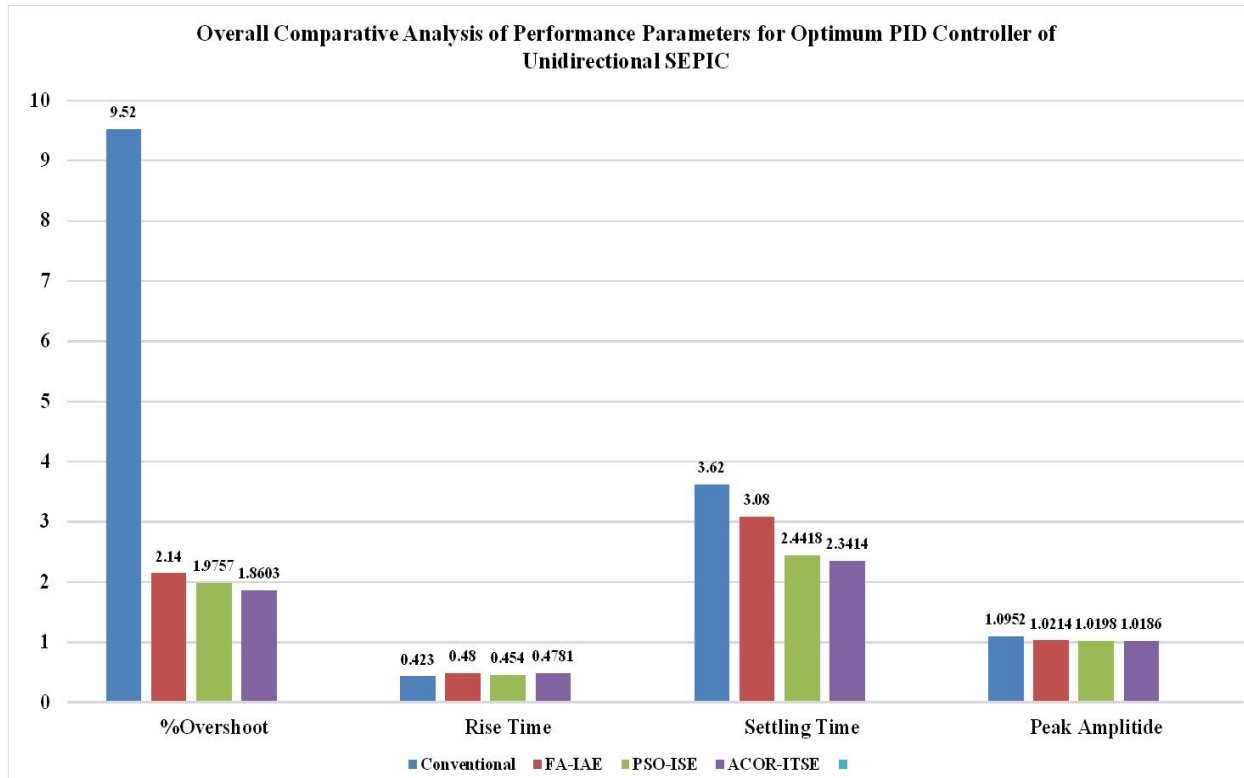


Fig. 6.24. Overall Comparative Chart of Optimum PID Controller (Unidirectional SEPIC Converter)

6.3 Bidirectional SEPIC Converter

6.3.1. Open-Loop Response

Using Simulink, the circuit for bidirectional SEPIC has been designed, which is depicted in Fig. 6.25. With the help of the system identification toolbox, the transfer function for the open-loop system has been obtained through exploring the input and output data from Simulink, with four poles and three zeros. Table 6.13 presents the parameters of the bidirectional SEPIC converter that have been used in the simulation.

TABLE 6.13. PARAMETERS OF BIDIRECTIONAL SEPIC CONVERTER

Parameter	Symbol	Value
Input Voltage	V_{in}	20 V
Output Voltage	V_o	20 V
Duty Cycle	d	50%
Switching Frequency	f_s	100 KHz
Inductor	L_1, L_2	10 μ H
Capacitor	C_1, C_2	47.62 μ F, 125 μ F
Load Resistance	R_o	1 Ω

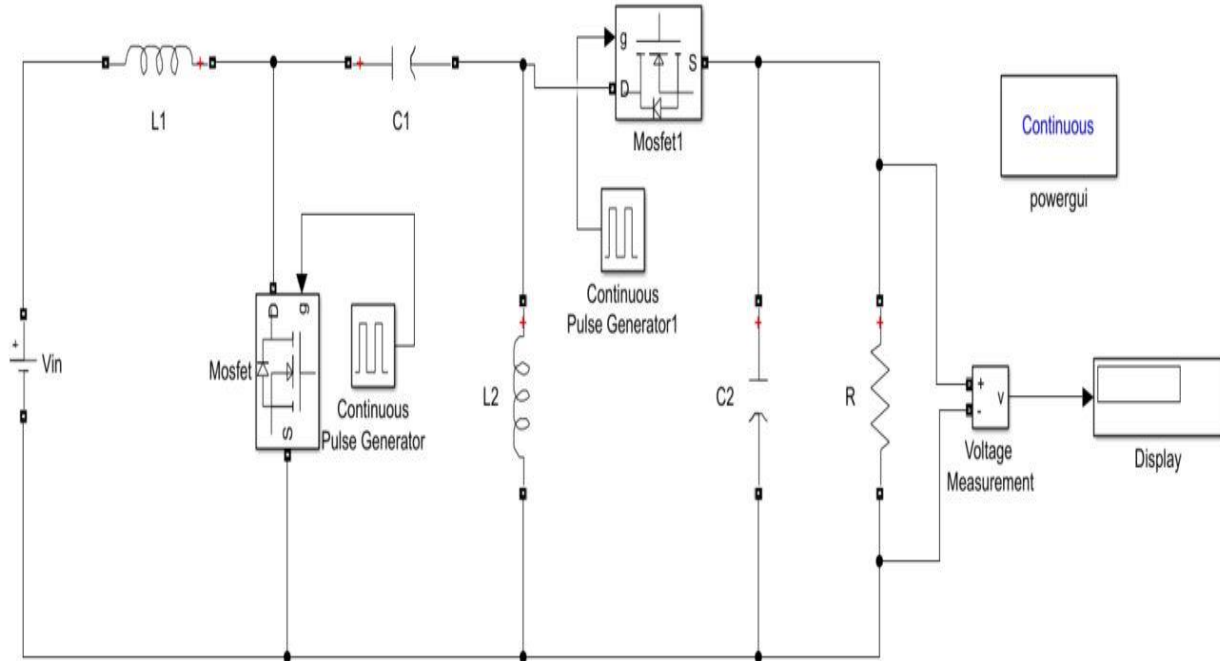


Fig. 6.25. Model of Open-Loop Bidirectional SEPIC by Simulink

The transfer function of the open-loop unidirectional SEPIC converter is as follows:

$$\frac{0.03706s^3 - 8.257 \times 10^{-5}s^2 + 3.128 \times 10^{-6}s + 4.756 \times 10^{-10}}{s^4 + 0.1188s^3 + 0.0002963s^2 + 3.286 \times 10^{-6}s + 84.919 \times 10^{-10}}$$

The step response for open-loop system of unidirectional SEPIC converter is depicted in Fig. 6.25.

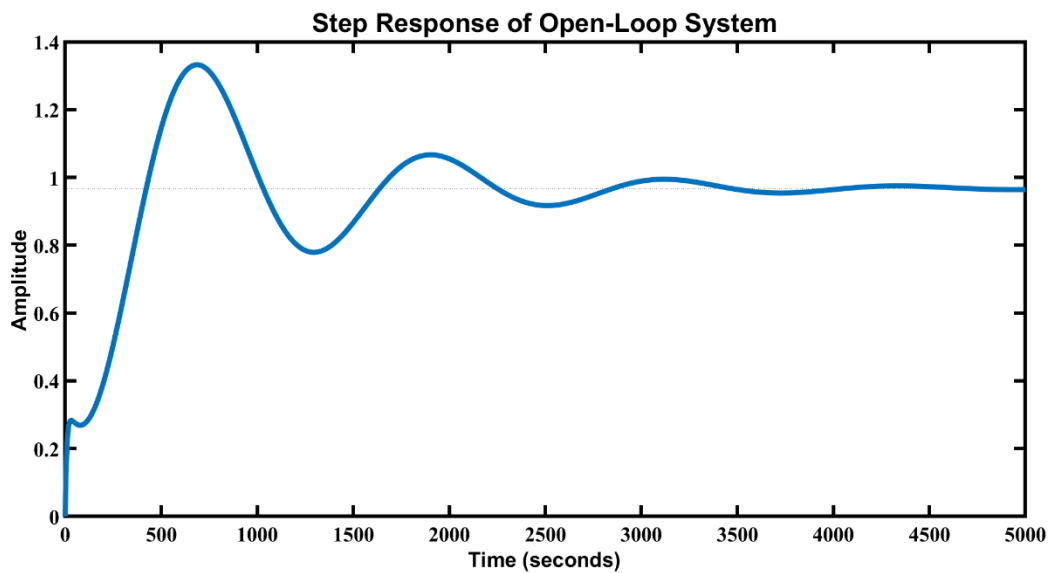


Fig. 6.26. Step Response of Open-Loop System of Bidirectional SEPIC

The step response shown in Fig. 6.26, shows that the percentage of overshoot is 37.7691%, rise time is 382.1369 seconds, settling time is 3282.0 seconds, and peak amplitude is 1.3320. So, it can be said that overshoot is very high for this open-loop response which must be reduced for having the safe application of the converters.

6.3.2. Closed-Loop Response with PID Controller

The PID controller for the closed-loop system has been used for the Bidirectional SEPIC converter as well. The circuit for closed-loop bidirectional SEPIC with conventional PID controller has been designed in Simulink, which is depicted in Fig. 6.27. The controller was manually tuned using the MATLAB PID Tuner App, and gain values ($K_P=415.212$, $K_I=1294.1967$, $K_D=2.127$) were achieved for the typical PID controller. After then, a step response, as shown in Fig. 6.28, is examined for its many properties in order to assess the system's stability.

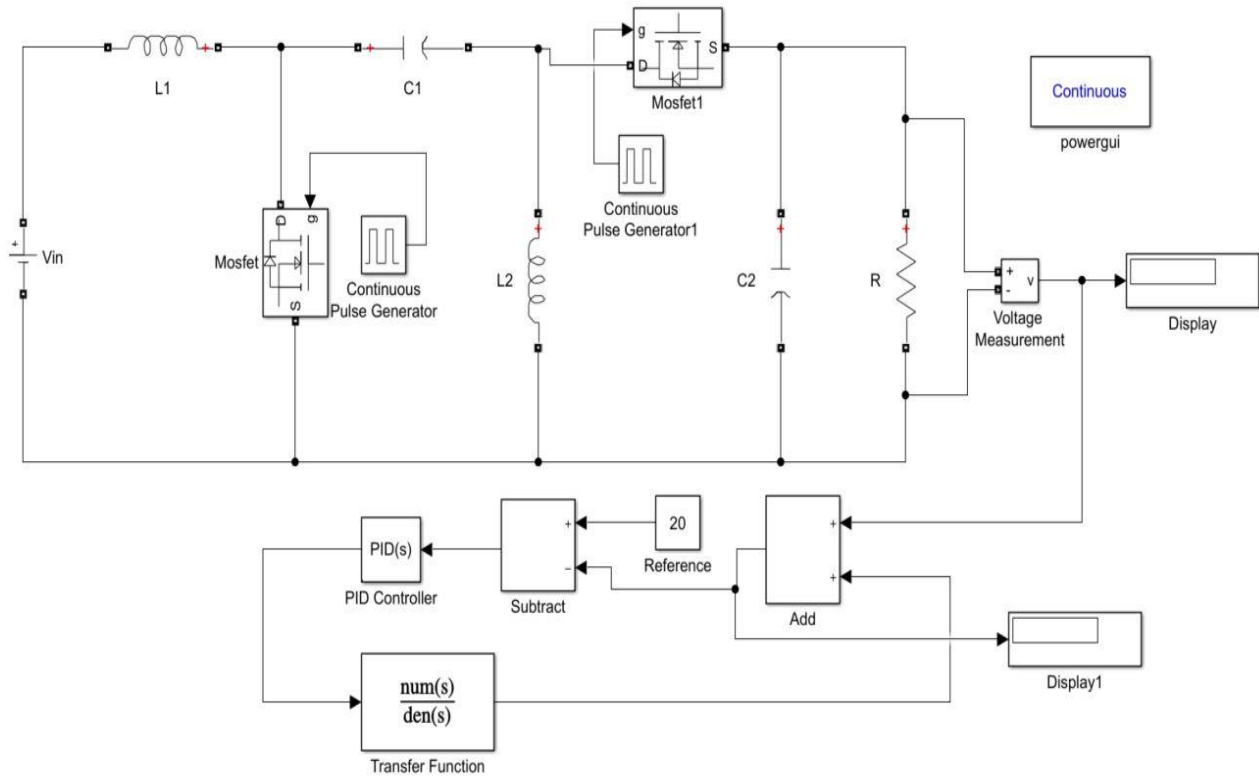


Fig. 6.27. Step Response of Closed-Loop System with PID Controller of Bidirectional SEPIC

The transfer function closed-loop of bidirectional SEPIC converter is as follows:

$$\frac{0.07883s^5 + 15.39s^4 + 47.93s^3 - 0.1056s^2 + 0.004048s + 6.155 \times 10^{-7}}{1.079s^5 + 15.51s^4 + 47.93s^3 - 0.1056s^2 + 0.004048s + 6.155 \times 10^{-7}}$$

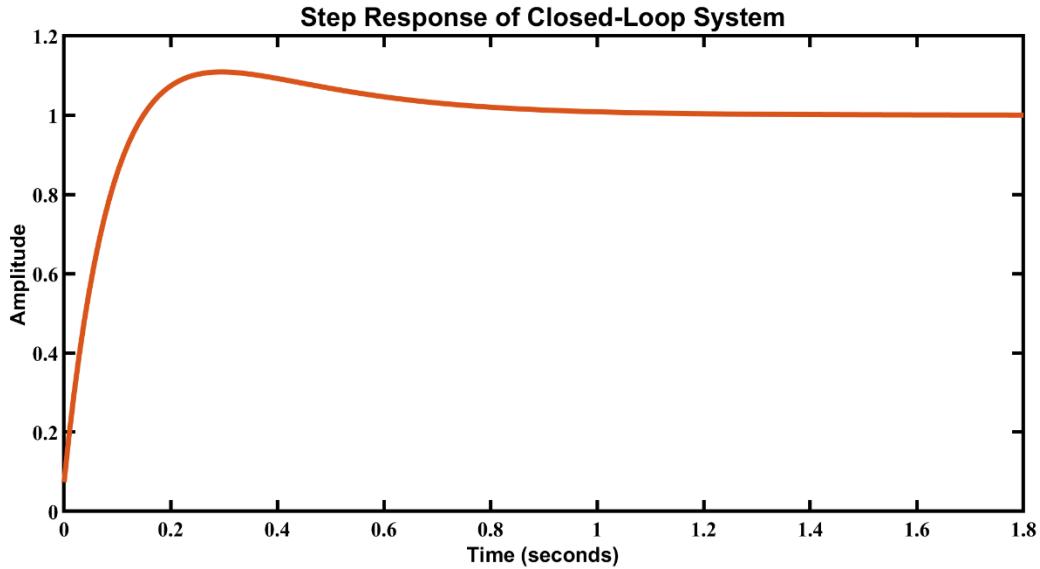


Fig. 6.28. Step Response of Closed-Loop System with Conventional PID of Bidirectional SEPIC

From the step response shown in Fig. 5.22, it is observed that the percentage of overshoot is 10.8875%, rise time is 0.1070 seconds, settling time is 0.8173 seconds, and peak amplitude is 1.1089. These values are less than the open-loop system but not so good as expected. The performance parameters; Percentage of Overshoot (%OS), Rise Time (T_r), Settling Time (T_s), and Peak Amplitude, are tabulated for both open-loop and closed-loop analysis, which is presented in Table 6.14.

TABLE 6.14. PERFORMANCE ANALYSIS OF OPEN-LOOP AND CLOSED-LOOP RESPONSE [BIDIRECTIONAL SEPIC]

Performance Parameters	Open-Loop Response	Closed-Loop Response
%OS	37.7691	10.8875
T_r (sec)	382.1369	0.1070
T_s (sec)	3282.0	0.8173
Peak Amplitude	1.3320	1.1089

6.2.3. Swarm Intelligence Algorithms based PID Controller

Though the closed-loop system with conventional PID controller provides better performance than the open-loop system, it is not good enough. So, bio-inspired swarm intelligence optimization algorithms are employed in the controller to reduce the overshoot, get faster rise time and settling time. Moreover, step responses are observed, and gain values and performance parameters are tabulated for FA-PID, PSO-PID, and ACO_R-PID.

6.3.3.1. FA-PID Controller

The Firefly Algorithm is first applied to have the optimized gain values for the controller. Then, the same parameters of firefly algorithm stated in Table 6.3 have been used in the bidirectional SEPIC converter. In comparison to the gain values of the traditional PID controller, improved values of the gain parameters for the four performance indices (IAE, ISE, ITSE, ITAE) of the FA-PID controller have been attained after several simulations in MATLAB, as shown in Table 6.15. The step responses of the FA-PID controller's IAE, ISE, ITSE, and ITAE for bidirectional SEPIC Converter are shown in Figures 6.29, 6.30, 6.31, and 6.32, respectively.

TABLE 6.15. GAIN VALUES OF FA-PID CONTROLLER FOR BIDIRECTIONAL SEPIC

Gains	FA-PID			
	<i>IAE</i>	<i>ISE</i>	<i>ITSE</i>	<i>ITAE</i>
K_p	827.5014	868.6958	893.0344	869.1520
K_i	209.9814	356.2909	484.1214	1500
K_d	2.9901	5.2010	4.7019	3.4094

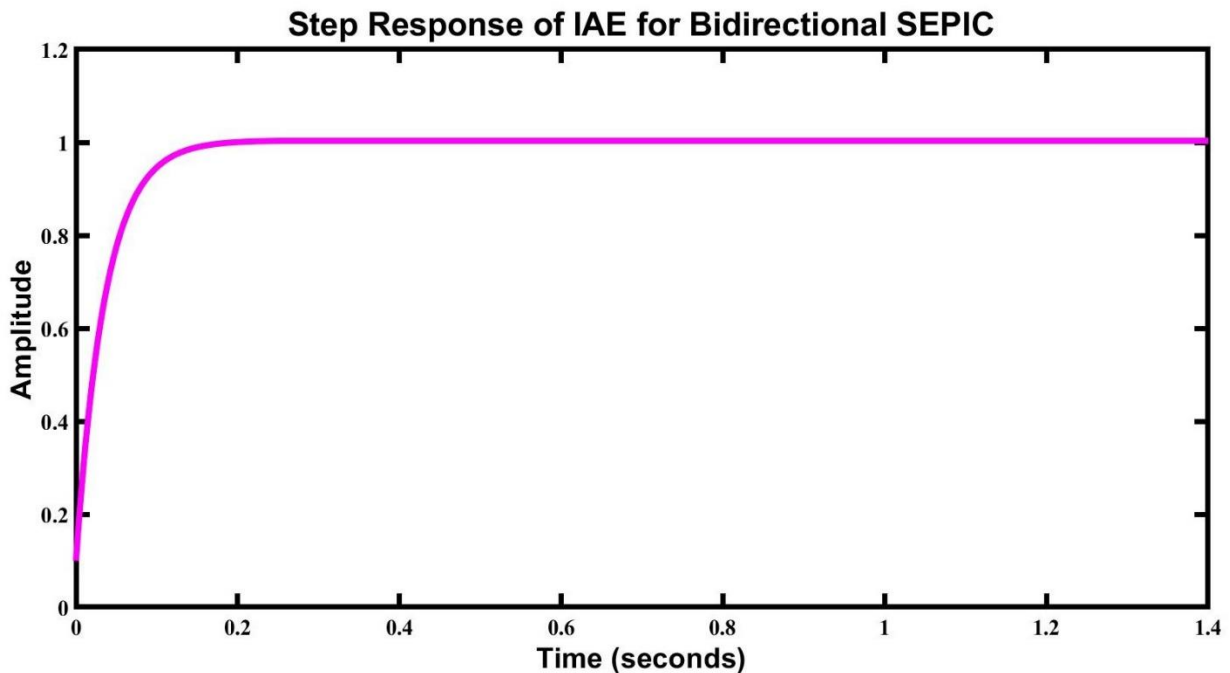


Fig. 6.29. Step Response of IAE for FA-PID (Bidirectional SEPIC Converter)

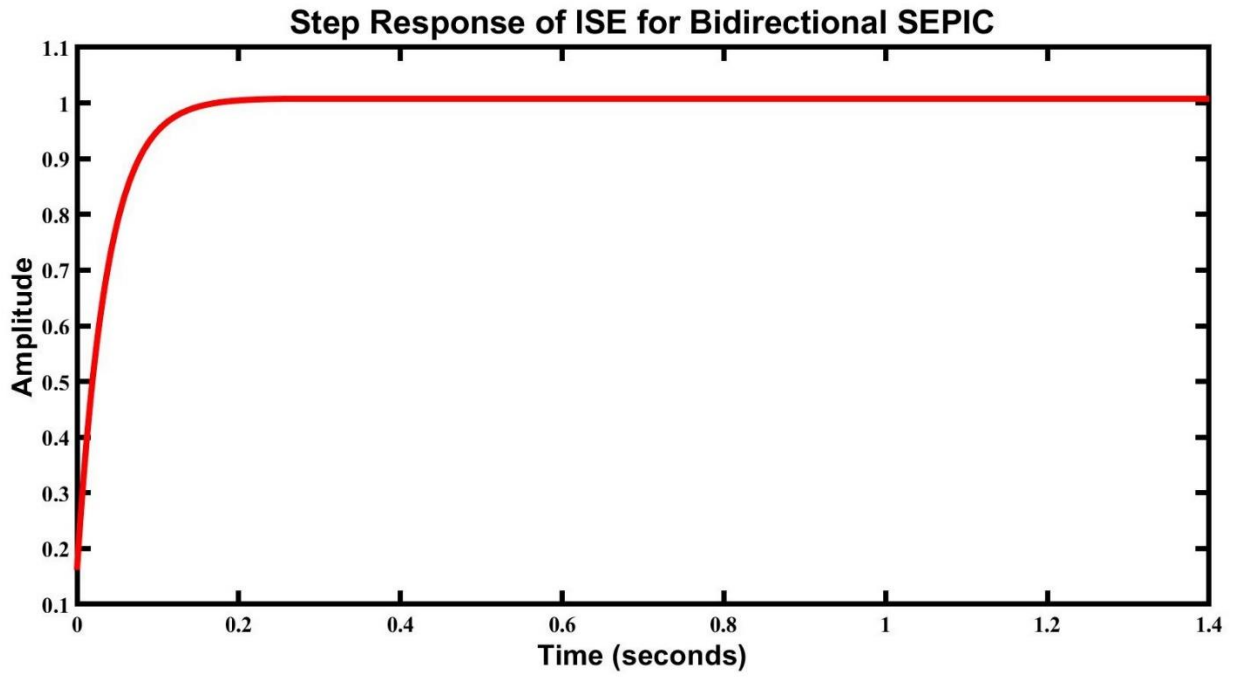


Fig. 6.30. Step Response of ISE for FA-PID (Bidirectional SEPIC Converter)

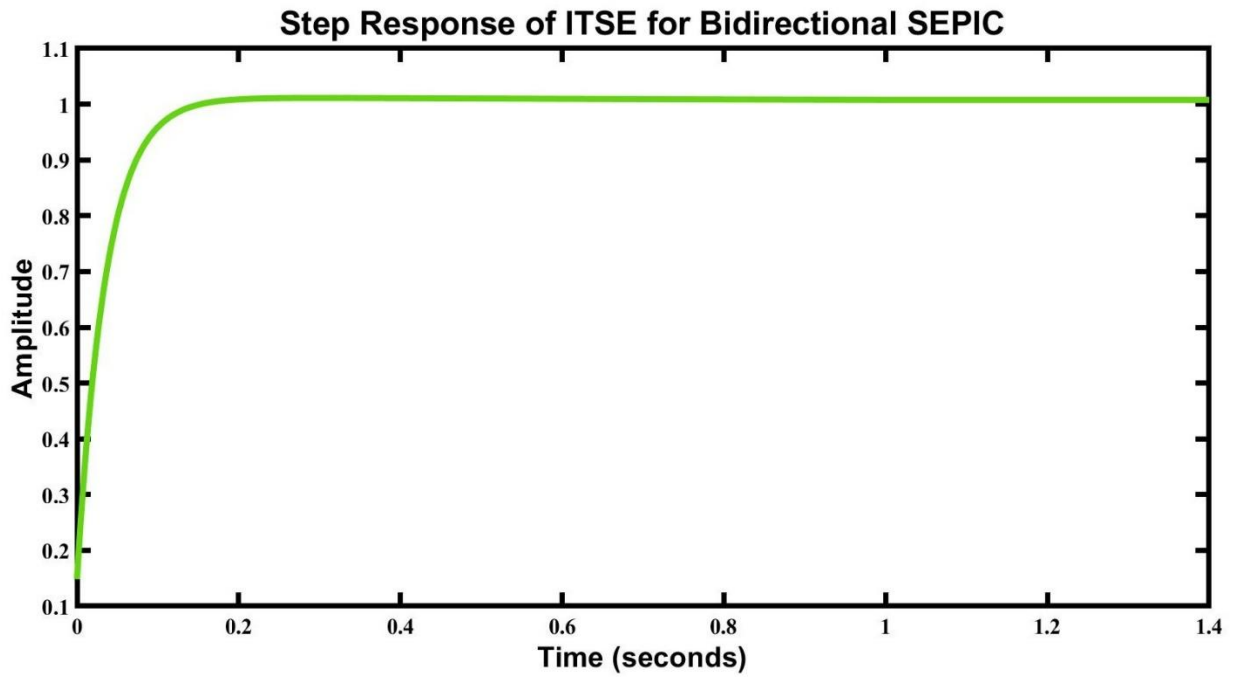


Fig. 6.31. Step Response of ITSE for FA-PID (Bidirectional SEPIC Converter)

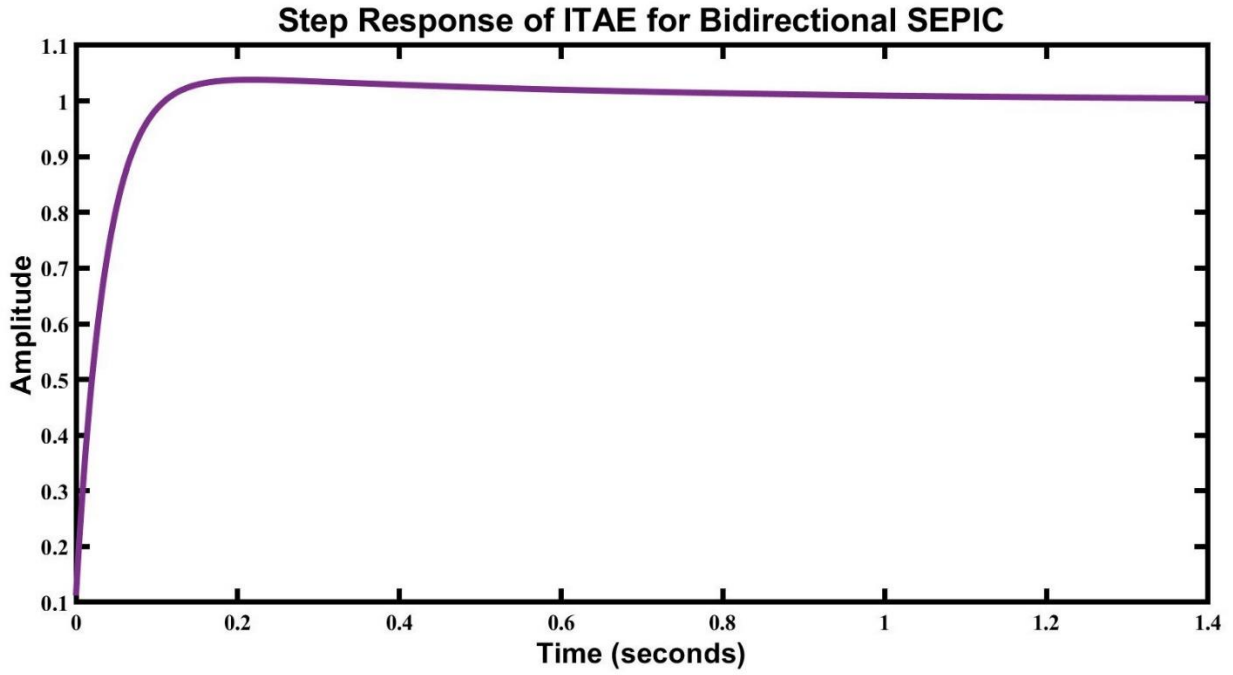


Fig. 6.32. Step Response of ITAE for FA-PID (Bidirectional SEPIC Converter)

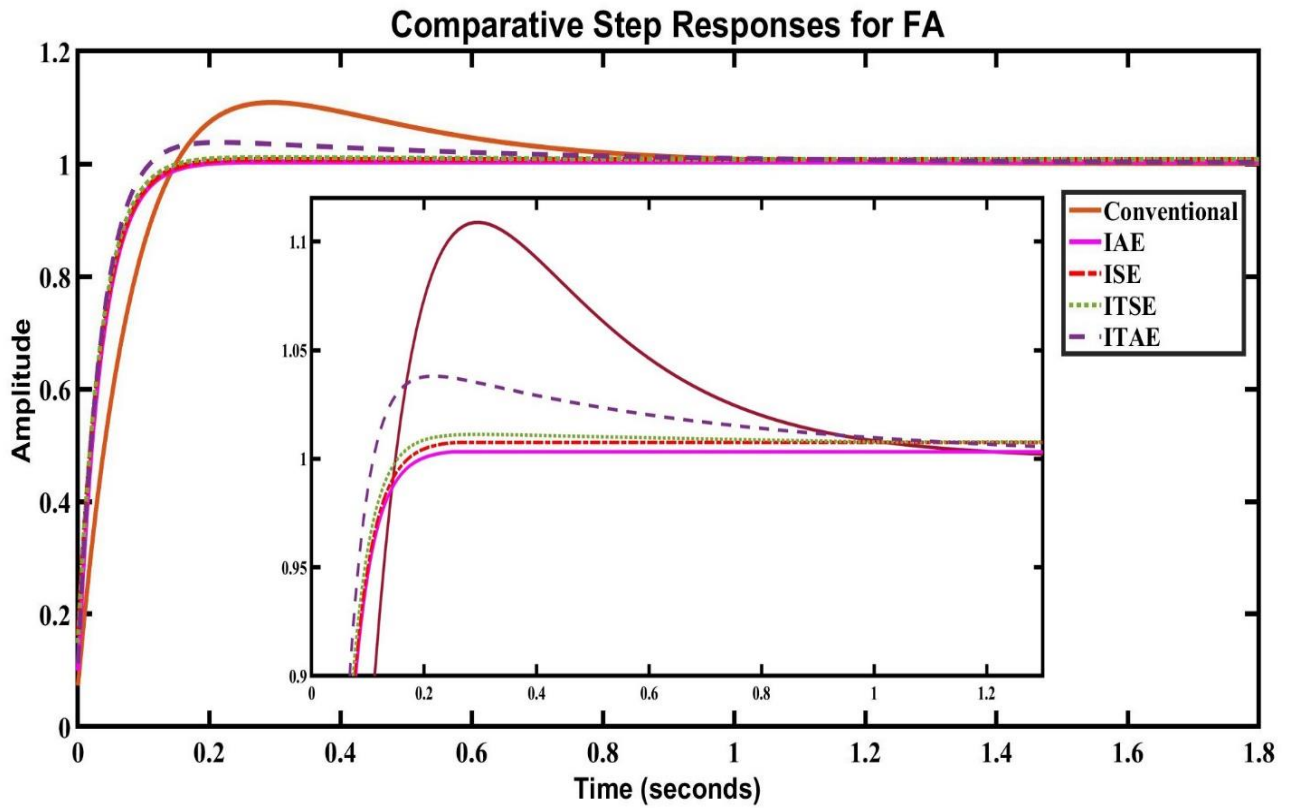


Fig. 6.33. Comparative Analysis of Step Responses for FA-PID (Bidirectional SEPIC Converter)

The performance parameters such as Percentage of Overshoot (%OS), Rise Time (Tr), Settling Time (Ts), and Peak Amplitude are tabulated for FA-PID which is presented in Table 6.16.

TABLE 6.16. PERFORMANCE PARAMETERS OF CONVENTIONAL AND FA-PID CONTROLLER FOR BIDIRECTIONAL SEPIC

Performance Parameters	Conventional PID	FA-PID			
		<i>IAE</i>	<i>ISE</i>	<i>ITSE</i>	<i>ITAE</i>
%OS	10.8875	0.3212	0.7543	1.1200	3.8034
Tr (sec)	0.1070	0.0785	0.0790	0.0748	0.0670
Ts (sec)	0.8173	0.1349	0.1311	0.1217	0.6704
Peak Amplitude	1.1089	1.0032	1.0075	1.0112	1.0381

By the observation from Fig. 6.33 and Table 6.16, it is visible that FA-PID of IAE performs better than conventional PID and other fitness functions in percentage of overshoot and peak amplitude. FA-PID of ITSE performs better in terms of settling time. FA-PID of ITAE performs better in terms of rise time. Fig. 6.34 depicts the comparative chart of performance parameters for FA-PID for bidirectional SEPIC.

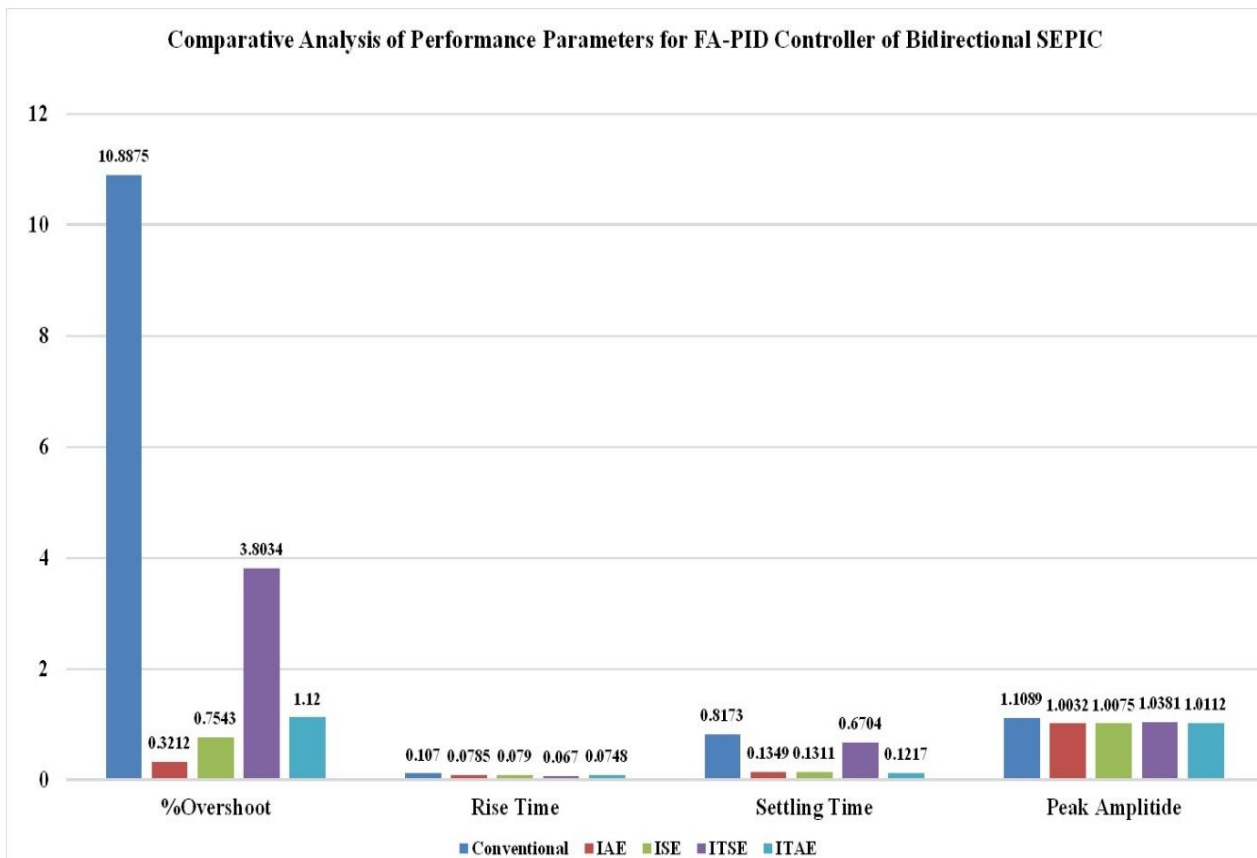


Fig. 6.34. Comparative Chart of Performance Parameters for FA-PID (Bidirectional SEPIC Converter)

6.3.3.2. PSO-PID Controller

The Particle Swarm Optimization (PSO) is applied to have the controller's optimized gain values. The exact parameters of the particle swarm optimization algorithm stated in Table 6.6 have been used in the bidirectional SEPIC converter. In comparison to the gain values of the conventional PID controller, improved values of the gain parameters for the four performance indices (IAE, ISE, ITSE, ITAE) of the PSO-PID controller have been attained after several simulations in MATLAB, as shown in Table 6.17. The step responses of the PSO-PID controller's IAE, ISE, ITSE, and ITAE for bidirectional SEPIC Converter are shown in Figs. 6.35, 6.36, 6.37, and 6.38, respectively.

TABLE 6.17. GAIN VALUES OF PSO-PID CONTROLLER [BIDIRECTIONAL SEPIC]

Gains	PSO-PID			
	<i>IAE</i>	<i>ISE</i>	<i>ITSE</i>	<i>ITAE</i>
K _p	798.2994	879.5768	884.3250	866.2155
K _i	217.1921	471.5866	213.99	1376.8
K _d	3.4709	4.8195	5.2295	5.6239

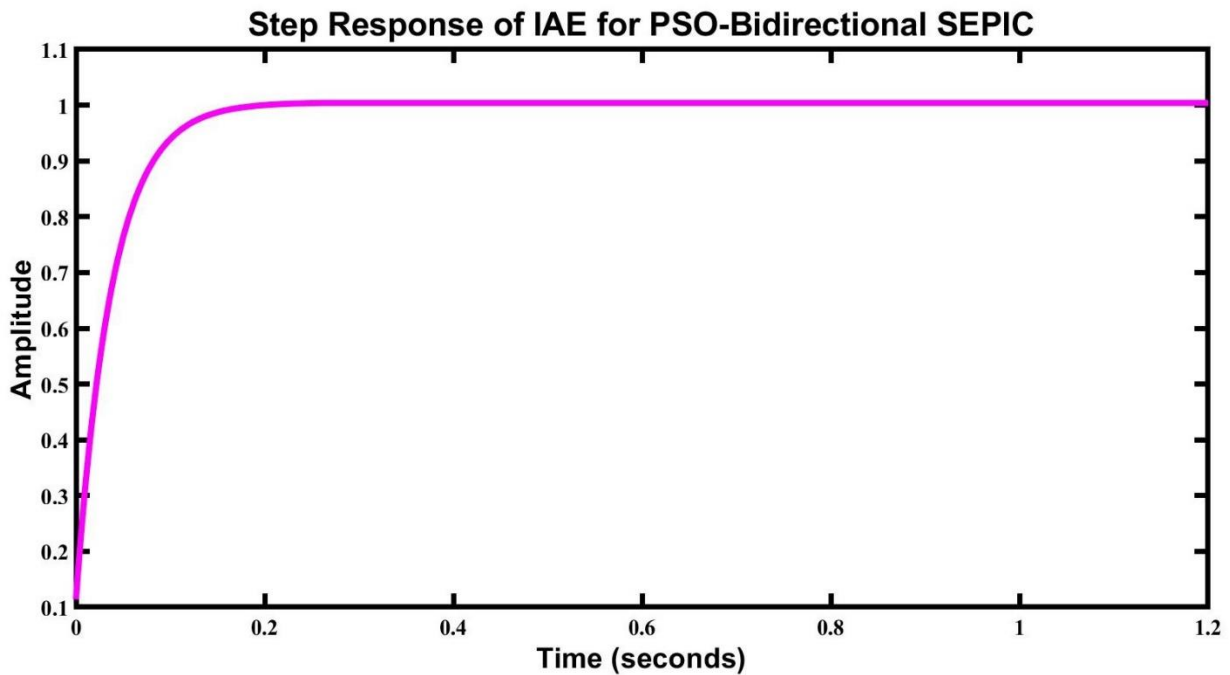


Fig. 6.35. Step Response of IAE for PSO-PID (Bidirectional SEPIC Converter)

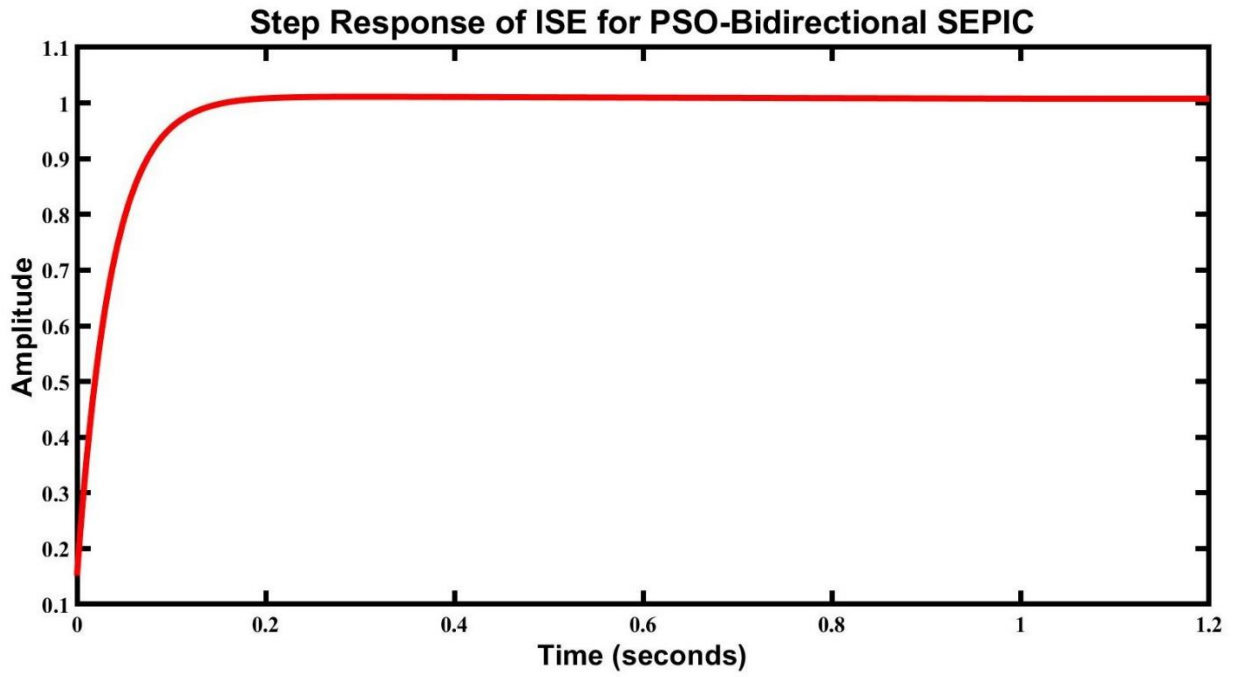


Fig. 6.36. Step Response of ISE for PSO-PID (Bidirectional SEPIC Converter)

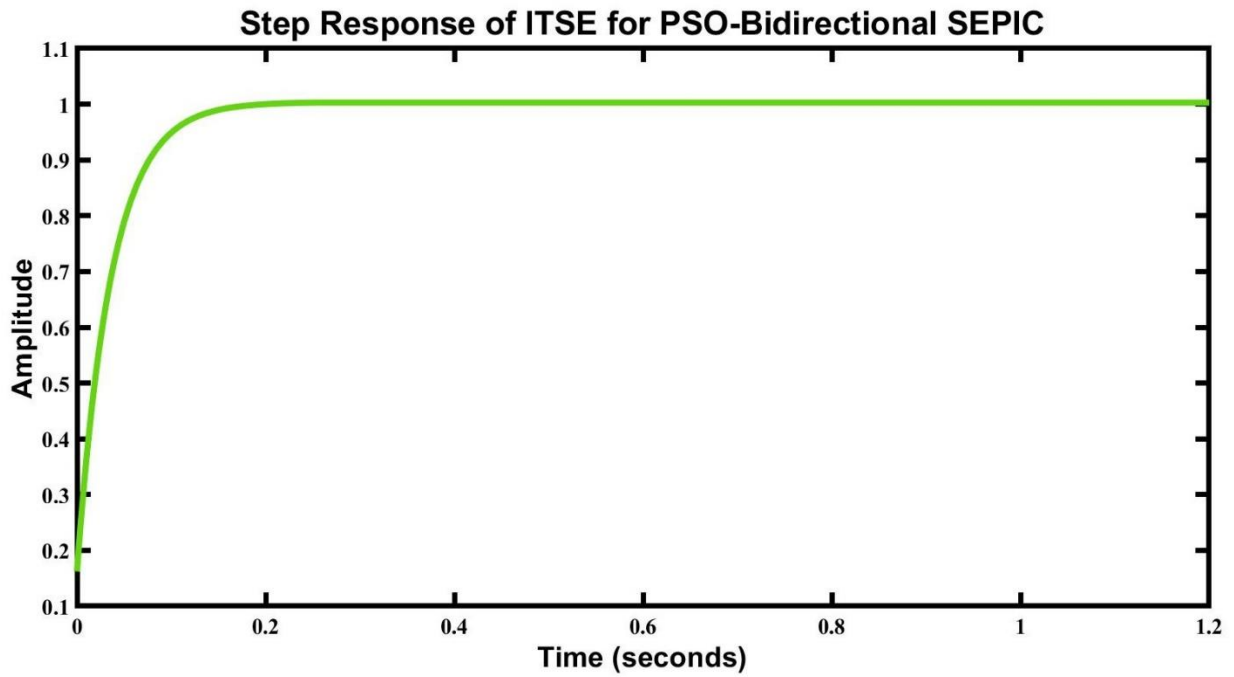


Fig. 6.37. Step Response of ITSE for PSO-PID (Bidirectional SEPIC Converter)

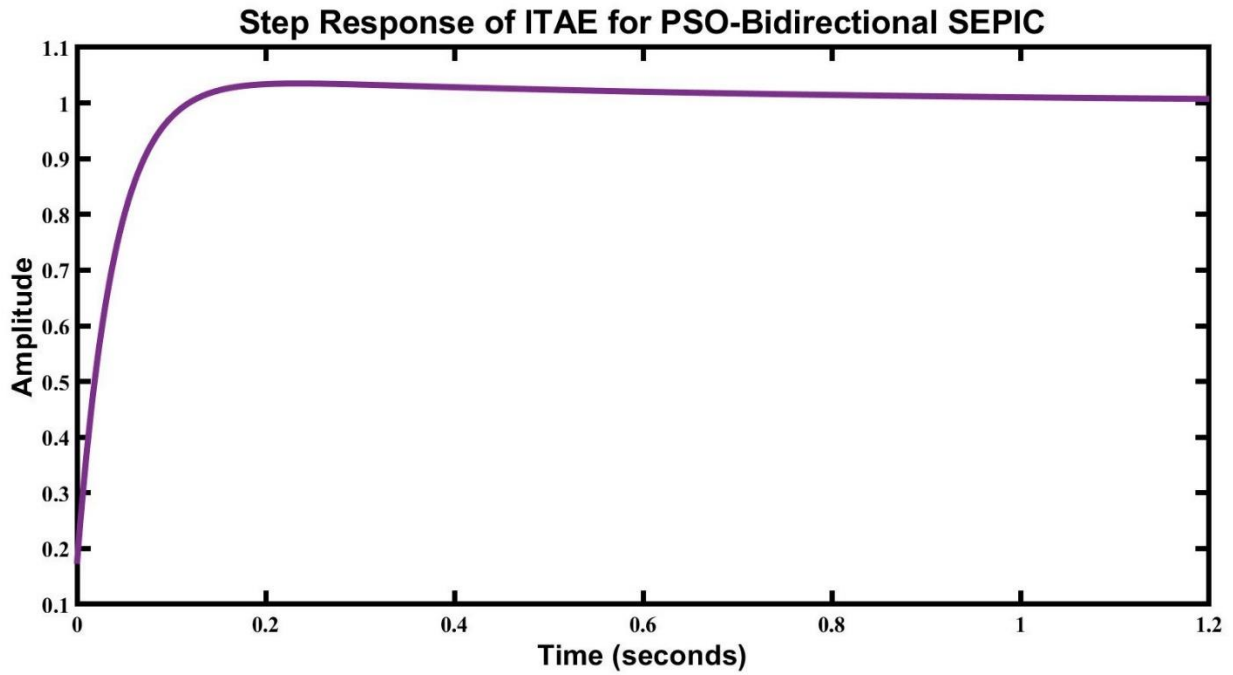


Fig. 6.38. Step Response of ITAE for PSO-PID (Bidirectional SEPIC Converter)

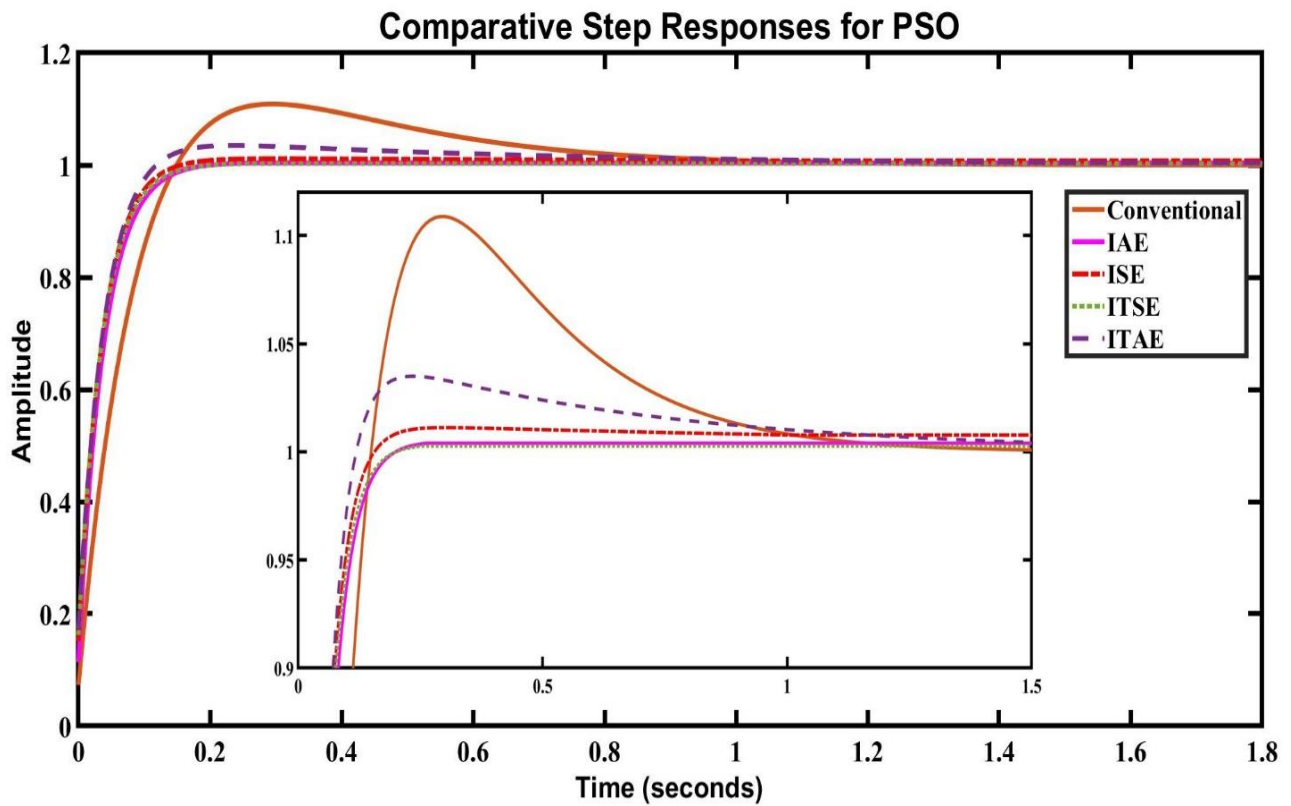


Fig. 6.39. Comparative Analysis of Step Responses for PSO-PID (Bidirectional SEPIC Converter)

The performance parameters such as Percentage of Overshoot (%OS), Rise Time (Tr), Settling Time (Ts), and Peak Amplitude are tabulated for PSO-PID which is presented in Table 6.18.

TABLE 6.18. PERFORMANCE PARAMETERS OF CONVENTIONAL AND PSO-PID CONTROLLER [BIDIRECTIONAL SEPIC]

Performance Parameters	Conventional PID	PSO-PID			
		<i>IAE</i>	<i>ISE</i>	<i>ITSE</i>	<i>ITAE</i>
%OS	10.8875	0.3950	1.1202	0.2674	3.4997
Tr (sec)	0.1070	0.0824	0.0762	0.0790	0.0722
Ts (sec)	0.8173	0.1408	0.1239	0.1362	0.7185
Peak Amplitude	1.1089	1.0040	1.0112	1.0027	1.0350

By the observation from Fig. 6.39 and Table 6.18, it is visible that PSO-PID of ITSE performs better than conventional PID and other fitness functions in percentage of overshoot, and peak amplitude. PSO-PID of ITAE performs better in terms of rise time. FA-PID of ISE performs better in terms of settling time. Fig. 6.40 depicts the comparative chart of performance parameters for PSO-PID for the bidirectional SEPIC.

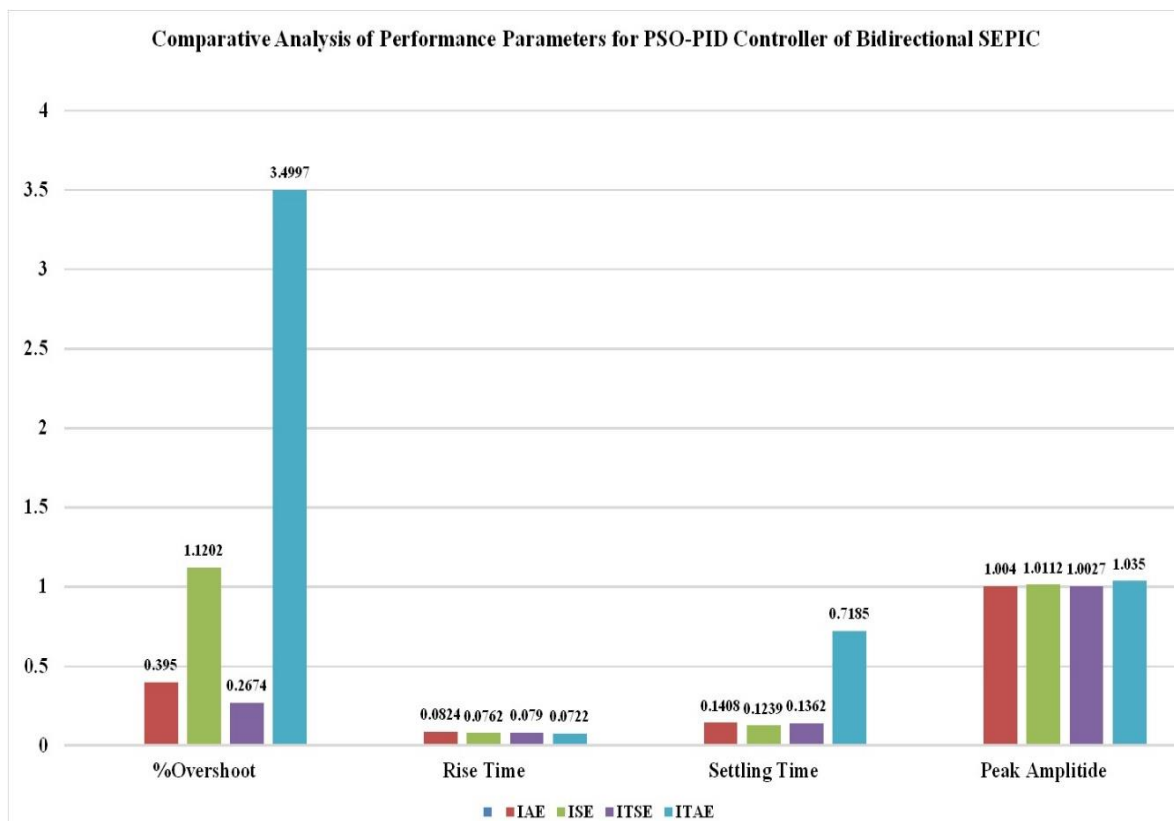


Fig. 6.40. Comparative Chart of Performance Parameters for PSO-PID (Bidirectional SEPIC Converter)

6.3.3.3. ACO_R-PID Controller

The Ant Colony Optimization for continuous domain (ACO_R) is applied to have the controller's optimized gain values. The same parameters of the ant colony optimization algorithm for continuous domain stated in Table 6.9 have been used in bidirectional SEPIC converter. In comparison to the gain values of the conventional PID controller, improved values of the gain parameters for the four performance indices (IAE, ISE, ITSE, ITAE) of the ACO_R-PID controller have been attained after several simulations in MATLAB, as shown in Table 6.19. The step responses of the ACO_R-PID controller's IAE, ISE, ITSE, and ITAE for bidirectional SEPIC Converter are shown in Figures 6.41, 6.42, 6.43, and 6.44, respectively.

TABLE 6.19. GAIN VALUES OF ACO_R-PID CONTROLLER [BIDIRECTIONAL SEPIC]

Gains	ACO _R -PID			
	<i>IAE</i>	<i>ISE</i>	<i>ITSE</i>	<i>ITAE</i>
K _p	864.7406	894.677	881.4950	834.5024
K _i	355.2797	709.5692	203.5099	1444.5
K _d	0.4070	5.3354	1.1169	1.5396

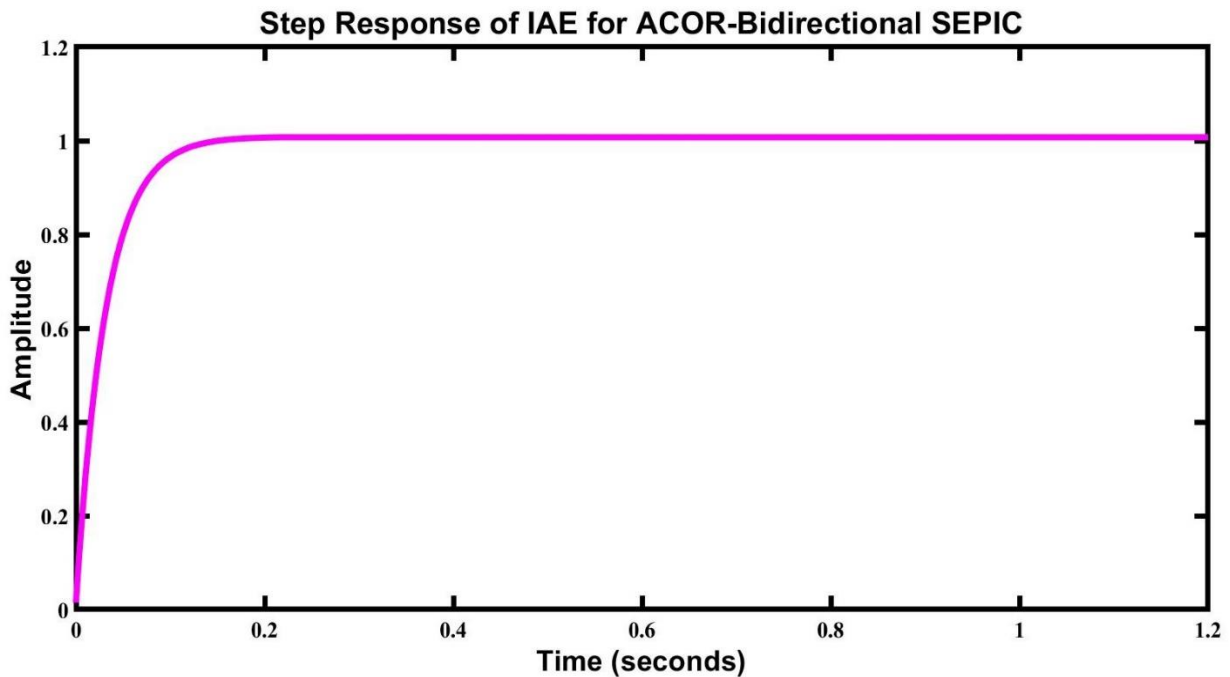


Fig. 6.41. Step Response of IAE for ACO_R-PID (Bidirectional SEPIC Converter)

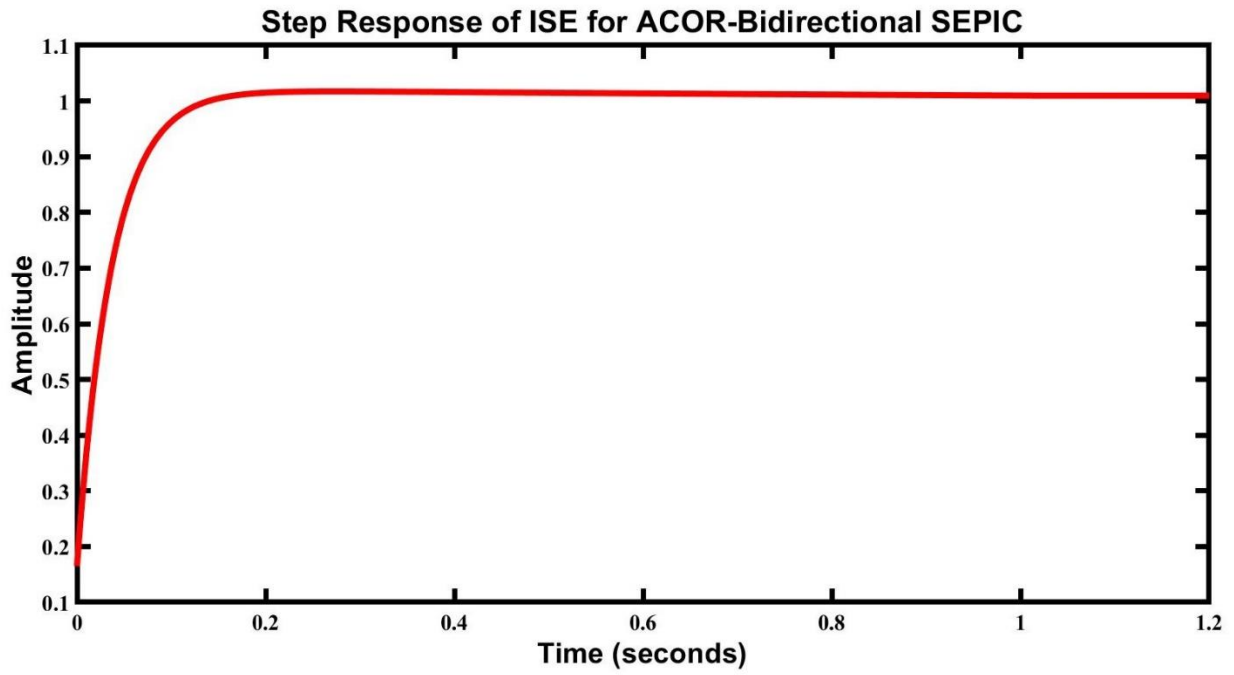


Fig. 6.42. Step Response of ISE for $ACOR$ -PID (Bidirectional SEPIC Converter)

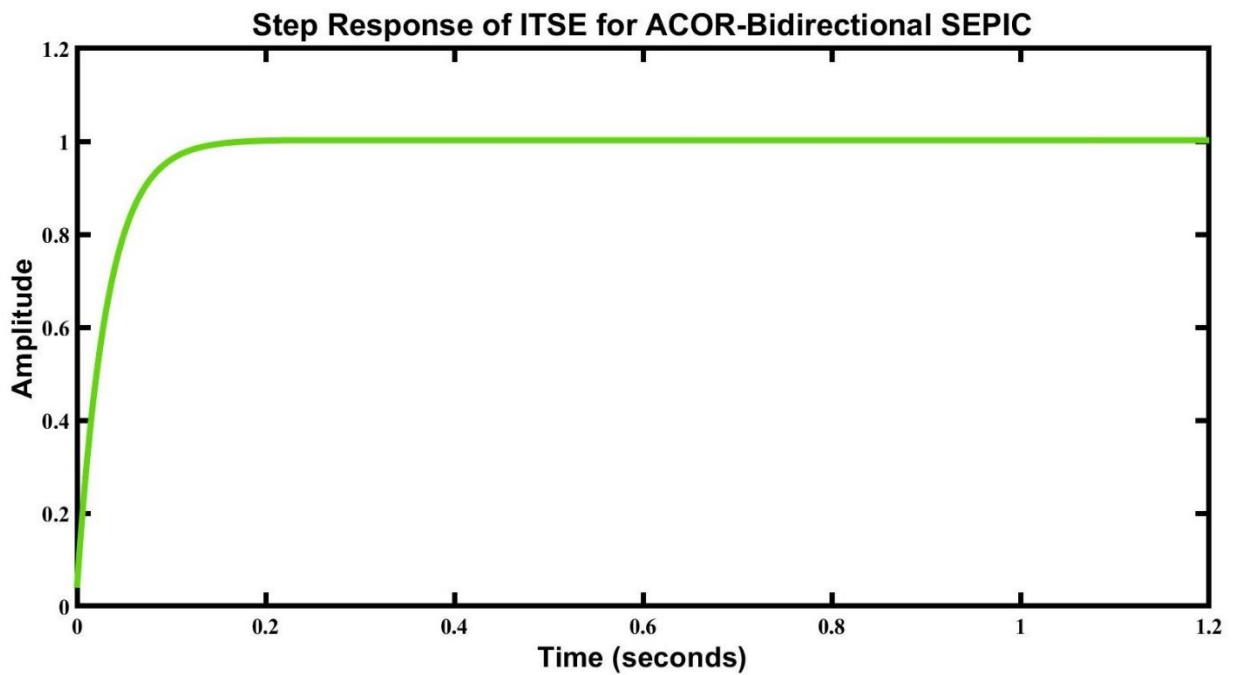


Fig. 6.43. Step Response of ITSE for $ACOR$ -PID (Bidirectional SEPIC Converter)

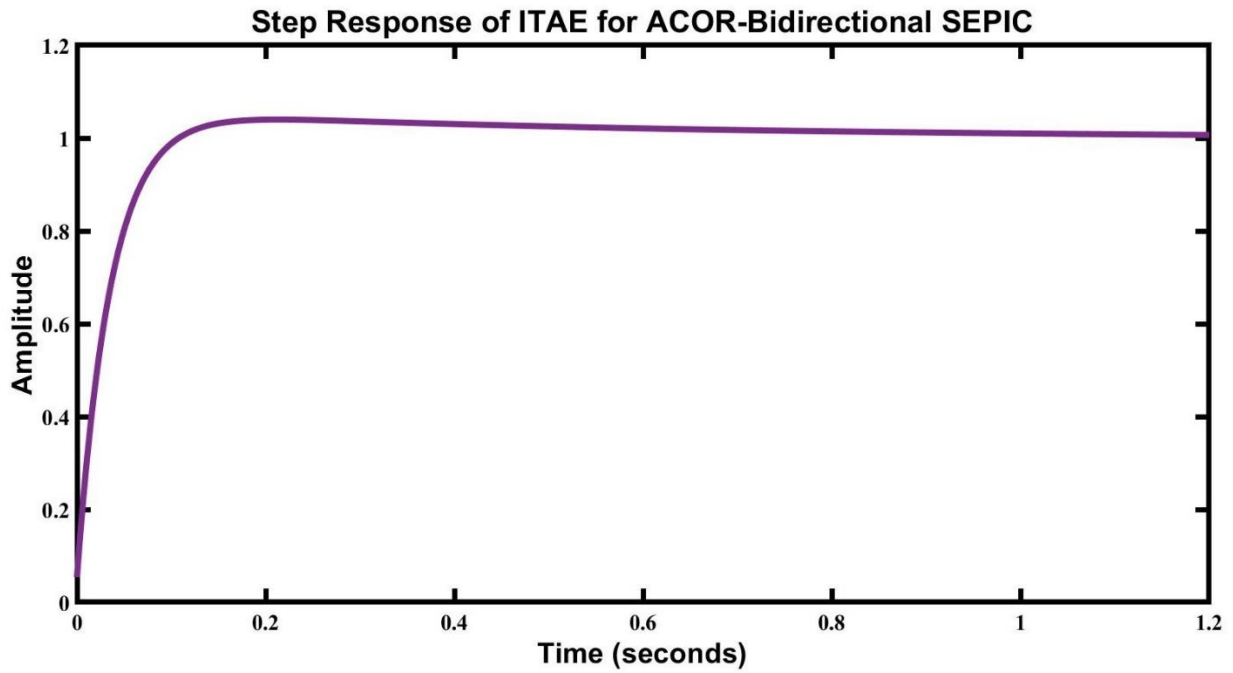


Fig. 6.44. Step Response of ITAE for ACOR-PID (Bidirectional SEPIC Converter)

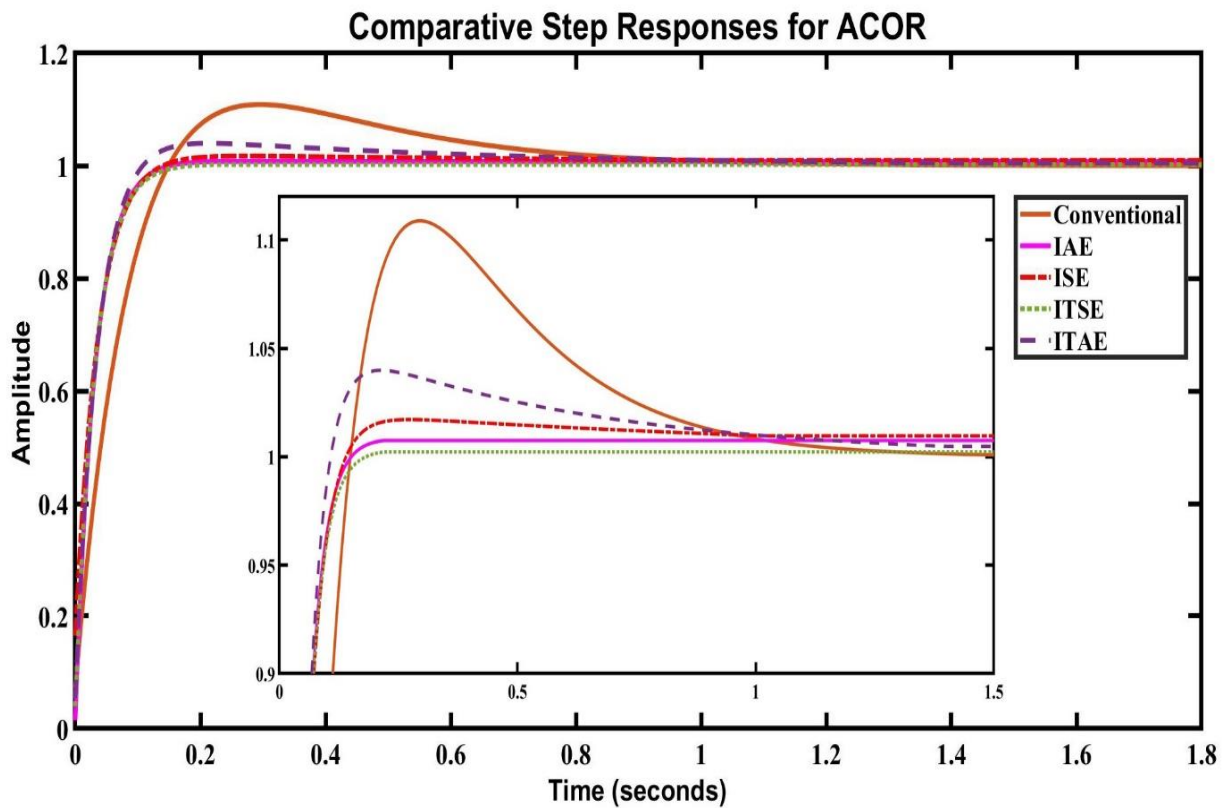


Fig. 6.45. Comparative Analysis of Step Responses for ACOR-PID (Unidirectional SEPIC Converter)

The performance parameters such as Percentage of Overshoot (%OS), Rise Time (Tr), Settling Time (Ts), and Peak Amplitude are tabulated for ACO_R-PID, which is presented in Table 6.20.

TABLE 6.20. PERFORMANCE PARAMETERS OF CONVENTIONAL AND ACO_R-PID CONTROLLER [BIDIRECTIONAL SEPIC]

Performance Parameters	Conventional PID	ACO _R -PID			
		IAE	ISE	ITSE	ITAE
%OS	10.8875	0.7517	1.7167	0.2245	3.9894
Tr (sec)	0.1070	0.0678	0.0743	0.0693	0.0656
Ts (sec)	0.8173	0.1134	0.3384	0.1202	0.6561
Peak Amplitude	1.1089	1.0075	1.0172	1.0022	1.0399

By the observation from Fig. 6.45 and Table 6.20, it is clearly visible that ACO_R-PID of ITSE performs better than conventional PID and other fitness functions in percentage of overshoot and peak amplitude. ACO_R-PID of ITAE performs better in terms of rise time. ACO_R-PID of IAE performs better in terms of settling time. Fig. 6.46 depicts the comparative chart of performance parameters for ACO_R-PID.

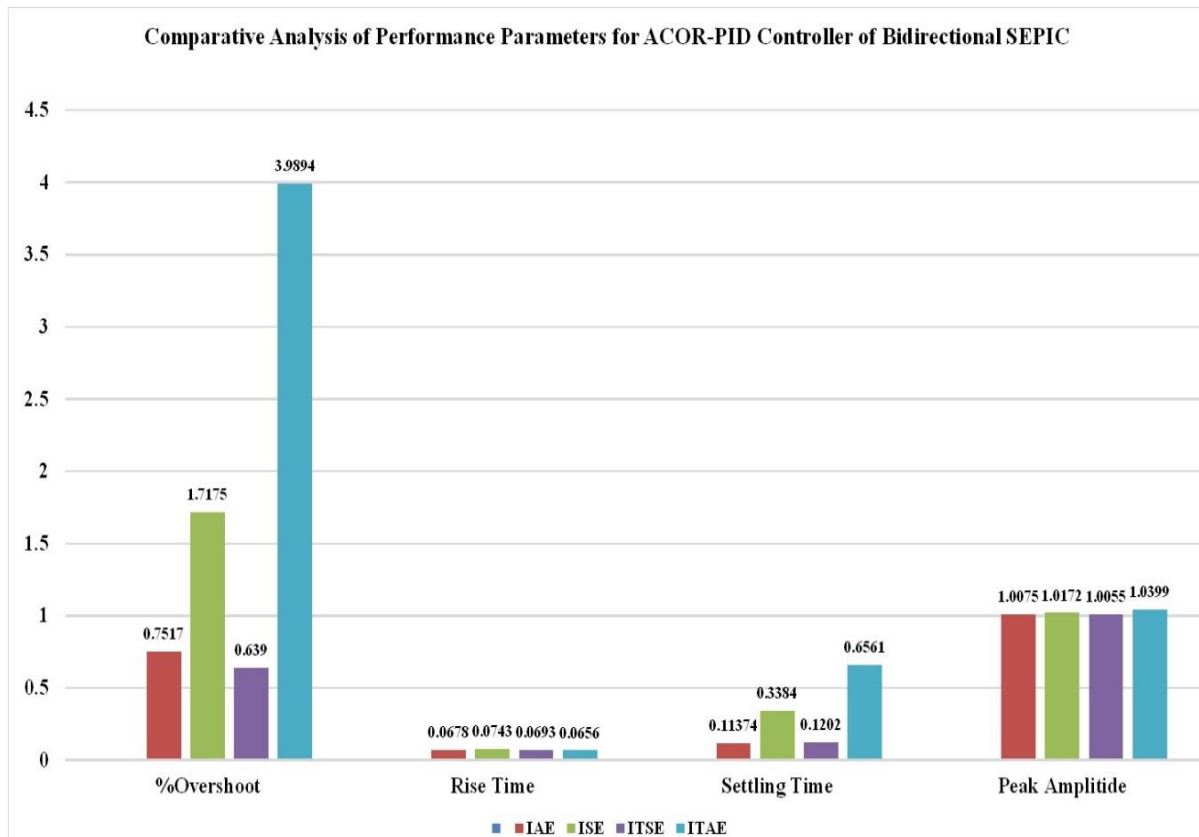


Fig. 6.46. Comparative Chart of Performance Parameters for ACO_R-PID (Bidirectional SEPIC Converter)

6.3.3.4. Comparative Analysis

After implementing all three swarm intelligence optimization algorithms in the Bidirectional SEPIC converter, a comparison of performance parameters for optimum PID controller is shown in Table 6.21 based on the better performing fitness function of Table 6.16, 6.18, 6.20. Furthermore, an overall comparative analysis of step responses is shown in Fig. 6.47 based on the best performing gain values for the Bidirectional SEPIC converter.

TABLE 6.21. COMPARATIVE PERFORMANCE PARAMETERS OF PID CONTROLLER [BIDIRECTIONAL SEPIC]

Attributes	Symbols	PID Controllers			
		Conventional PID	<i>FA-IAE</i>	<i>PSO-ITSE</i>	<i>ACOR-ITSE</i>
Performance Parameters	%OS	10.8875	0.3212	0.2674	0.2245
	Tr (sec)	0.1070	0.0785	0.0790	0.0693
	Ts (sec)	0.8173	0.1349	0.1362	0.1202
	Peak Amplitude	1.1089	1.0032	1.0027	1.0022
Gain Values	Kp	415.212	827.5014	884.5768	881.4950
	Ki	1294.1967	209.9814	213.99	203.5099
	Kd	2.127	2.9901	5.2295	1.1169

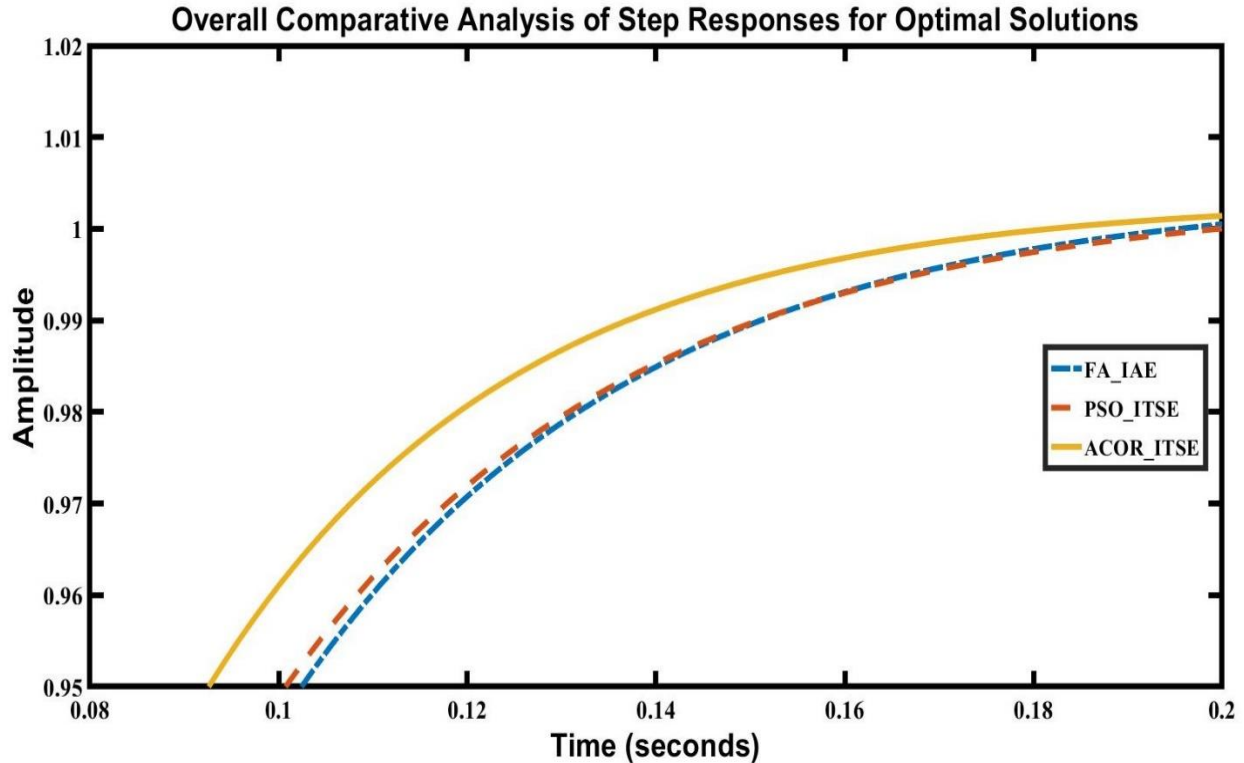


Fig. 6.47. Overall Comparative Step Response Analysis of PID Controller (Bidirectional SEPIC Converter)

By the observation from Table 6.21 and Fig. 6.47, it is evident that ACO_R -ITSE performs better in terms of percentage of overshoot (0.2245%), rise time (0.0693 sec), settling time (0.1202 sec), and peak amplitude (1.0022). Fig. 6.48 depicts an overall comparative chart of optimum PID controller for bidirectional SEPIC converter.

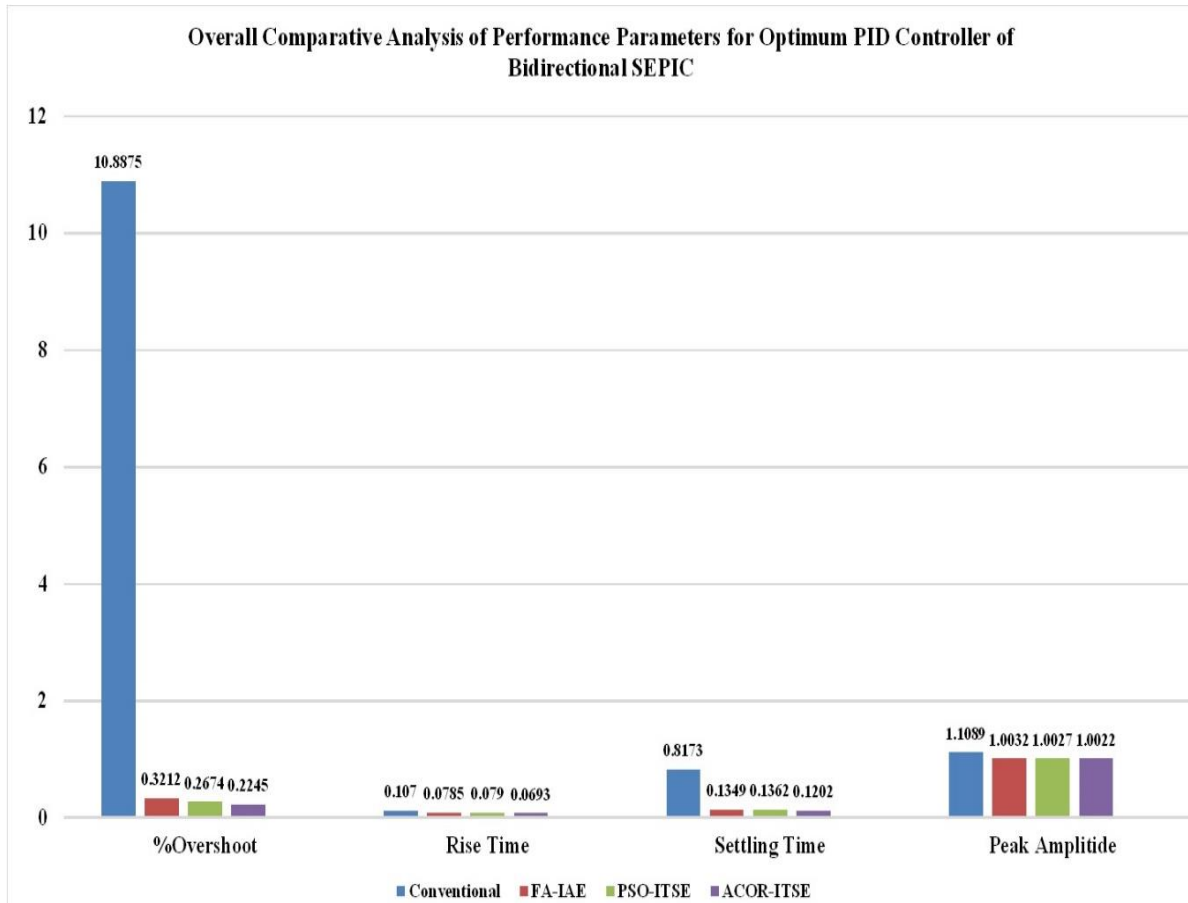


Fig. 6.48. Overall Comparative Chart of Optimum PID Controller (Bidirectional SEPIC Converter)

6.4 Interleaved SEPIC Converter

6.4.1. Open-Loop Response

Using Simulink, the circuit for Interleaved SEPIC has been designed, which is depicted in Fig. 6.49. With the help of the system identification toolbox, the transfer function for the open-loop system has been obtained through exploring the input and output data from Simulink, with four poles and three zeros. Table 6.22 presents the parameters of Interleaved SEPIC converter that have been used in the simulation.

TABLE 6.22. PARAMETERS OF INTERLEAVED SEPIC CONVERTER

Variable Name	Symbol	Value
Input Voltage	V_{in}	20 V
Output Voltage	V_o	20 V
Duty Cycle	D	50%
Switching Frequency	f_s	100 kHz
Inductor	L_1, L_2, L_3, L_4	$366 \mu\text{H}$
Capacitor	C_1, C_2	$1.9 \mu\text{F}$
Load Capacitor	V_{c1}	$470 \mu\text{F}$
Load Resistance	R	20Ω

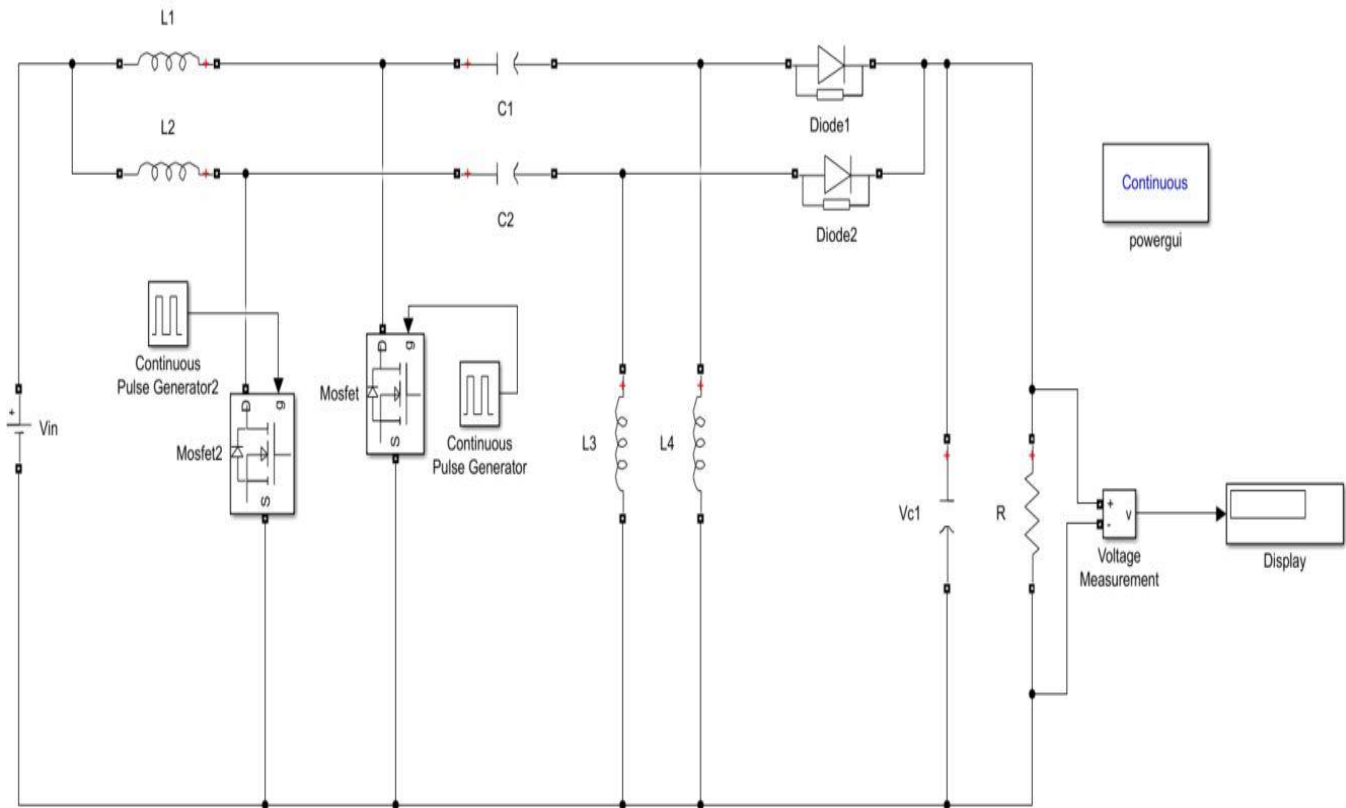


Fig. 6.49. Model of Open-Loop Interleaved SEPIC by Simulink

The transfer function of the open-loop Interleaved SEPIC converter is as follows:

$$\frac{-0.001328s^3 + 1.21 \times 10^{-5}s^2 + 2.438 \times 10^{-9}s + 9.775 \times 10^{-14}}{s^4 + 0.003659s^3 + 7.64 \times 10^{-6}s^2 + 1.374 \times 10^{-9}s + 1.013 \times 10^{-13}}$$

The step response for open-loop system of Interleaved SEPIC converter is depicted in Fig. 6.50.

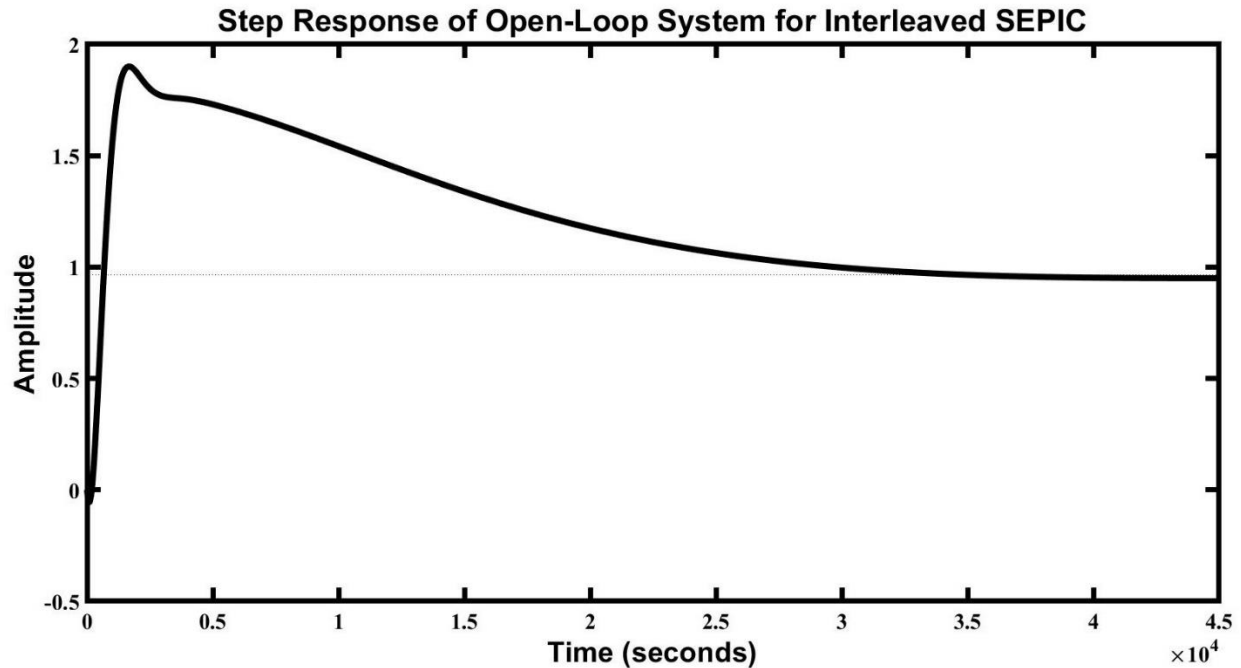


Fig. 6.50. Step Response of Open-Loop Interleaved Converter

From the step response shown in Fig. 6.50, it is observed that the percentage of overshoot is 96.9095%, rise time is 362.0327 seconds, settling time is 31495.0 seconds, and peak amplitude is 1.9001. So, it can be said that overshoot is very high for this open-loop response which must be reduced for having the safe application of the converters.

6.4.2. Closed-Loop Response with PID Controller

To improve the system's performance, closed-loop techniques are used in many aspects. In our research, we used PID controller for the closed-loop system. The circuit for closed-loop unidirectional SEPIC with conventional PID controller has been designed in Simulink, which is depicted in Fig. 6.51. Then, the controller was then manually adjusted using the MATLAB PID Tuner App, yielding gain values ($K_P = -7357.6859$, $K_I = -11950.1831$, $K_D = -61.2834$) for the typical PID controller. Afterward, a step response, as shown in Fig. 6.51, is examined for its many properties in order to determine the system's stabilization.

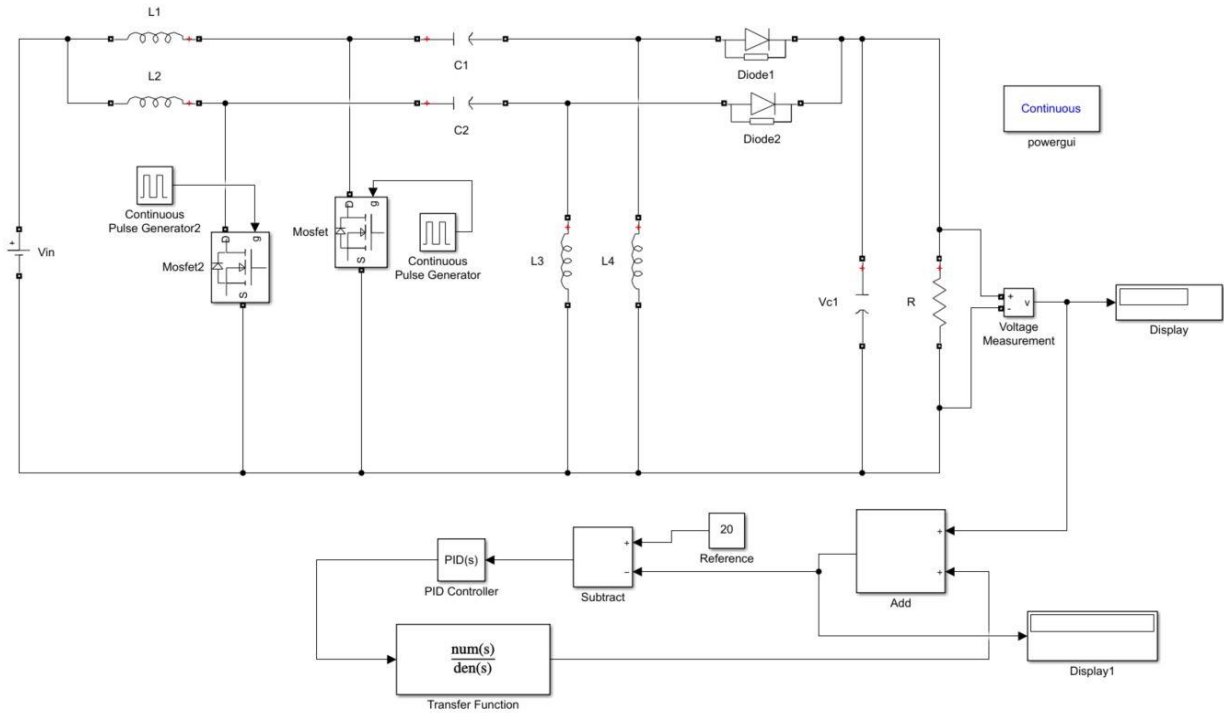


Fig. 6.51. Step Response of Closed-Loop Interleaved Converter with PID Controller

The transfer function of Interleaved SEPIC converter is as follows:

$$\frac{0.08138s^5 + 9.77s^4 + 15.78s^3 - 0.1446s^2 - 2.914 \times 10^{-5}s - 1.168 \times 10^{-9}}{1.081s^5 + 9.774s^4 + 15.78s^3 - 0.1446s^2 - 2.914 \times 10^{-5}s - 1.168 \times 10^{-9}}$$

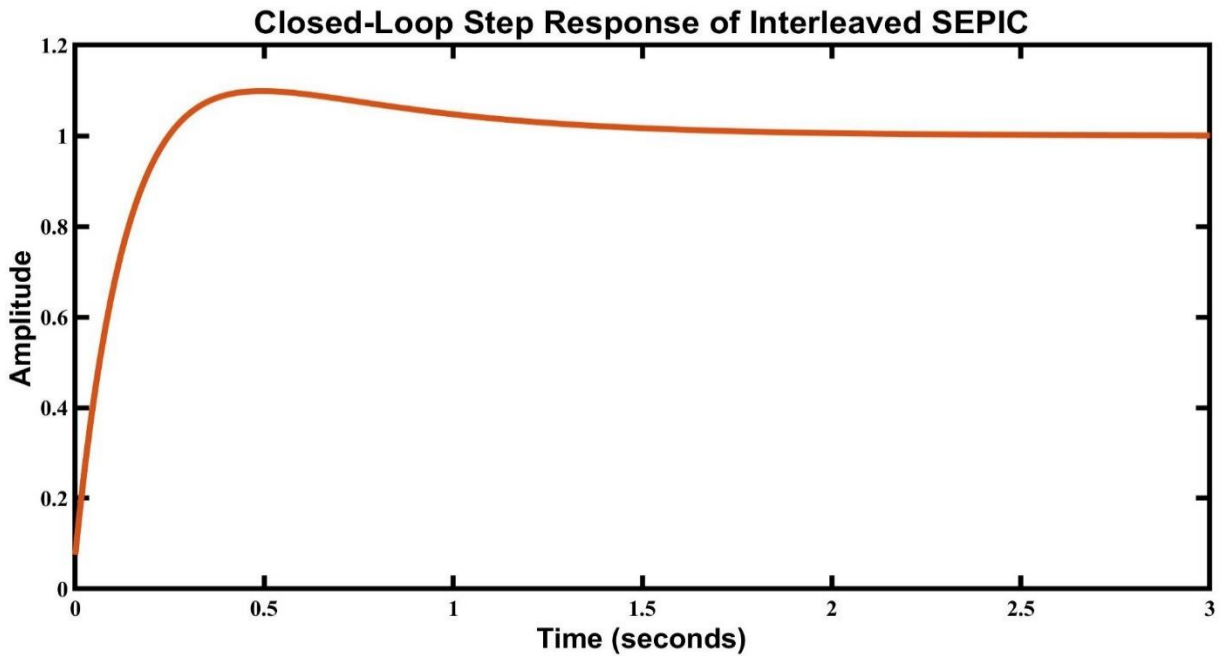


Fig. 6.52. Step Response of Closed-Loop System with Conventional PID of Bidirectional SEPIC

The step response shown in Fig. 6.52 shows that the percentage of overshoot is 9.8756%, rise time is 0.1749 seconds, settling time is 1.4553 seconds, and peak amplitude is 1.0988. These values are less than the open-loop system but not so good as expected. Therefore, the performance parameters; Percentage of Overshoot (%OS), Rise Time (T_r), Settling Time (T_s), and Peak Amplitude are tabulated for both open-loop and closed-loop analysis, which is presented in Table 6.23.

TABLE 6.23. PERFORMANCE ANALYSIS OF OPEN-LOOP AND CLOSED-LOOP RESPONSE [INTERLEAVED SEPIC]

Performance Parameters	Open-Loop Response	Closed-Loop Response
%OS	96.9095	9.8756
T_r (sec)	362.0327	0.1749
T_s (sec)	314950	1.4553
Peak Amplitude	1.9001	1.0988

6.4.3. Swarm Intelligence Algorithms based PID Controller

Though the closed-loop system with conventional PID controller provides better performance than the open-loop system, it is not good enough. So, bio-inspired swarm intelligence optimization algorithms are employed in the controller to reduce overshoot, get faster rise time and settling time. Moreover, step responses are observed, and gain values along with performance parameters are tabulated for FA-PID, PSO-PID, and ACO_R-PID.

6.4.3.1. FA-PID Controller

The Firefly Algorithm is first applied to have the optimized gain values for the controller. Then, the same parameters of firefly algorithm stated in Table 6.3 have been used in Interleaved SEPIC converter. In comparison to the gain values of the traditional PID controller, improved values of the gain parameters for the four performance indices (IAE, ISE, ITSE, ITAE) of the FA-PID controller have been attained after several simulations in MATLAB, as shown in Table 6.24. The step responses of the FA-PID controller's IAE, ISE, ITSE, and ITAE for Interleaved SEPIC Converter are shown in Figures 6.53, 6.54, 6.55, and 6.56, respectively.

TABLE 6.24. GAIN VALUES OF FA-PID CONTROLLER FOR INTERLEAVED SEPIC

Gains	FA-PID			
	IAE	ISE	ITSE	ITAE
K _p	-8989.1	-8976.3	-8997.1	-8859.3
K _i	-9630.3	-8118.9	-8767.5	-13789
K _d	-58.8220	-776868	-28.8978	-37.3095

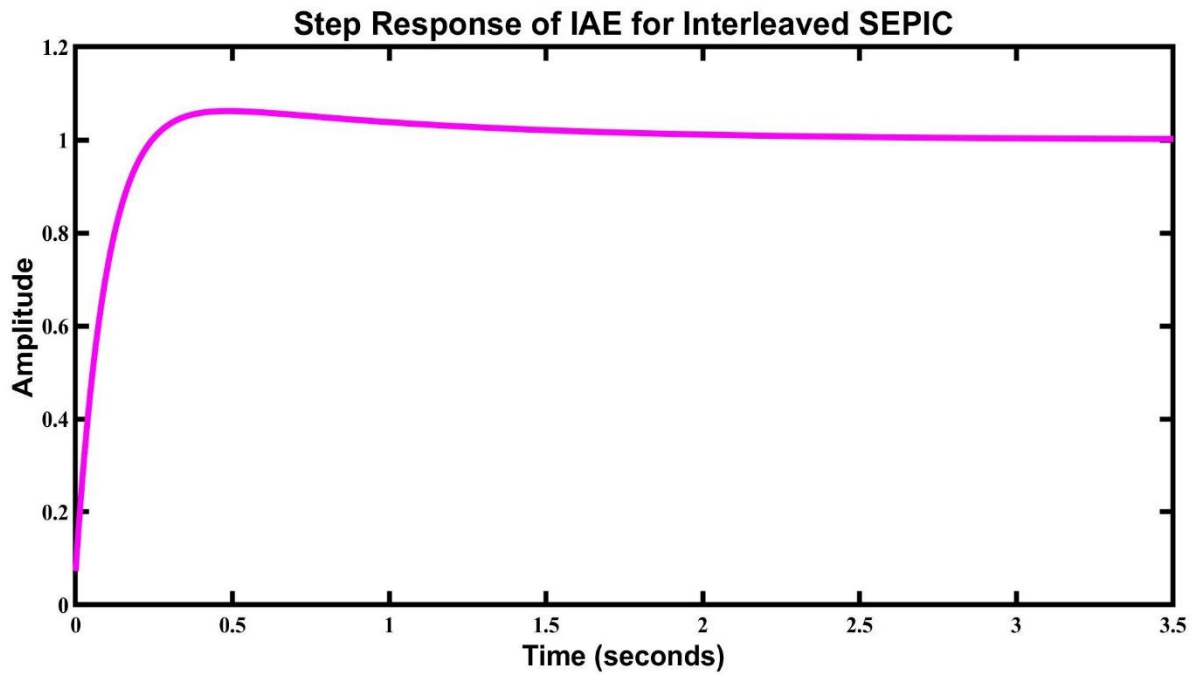


Fig. 6.53. Step Response of IAE for FA-PID (Interleaved SEPIC Converter)

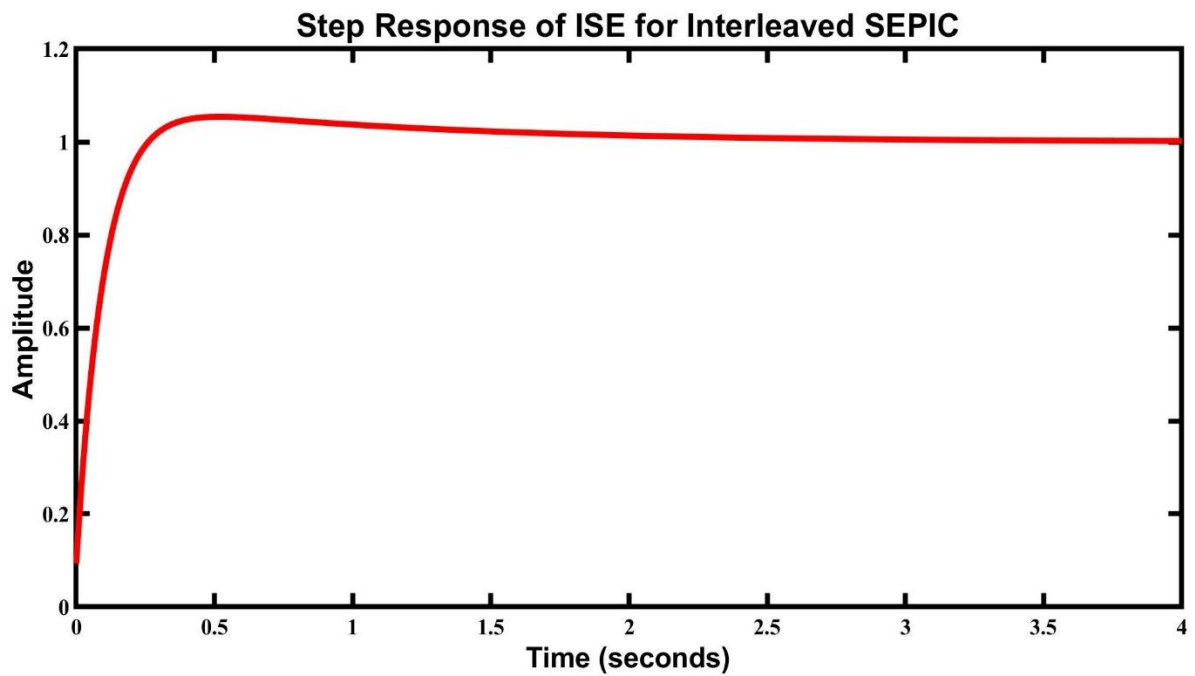


Fig. 6.54. Step Response of ISE for FA-PID (Interleaved SEPIC Converter)

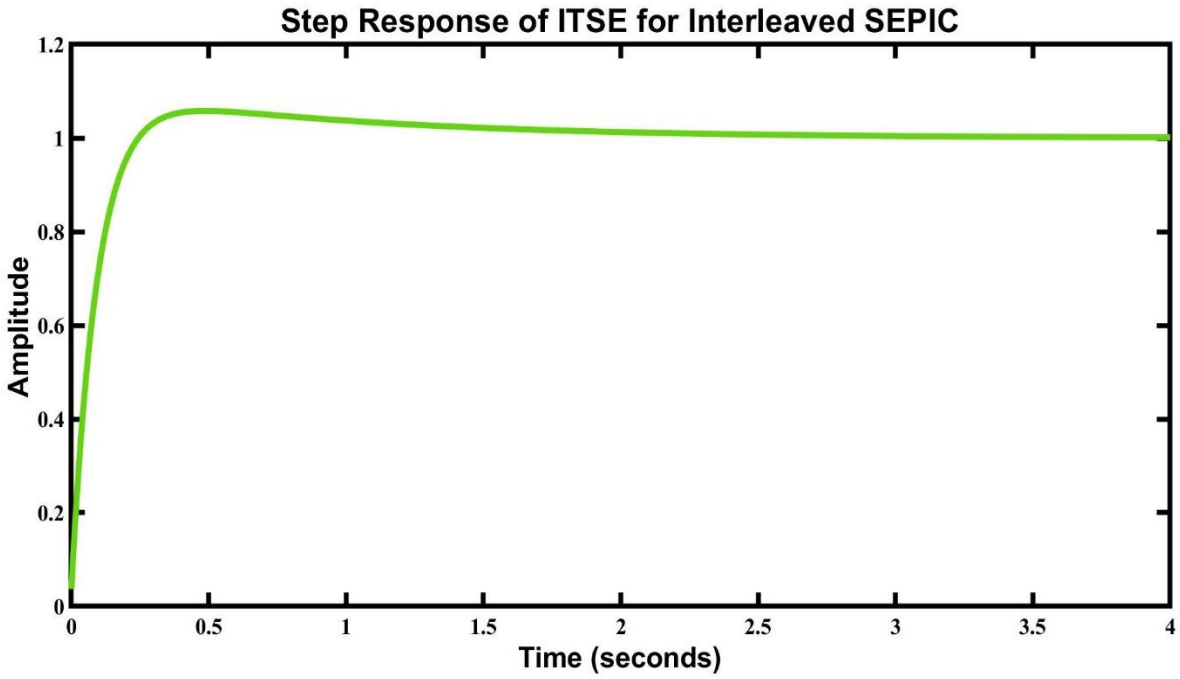


Fig. 6.55. Step Response of ITSE for FA-PID (Interleaved SEPIC Converter)

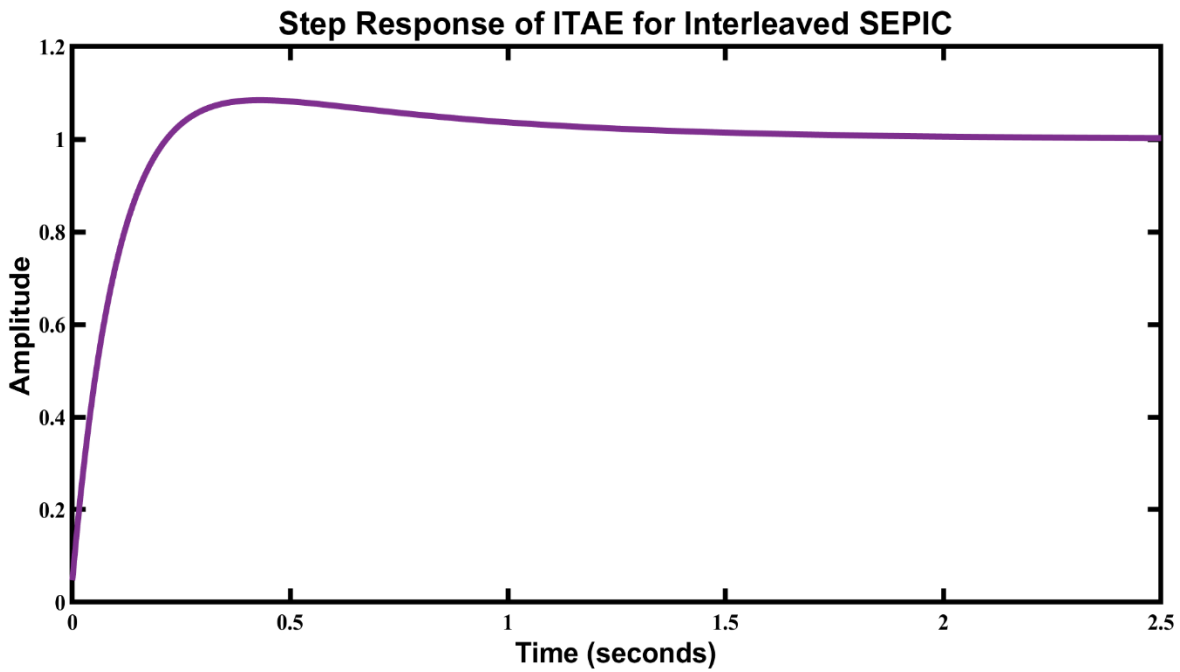


Fig. 6.56. Step Response of ITAE for FA-PID (Interleaved SEPIC Converter)

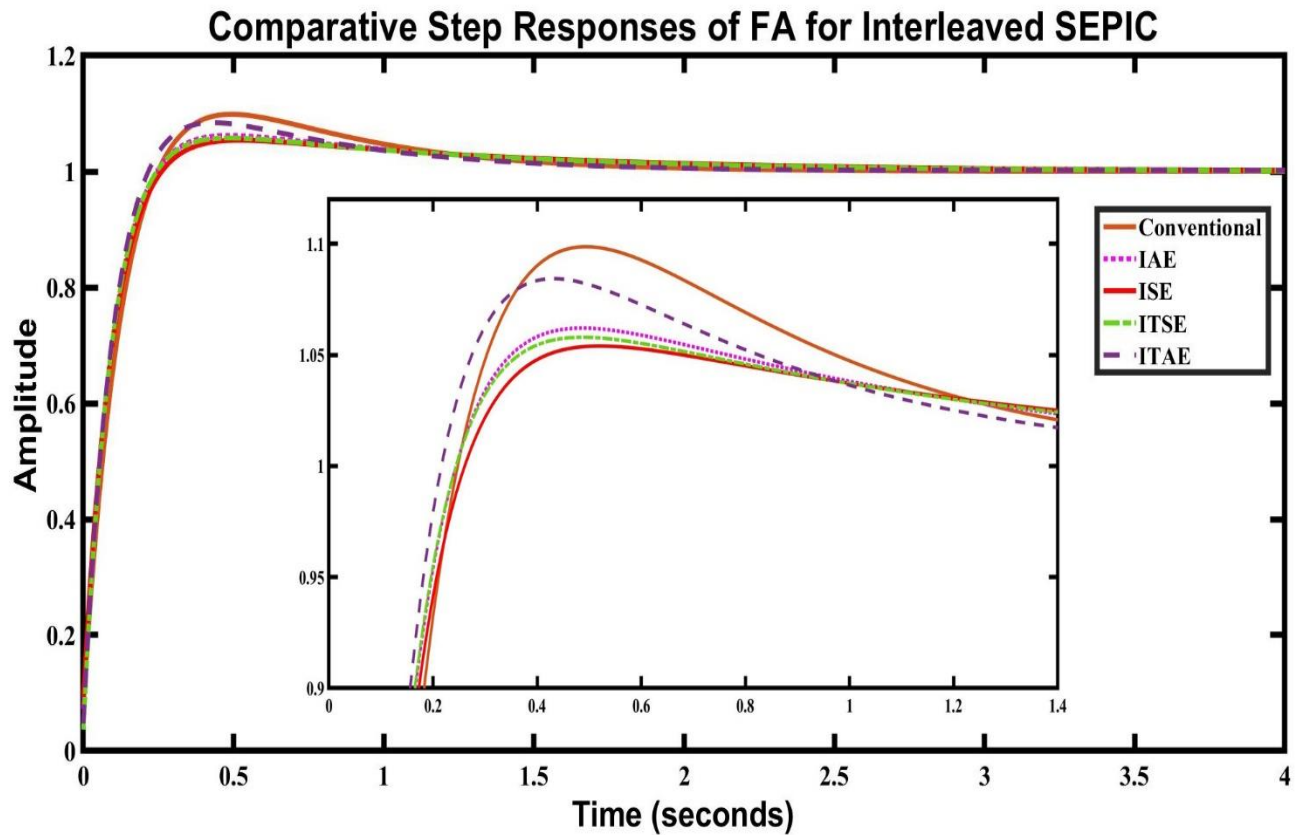


Fig. 6.57. Comparative Analysis of Step Responses for FA-PID (Interleaved SEPIC Converter)

The performance parameters such as Percentage of Overshoot (%OS), Rise Time (Tr), Settling Time (Ts), and Peak Amplitude are tabulated for FA-PID which is presented in Table 6.25.

TABLE 6.25. PERFORMANCE PARAMETERS OF CONVENTIONAL AND FA-PID CONTROLLER FOR INTERLEAVED SEPIC

Performance Parameters	Conventional PID	FA-PID			
		IAE	ISE	ITSE	ITAE
%OS	9.8756	6.2126	5.4021	5.7994	8.4361
Tr (sec)	0.1749	0.1608	0.1684	0.1579	0.1488
Ts (sec)	1.4553	1.6013	1.7243	1.6142	1.3481
Peak Amplitude	1.0988	1.0621	1.0540	1.0580	1.0844

By the observation from Fig. 6.57 and Table 6.25, it is visible that FA-PID of ISE performs better than conventional PID and other fitness functions in percentage of overshoot and peak amplitude. FA-PID of ITAE performs better in terms of settling time and rise time. Fig. 6.58 depicts the comparative chart of performance parameters for FA-PID for the Interleaved SEPIC.

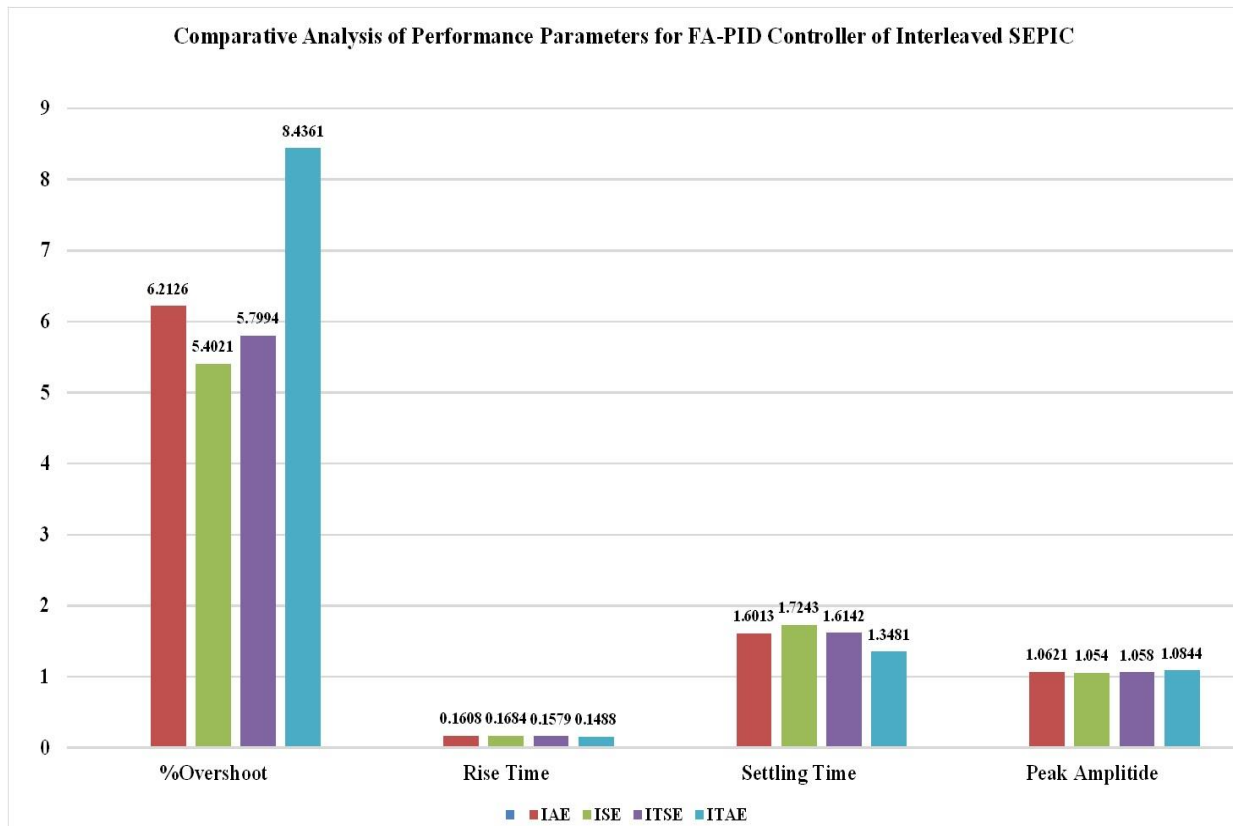


Fig. 6.58. Comparative Chart of Performance Parameters for FA-PID (Interleaved SEPIC Converter)

6.4.3.2. PSO-PID Controller

The Particle Swarm Optimization (PSO) is applied to have the optimized gain values for the controller. The same parameters of the particle swarm optimization algorithm stated in Table 6.6 has been used in bidirectional SEPIC converter. In comparison to the gain values of the conventional PID controller, improved values of the gain parameters for the four performance indices (IAE, ISE, ITSE, ITAE) of the PSO-PID controller have been attained after several simulations in MATLAB, as shown in Table 6.26. The step responses of the PSO-PID controller's IAE, ISE, ITSE, and ITAE for bidirectional SEPIC Converter are shown in Figs. 6.59, 6.60, 6.61, and 6.62, respectively.

TABLE 6.26. GAIN VALUES OF PSO-PID CONTROLLER FOR INTERLEAVED SEPIC

Gains	PSO-PID			
	IAE	ISE	ITSE	ITAE
Kp	-8624.2	-8808.1	-8898.1	-8923.3
Ki	-12130	-8156.7	-7556.3	-13973
Kd	-83.6360	-87.5893	-43.3105	-32.6779

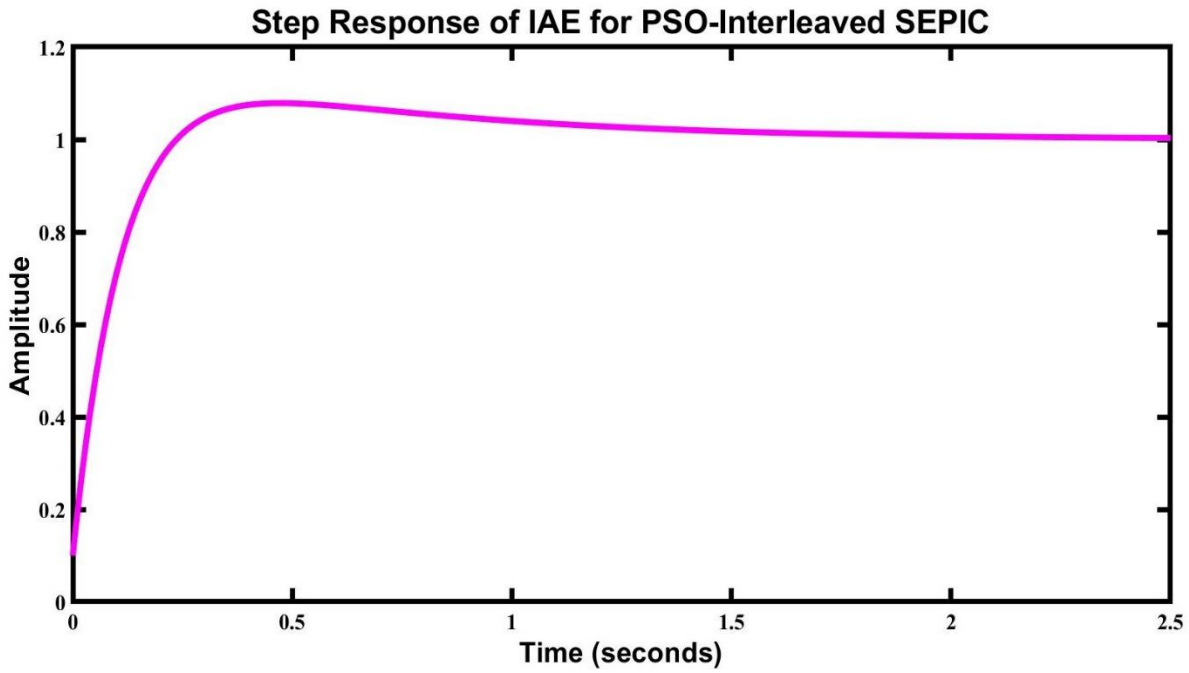


Fig. 6.59. Step Response of IAE for PSO-PID (Interleaved SEPIC Converter)

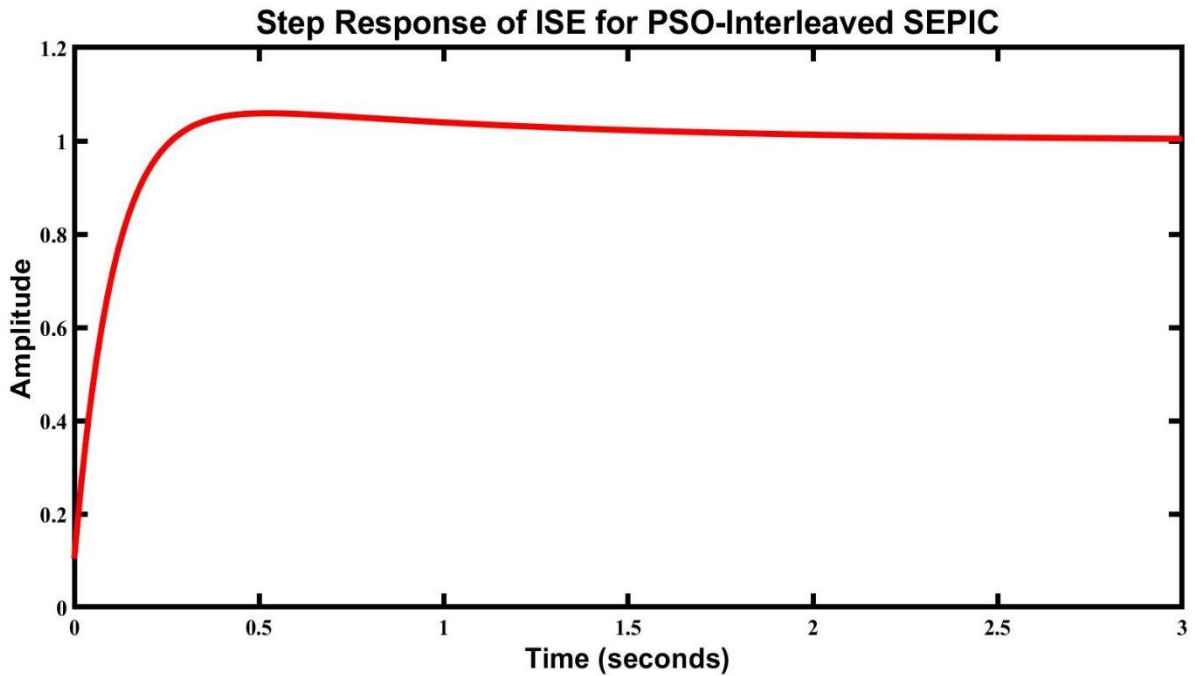


Fig. 6.60. Step Response of ISE for PSO-PID (Interleaved SEPIC Converter)

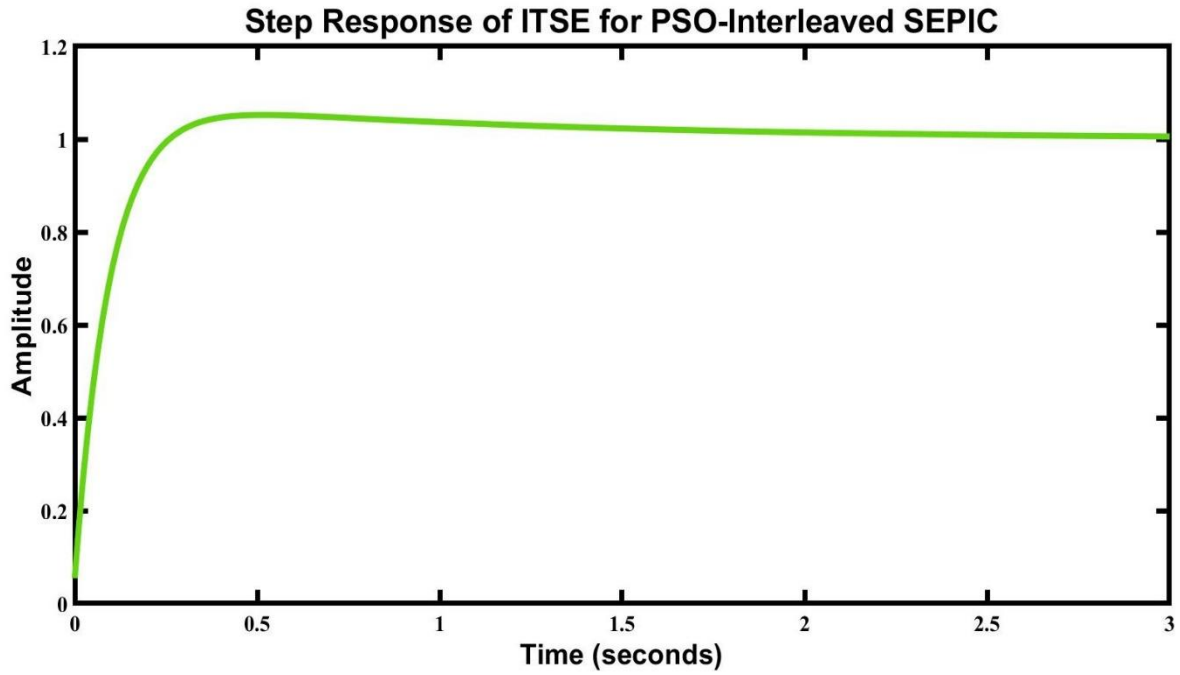


Fig. 6.61. Step Response of ITSE for PSO-PID (Interleaved SEPIC Converter)

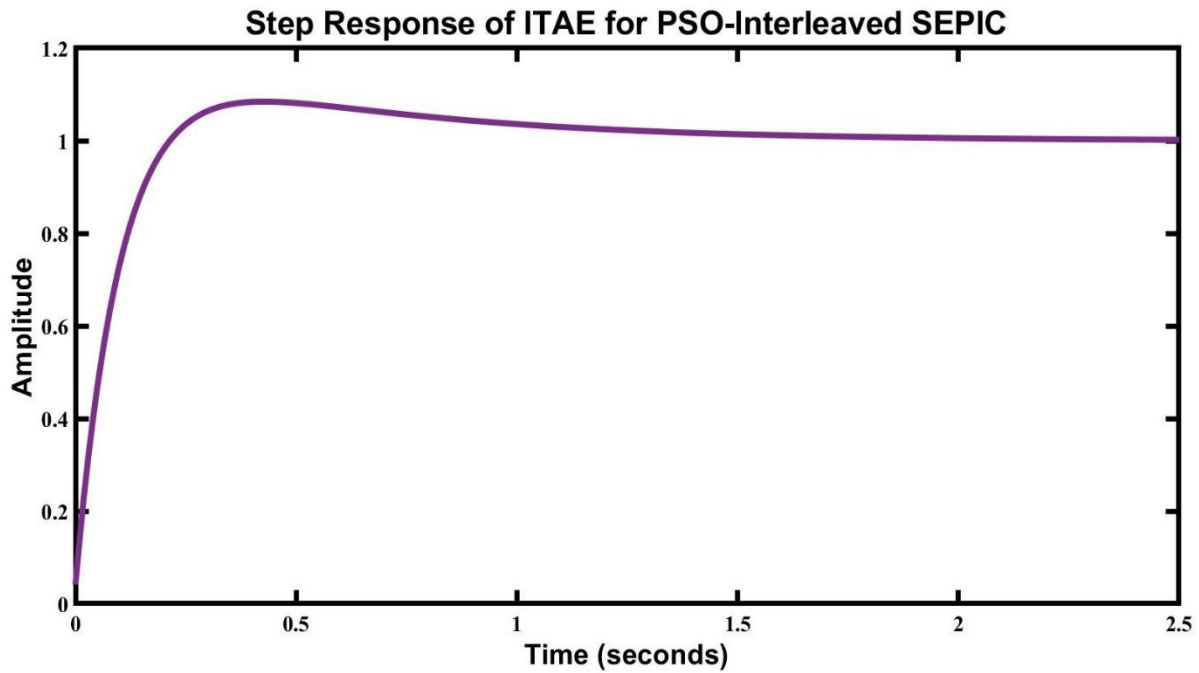


Fig. 6.62. Step Response of ITAE for PSO-PID (Interleaved SEPIC Converter)

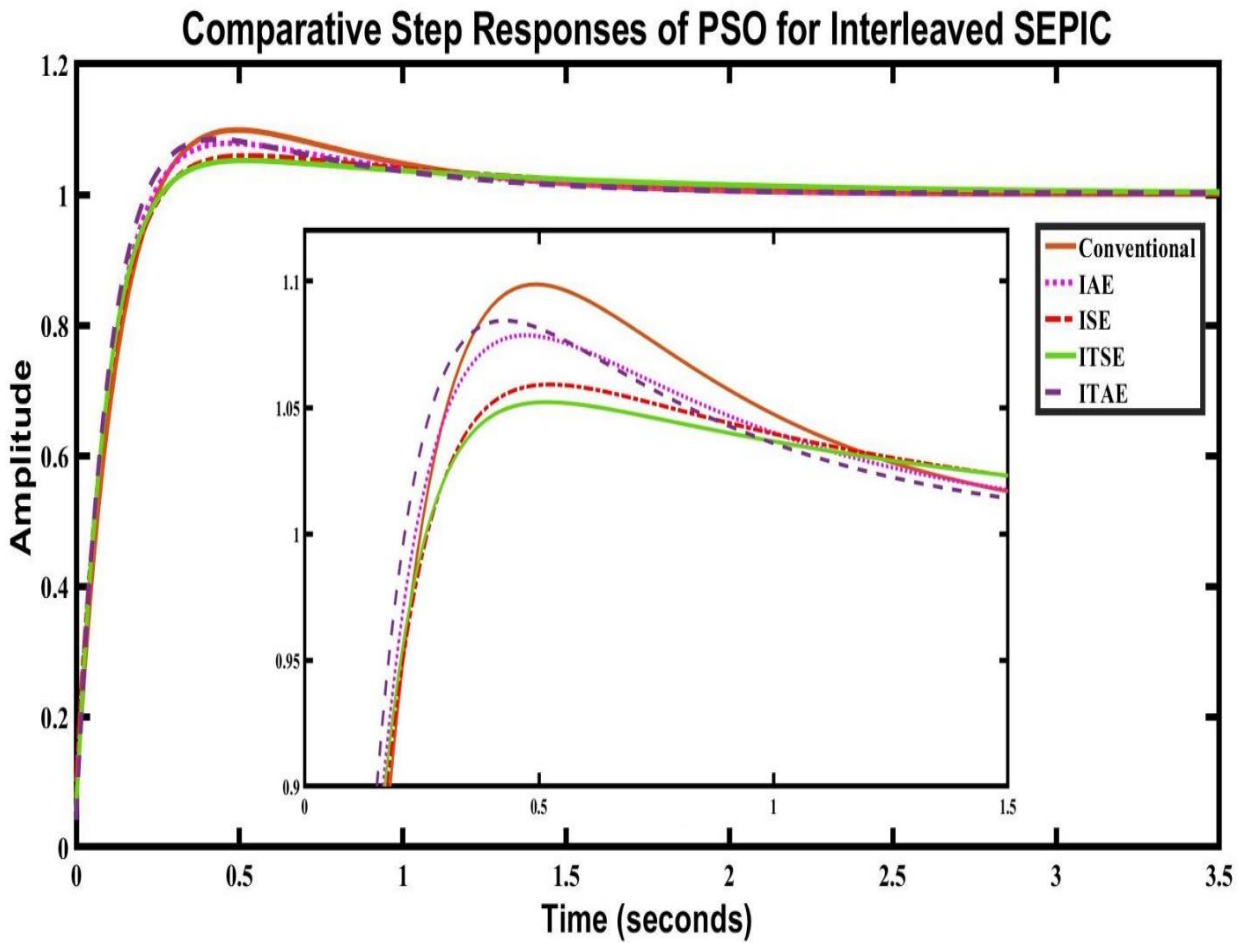


Fig. 6.63. Comparative Analysis of Step Responses for PSO-PID (Interleaved SEPIC Converter)

The performance parameters such as Percentage of Overshoot (%OS), Rise Time (T_r), Settling Time (T_s), and Peak Amplitude are tabulated for PSO-PID which is presented in Table 6.27.

TABLE 6.27. PERFORMANCE PARAMETERS OF CONVENTIONAL AND PSO-PID CONTROLLER [INTERLEAVED SEPIC]

Performance Parameters	Conventional PID	PSO-PID			
		<i>IAE</i>	<i>ISE</i>	<i>ITSE</i>	<i>ITAE</i>
%OS	9.8756	7.8590	5.9105	5.2104	8.4425
T_r (sec)	0.1749	0.1624	0.1726	0.1651	0.1471
T_s (sec)	1.4553	1.4785	1.7247	1.7144	1.3354
Peak Amplitude	1.0988	1.0786	1.0591	1.0521	1.0844

The observation from Fig. 6.63 and Table 6.27 clearly shows that PSO-PID of ITSE performs better than conventional PID and other fitness function in the percentage of overshoot and peak amplitude. PSO-PID of ITAE performs better in terms of rise time and settling time. Fig. 6.64 depicts the comparative chart of performance parameters for PSO-PID for Interleaved SEPIC.

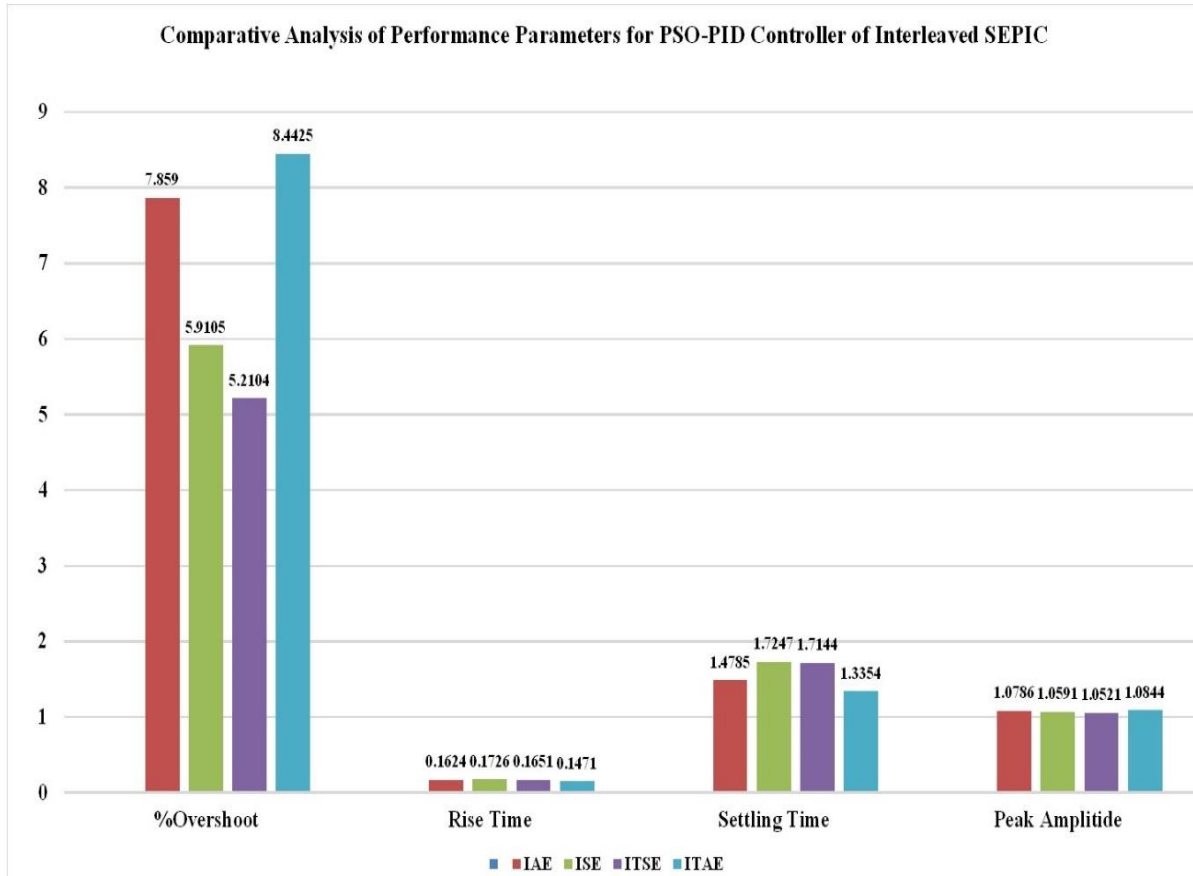


Fig. 6.64. Comparative Chart of Performance Parameters for PSO-PID (Interleaved SEPIC Converter)

6.4.3.3. ACO_R-PID Controller

The Ant Colony Optimization for continuous domain (ACO_R) is applied to have the controller's optimized gain values. The same parameters of ant colony optimization algorithm for continuous domain stated in Table 6.9 have been used in Interleaved SEPIC converter. In comparison to the gain values of the conventional PID controller, improved values of the gain parameters for the four performance indices (IAE, ISE, ITSE, ITAE) of the ACO_R-PID controller have been attained after several simulations in MATLAB, as shown in Table 6.28. The step responses of the ACO_R-PID controller's IAE, ISE, ITSE, and ITAE for Interleaved SEPIC Converter are shown in Figures 6.65, 6.66, 6.67, and 6.68, respectively.

TABLE 6.28. GAIN VALUES OF ACO_R-PID CONTROLLER FOR INTERLEAVED SEPIC

Gains	ACO _R -PID			
	<i>IAE</i>	<i>ISE</i>	<i>ITSE</i>	<i>ITAE</i>
K _p	-8992.6	-8974.3	-8833.3	-8999.5
K _i	-11144	-8472.9	-9595.9	-13946
K _d	-48.4142	-85.1738	-90.2914	-52.1138

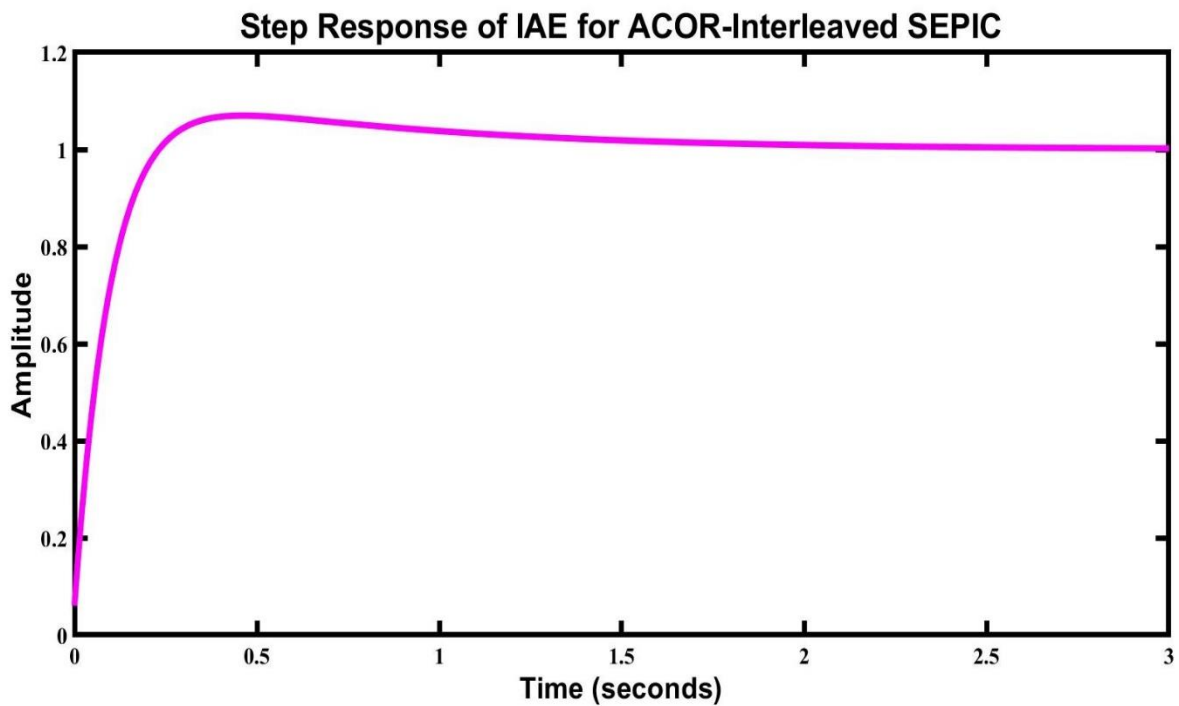


Fig. 6.65. Step Response of IAE for ACO_R-PID (Interleaved SEPIC Converter)

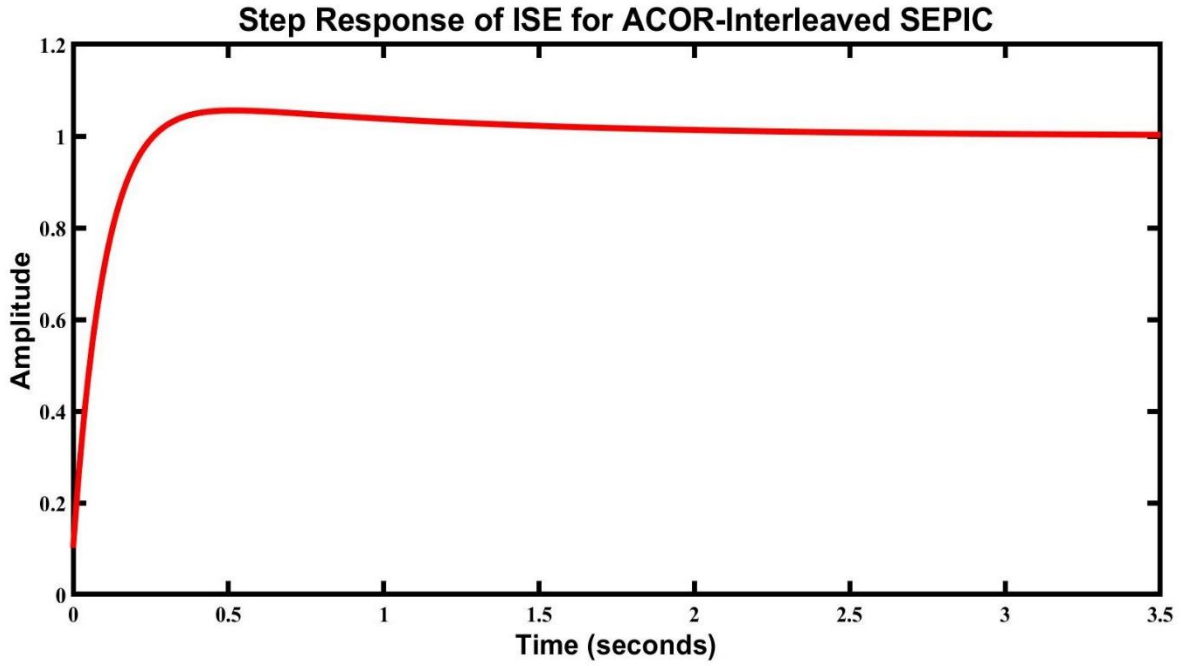


Fig. 6.66. Step Response of ISE for ACOR-PID (Interleaved SEPIC Converter)

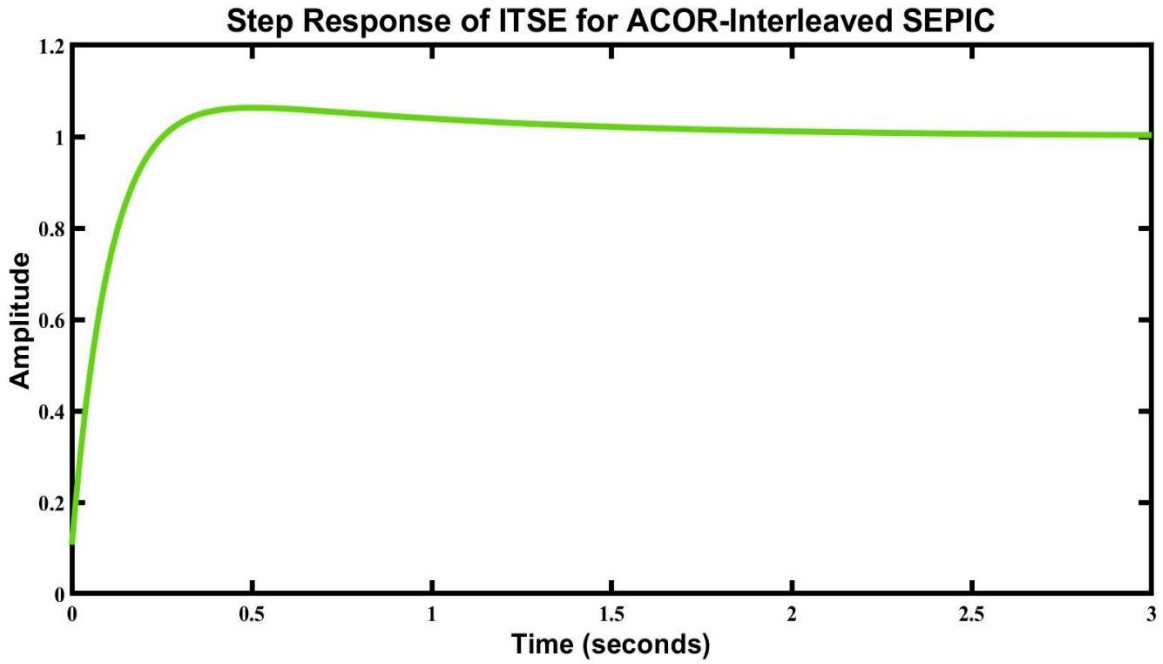


Fig. 6.67. Step Response of ITSE for ACOR-PID (Interleaved SEPIC Converter)

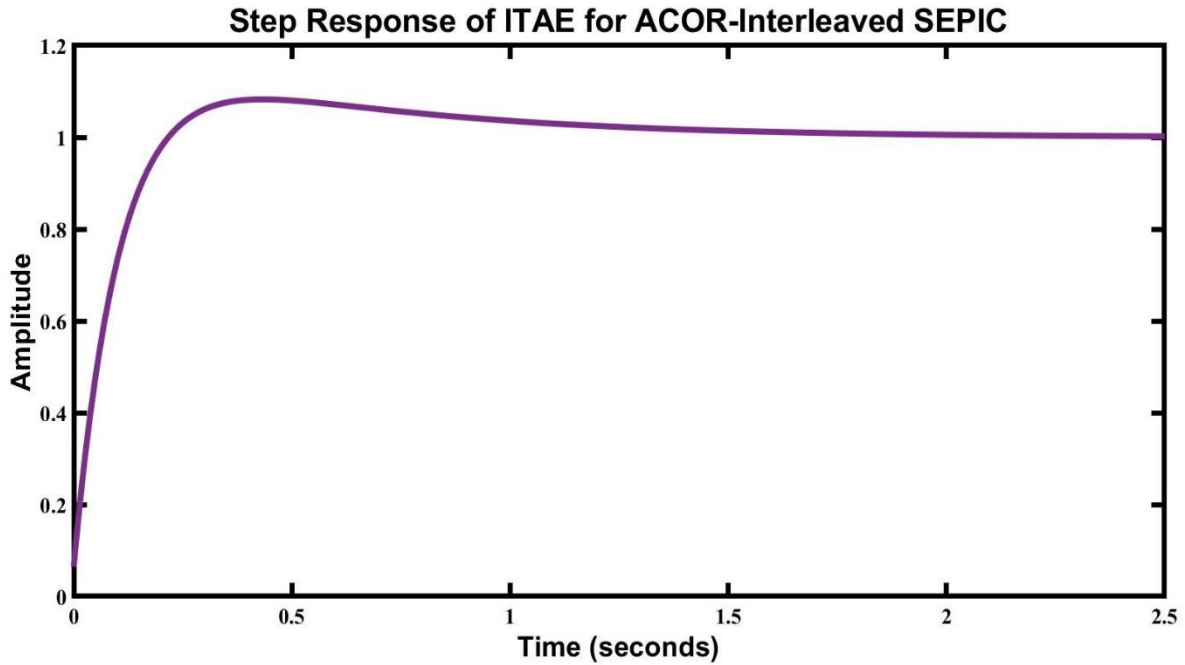


Fig. 6.68. Step Response of ITAE for $ACOR_R$ -PID (Interleaved SEPIC Converter)

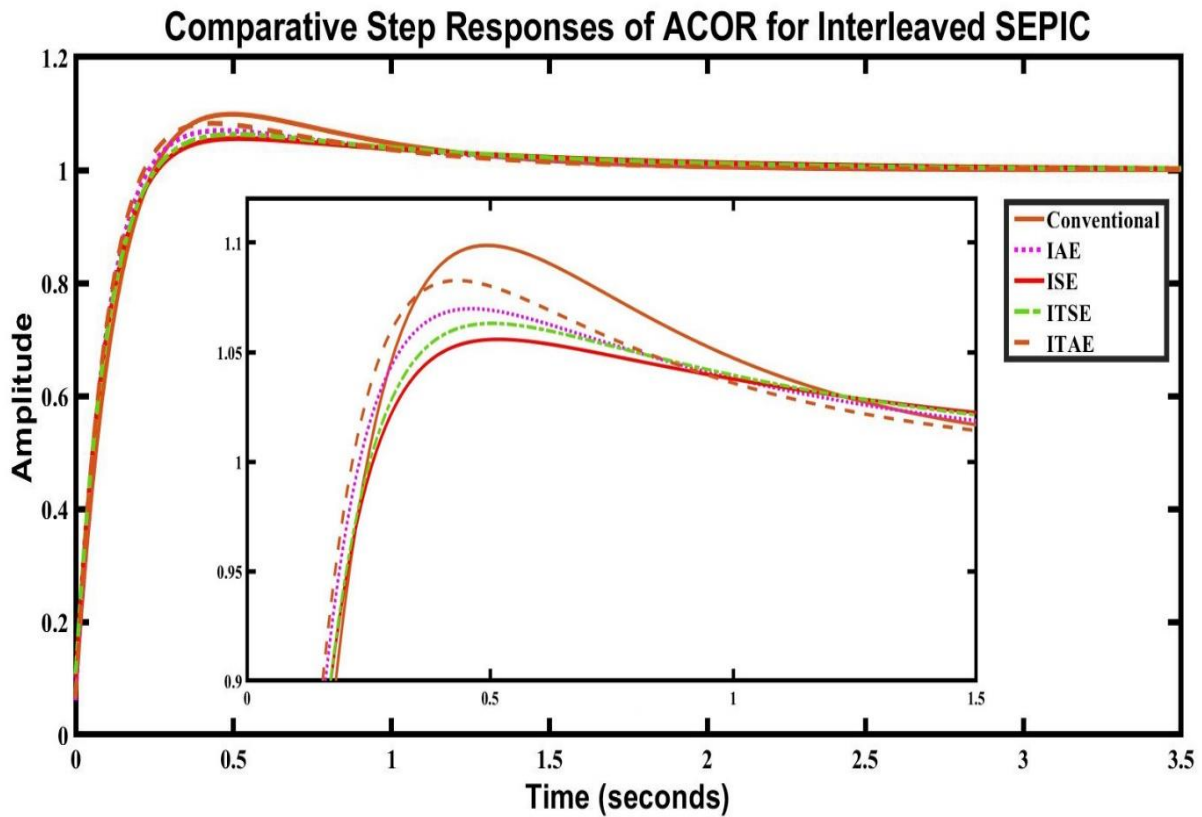


Fig. 6.69. Comparative Analysis of Step Responses for $ACOR_R$ -PID (Interleaved SEPIC Converter)

The performance parameters such as Percentage of Overshoot (%OS), Rise Time (Tr), Settling Time (Ts), and Peak Amplitude are tabulated for ACO_R-PID which is presented in Table 6.29.

TABLE 6.29. PERFORMANCE PARAMETERS OF CONVENTIONAL AND ACO_R-PID CONTROLLER [INTERLEAVED SEPIC]

Performance Parameters	Conventional PID	ACO _R -PID			
		<i>IAE</i>	<i>ISE</i>	<i>ITSE</i>	<i>ITAE</i>
%OS	9.8756	6.9845	5.5839	6.3136	8.2717
Tr (sec)	0.1749	0.1552	0.1687	0.1680	0.1493
Ts (sec)	1.4553	1.4984	1.7112	1.6470	1.3530
Peak Amplitude	1.0988	1.0698	1.0558	1.0631	1.0827

By the observation from Fig. 6.69 and Table 6.29, it is visible that ACO_R-PID of ISE performs better than conventional PID and other fitness functions in percentage of overshoot and peak amplitude. ACO_R-PID of ITAE performs better in terms of rise time and settling time. Fig. 6.70 depicts the comparative chart of performance parameters for ACO_R-PID.

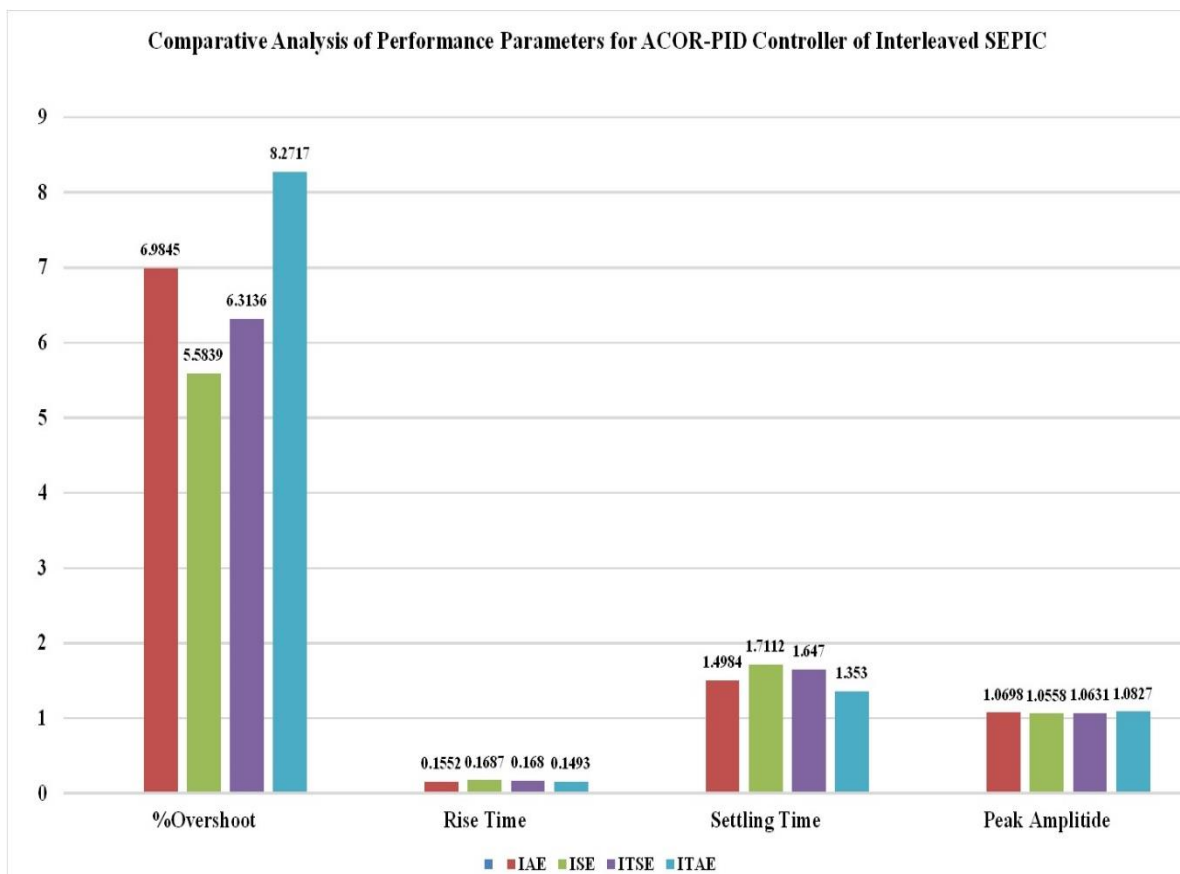


Fig. 6.70. Comparative Chart of Performance Parameters for ACO_R-PID (Interleaved SEPIC Converter)

6.4.3.4. Comparative Analysis

After implementing all three swarm intelligence optimization algorithms in Interleaved SEPIC converter, a comparison of performance parameters for optimum PID controller is shown in Table 6.30 based on the better performing fitness function of Table 6.25, 6.27, 6.29. Furthermore, an overall comparative analysis of step responses is shown in Fig. 6.70 based on the best performing gain values for the Interleaved SEPIC converter.

TABLE 6.30. COMPARATIVE PERFORMANCE PARAMETERS OF PID CONTROLLER (INTERLEAVED SEPIC CONVERTER)

Attributes	Symbols	PID CONTROLLER			
		Conventional PID	<i>FA-ISE</i>	<i>PSO-ITSE</i>	<i>ACOR-ISE</i>
Performance Parameters	%OS	9.8756	5.4021	5.2104	5.5839
	Tr (sec)	0.1749	0.1684	0.1651	0.1687
	Ts (sec)	1.4553	1.7243	1.7144	1.7112
	Peak Amplitude	1.0988	1.0540	1.0521	1.0558
Gain Values	Kp	-7357.6859	-8976.3	-8898.1	-8974.3
	Ki	-11950.1831	-8118.9	-7556.3	-8472.3
	Kd	-61.2834	-77.6868	-43.3105	-85.1738

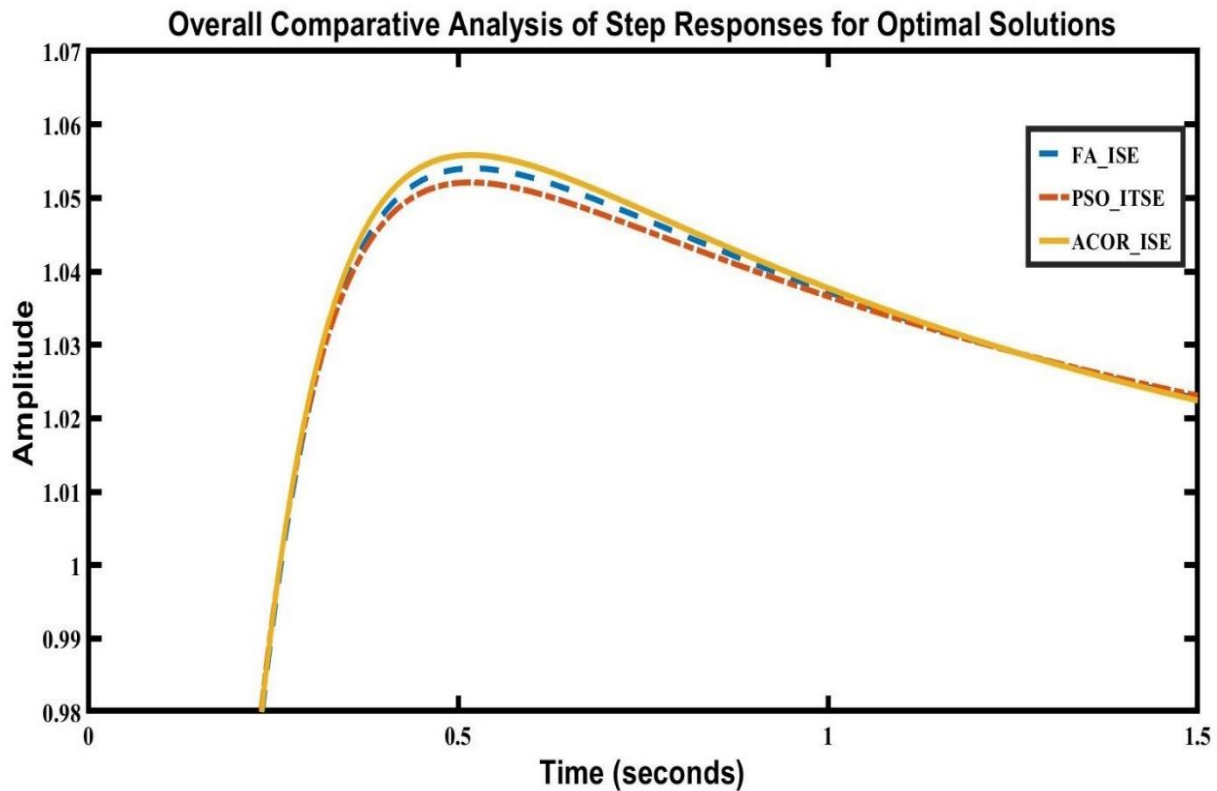


Fig. 6.71. Overall Comparative Step Response Analysis of PID Controller (Interleaved SEPIC Converter)

By the observation from Table 6.31 and Fig. 6.71, it is evident that $ACOR$ -ITSE performs better in terms of percentage of overshoot (0.2245%), rise time (0.0693 sec), settling time (0.1202 sec), and peak amplitude (1.0022). Fig. 6.72 depicts an overall comparative chart of optimum PID controller for bidirectional SEPIC converter.

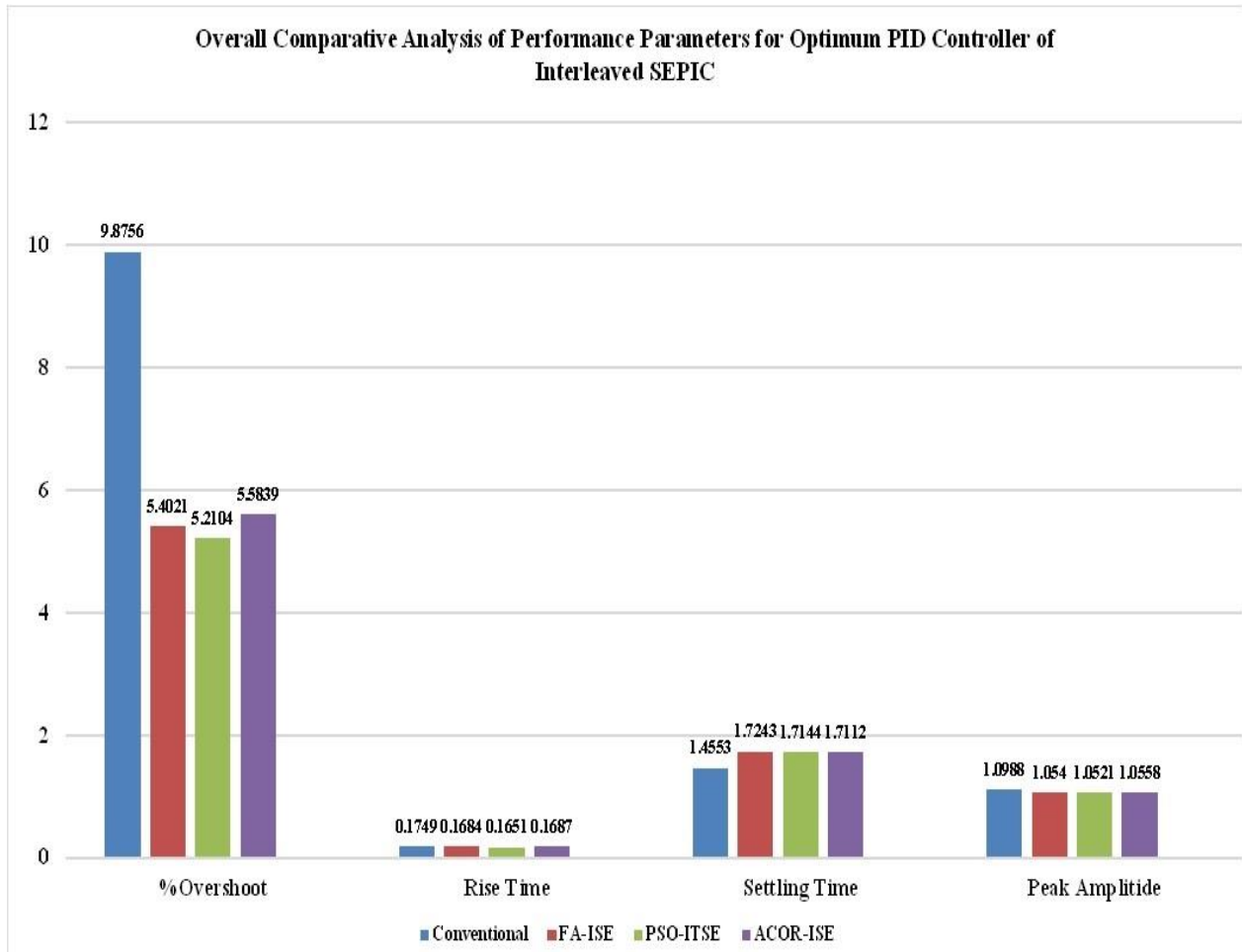


Fig. 6.72. Overall Comparative Chart of Optimum PID Controller (Interleaved SEPIC Converter)

CHAPTER 7

CONCLUSION AND FUTURE WORKS

7.1 Synopsis

This thesis focuses on optimizing the PID controller by implementing three types of Swarm Intelligence Algorithms for achieving better performance parameters and responses of Unidirectional SEPIC, Bidirectional SEPIC, and Interleaved SEPIC converter. Performance parameters named IAE, ITAE, ISE, and ITSE are used as objective functions to investigate the stability of the converters. **In Chapter 2**, different types of existing widely used dc-dc converters have been discussed. The methods and analysis dc-dc converters have also been presented in detail. **Chapter 3** has referred to the study of three different types of SEPIC converters: Unidirectional SEPIC, Bidirectional SEPIC and Interleaved SEPIC, with the illustration of State Space Modeling of the converters. Then, open-loop and closed-loop analyses of the converter were carried out. **Chapter 4** has demonstrated the overview of three different Swarm Intelligence Algorithms and an elaborate discussion has been reported about Firefly Algorithm (FA), Particle Swarm Optimization (PSO), and Ant Colony Optimization for Continuous Domain (ACO_R). **Chapter 5** referred to the implementation of the algorithms for designing an optimized PID controller. The tuning of the performance parameters has been discussed, and the required objective functions are stated in a short discussion. **Chapter 6** has dealt with the simulation results of the Swarm Intelligence Algorithm-based optimized PID controller for SEPIC converter and its variants separately. The performance parameters were investigated, and graphical and comparative analyses were presented.

So, after carrying out the graphical analysis of all the step responses in chapter 5, it is observed that for the Unidirectional SEPIC converter, ACO_R-PID (ITSE) is the most optimized controller among all the algorithms based PID controllers in terms of performance parameters. In this case, overshoot (1.8603%), settling time (2.3414 sec), and peak amplitude (1.0186) are the lowest. Moreover, rise time (0.4781 sec) is also within the acceptable limit. The lowest value of rise time (0.3798 sec) is for ACO_R-PID (ITAE). Again, for the Bidirectional SEPIC converter, PSO-PID (ITSE) is the most optimized controller among all the algorithms-based PID controllers in terms of performance parameters. In this case, overshoot (0.2674%) and peak amplitude (1.0027) are the lowest. Moreover, rise time (0.0790 sec) and settling time (0.1202 sec) are also within the acceptable limit. The lowest value of rise time (0.0656 sec) is for ACO_R-PID (ITAE), and the lowest value of settling time (0.1134 sec) is for ACO_R-PID (IAE). After that, for Interleaved SEPIC converter, PSO-PID (ITSE) is the most optimized controller among all the algorithms-based PID controllers in terms of performance parameters. In this case, overshoot (5.2104%) and peak amplitude (1.0521) are the lowest. Moreover, rise time (0.1651 sec) and settling time (1.7247 sec) are also within the acceptable limit. The lowest value of rise time (0.1471 sec) and settling time (1.3354 sec) are for PSO-PID (ITAE). So, it is evident that Swarm Intelligence Algorithm based optimized PID controller provides the more optimized results and performs far better than Conventional PID controller.

7.2 Future Work

In future work, different algorithms will be implemented in designing an optimized PID controller to investigate and enhance the stability of the converters. On top of that, the three algorithms utilized in this thesis can be performed to improve the stability of other converters. So, the overall comparative analysis can be very effective in observing the stable condition for different applications in power electronics. Moreover, hardware implementation will be performed to validate and inspect the simulation results with VHDL and FPGA devices in the future

References

- [1] Fang, X., Ding, X., Zhong, S. and Tian, Y., "Improved quasi-Y-source DC-DC converter for renewable energy," *CPSS transactions on Power Electronics and Applications*, 4(2), pp. 163-170, 2019
- [2] K. R. Kishore, B. F. Wang, K. N. Kumar, and P. L. So. "A new ZVS full-bridge DC-DC converter for battery charging with reduced losses over full-load range"; *In India Conference (INDICON)*, 2015 Annual IEEE, pp. 1-6. IEEE, 2015.
- [3] C. Gobbato, S. V. Kohler, I. H. de Souza, G. W. Denardin, and J. de P. Lopes. "Integrated Topology of DC-DC Converter for LED Street Lighting System Based on Modular Drivers" *IEEE Transactions on Industry Applications* (2018).
- [4] Qun Jhao and F.C. Lee, "High-efficiency, high step-up DC-DC converters," *IEEE Transactions on Power Electronics*, vol. 18, issue. 1, pp- 65-73, Jan. 2003
- [5] C. Lai, C. Pan and Cheng, "High-Efficiency Modular High Step-Up Interleaved Boost Converter for DC-Microgrid Applications," *IEEE Transactions on Industrial Electronics*, vol. 48, no. 1, pp.161-171, Jan/Feb. 2012.
- [6] Wuhua Li and Xiangning He, "Review of Nonisolated High-Step-Up DC/DC Converters in Photovoltaic Grid-Connected Applications," *IEEE Trans. on Ind. Electron.*, vol. 58, no. 4, pp- 1239-1251, April 2011
- [7] R.G Ganesan and M. Prabhakar, "Non-isolated high gain boost converter for photovoltaic applications," *in Proc. IEEE ICPEC*, pp.277-280, 2013.
- [8] M. H. Rashid, "Power Electronics-Circuits, Devices and Applications," Third Edition 2013- 2014
- [9] Hasanpour, Sara, Alfred Baghrmian, and Hamed Mojallali. "A Modified SEPIC-Based High Step-Up DC-DC Converter with Quasi-Resonant Operation for Renewable Energy Applications." *IEEE Transactions on Industrial Electronics* 66, no. 5 (2019): 3539-3549.
- [10] Gheisarnejad, Meysam, Hamed Farsizadeh, and Mohammad Hassan Khooban. "A novel non-linear deep reinforcement learning controller for DC/DC power buck converters." *IEEE Transactions on Industrial Electronics* (2020).
- [11] Li, R. and Shi, F., "Control and optimization of residential photovoltaic power generation system with high efficiency isolated bidirectional DC-DC converter," *IEEE Access*, 7, pp. 116107-116122, 2019.
- [12] Pachauri, R. K. and Chauhan, Y. K., "Modeling and simulation analysis of PV fed Cuk, Sepic, Zeta and Luo DC-DC converter," *In 2016 IEEE 1st international conference on power electronics, intelligent control and energy systems (ICPEICES)*, pp. 1-6, IEEE, 2016.
- [13] Wu, Bin, Lei Yang, Xiaobin Zhang, Keyue Ma Smedley, and Guann-pyng Li. "Modeling and Analysis of variable frequency one-cycle control on high-power switched-capacitor converters." *IEEE Transactions on Power Electronics* 33, no. 6 (2018): 5465-5475.
- [14] de Moraes, Julio CS, Roger Gules, Juliano LS de Moraes, and Leonardo G. Fernandes. "Transformerless DC-DC converter with high voltage gain based on a switched-inductor structure applied to photovoltaic systems." *Brazilian Power Electronics Conference (COBEP)*, IEEE, 2017
- [15] Gangavarapu, Sivanagaraju, and Akshay Kumar Rathore GAE. "Three Phase Buck-Boost Derived PFC Converter for More Electric Aircraft." *IEEE Transactions on Power Electronics* (2018).
- [16] de Moraes, Julio Cezar dos Santos, Juliano Luiz dos Santos de Moraes, and Roger Gules. "Photovoltaic AC Module Based on a Cuk Converter With a Switched-Inductor Structure." *IEEE Transactions on Industrial Electronics* 66, no. 5 (2019): 3881-3890
- [17] El Khateb, A., Abd Rahim, N., Selvaraj, J., & Uddin, M. N. (2014). Fuzzy-logic-controller-based SEPIC converter for maximum power point tracking. *IEEE Transactions on Industry Applications*, 50(4), 2349-2358.
- [18] Nathan, K., Ghosh, S., Siwakoti, Y. and Long, T., "A new DC-DC converter for photovoltaic systems: coupled-inductors combined Cuk- SEPIC converter," *IEEE Transactions on Energy Conversion*, 34(1), pp.191-201, 2018.

- [19] Ardi, Hossein, and Ali Ajami. "Study on a High Voltage Gain SEPIC-Based DC–DC Converter with Continuous Input Current for Sustainable Energy Applications." *IEEE Transactions on Power Electronics* 33, no. 12 (2018): 10403-10409.
- [20] Nishat, M. M., Faisal, F. and Hoque, M. A., "Modeling and Stability Analysis of a DC-DC SEPIC Converter by Employing Optimized PID Controller Using Genetic Algorithm," *International Journal of Electrical & Computer Sciences IJECS-IJENS*, 19(01), 2019
- [21] Nishat, M. M., Faisal, F., Rahman, M., and Hoque, M. A., "Modeling and Design of a Fuzzy Logic Based PID Controller for DC Motor Speed Control in Different Loading Condition for Enhanced Performance," *2019 1st International Conference on Advances in Science Engineering and Robotics Technology (ICASERT)*, pp. 1-6, 2019
- [22] Malwatkar, G. M., Khandekar, A. A. and Nikam, S. D., "PID controllers for higher order systems based on maximum sensitivity function," In *2011 3rd International Conference on Electronics Computer Technology*, vol. 1, pp. 259-263, IEEE, 2011.
- [23] Haalman, A. "Adjusting controllers for a deadtime process." *Control Engineering* (1965): 71-73.
- [24] Joseph, E. A., and O. O. Olaiya. "Cohen-coon PID Tuning Method; A Better Option to Ziegler Nichols-PID Tuning Method." *Engineering Research* 2.11 (2017): 141-145.
- [25] Rivera, Daniel E., Manfred Morari, and Sigurd Skogestad. "Internal model control: PID controller design." *Industrial & engineering chemistry process design and development* 25.1 (1986): 252-265.
- [26] Eberhart, R. and Kennedy, J., "A new optimizer using particle swarm theory," In *MHS'95. Proceedings of the Sixth International Symposium on Micro Machine and Human Science*, pp. 39-43., IEEE, 1995.
- [27] Nishat, M. M., Shagor, M. R. K., Akter, H., Mi, S. A., and Faisal, F., "An Optimal Design of PID controller for DC-DC Zeta converter using Particle Swarm Optimization," *2020 23rd International Conference on Computer and Information Technology (ICCIT)*, pp. 1-6, 2020
- [28] Holland, J. H., "Genetic algorithms," *Scientific american*, 267(1), pp.66- 73, 1992
- [29] Nishat, M. M., Faisal, F., Evan, A. J., Rahaman, M. M., Sifat, M. S., and Fazle Rabbi, H. M., "Development of genetic algorithm (ga) based optimized PID controller for stability analysis of DC-DC buck converter," *Journal of Power and Energy Engineering*, vol. 8, no. 9, 2020
- [30] Davendra, D. and Zelinka, I., "Self-organizing migrating algorithm," *New optimization techniques in engineering*, 2016
- [31] Geem, Z. W., Kim, J. H. and Loganathan, G. V., "A new heuristic optimization algorithm: harmony search," *simulation*, 76(2), pp.60-68, 2001.
- [32] Colorni, A., Dorigo, M. and Maniezzo, V., "Distributed optimization by ant colonies," In *Proceedings of the first European conference on artificial life*, vol. 142, pp. 134-142, 1991.
- [33] Yang, X. S., *Nature-inspired metaheuristic algorithms*, Luniver press, 2010.
- [34] Eusuff, M., Lansey, K. and Pasha, F., "Shuffled frog-leaping algorithm: a memetic meta-heuristic for discrete optimization," *Engineering optimization*, 38(2), pp.129-154. 2010.
- [35] Klir, George, and Bo Yuan. *Fuzzy sets and fuzzy logic*. Vol. 4. New Jersey: Prentice hall, 1995.
- [36] Nishat, Mirza Muntasir, et al. "Modeling and Design of a Fuzzy Logic Based PID Controller for DC Motor Speed Control in Different Loading Condition for Enhanced Performance." *2019 1st International Conference on Advances in Science, Engineering and Robotics Technology (ICASERT)*. IEEE, 2019.
- [37] Nishat, M. M., Faisal, F., Oninda, M. A. M., and Hoque, M. A., "Modeling Simulation and Performance Analysis of SEPIC Converter Using Hysteresis Current Control and PI Control Method," *2018 International Conference on Innovations in Science Engineering and Technology (ICISSET)*, pp. 7-12, 2018
- [38] Chen, L., Chen, G., Wu, R., Lopes, A. M., Machado, J. A. T. and Niu, H., "Variable coefficient fractional-order PID controller and its application to a SEPIC device," *IET Control Theory & Applications*, 14(6), pp. 900-908, 2020.
- [39] Alqudah, A., Malkawi, A. and Alwadi, A., "Adaptive Control of DC-DC Converter Using Simulated Annealing Optimization Method," *Journal of Signal and Information Processing*, 5(04), p.198, 2014

- [40] Haji, V. H. and Monje, C. A., "Fractional-order PID control of a chopper-fed DC motor drive using a novel firefly algorithm with dynamic control mechanism," *Soft Computing*, 22(18), pp.6135-6146, 2018
- [41] Yaqoob, M., Jianhua, Z., Nawaz, F., Ali, T., Saeed, U. and Qaisrani, R., "Optimization in transient response of DC-DC buck converter using firefly algorithm," In *2014 16th International Conference on Harmonics and Quality of Power (ICHQP)*, pp. 347-351, IEEE, 2014
- [42] M. R. K. Shagor, A. J. Mahmud, M. M. Nishat, F. Faisal, M. H. Mithun and M. A. Khan, "Firefly Algorithm Based Optimized PID Controller for Stability Analysis of DC-DC SEPIC Converter," *2021 IEEE 12th Annual Ubiquitous Computing, Electronics & Mobile Communication Conference (UEMCON)*, 2021, pp. 0957-0963, doi: 10.1109/UEMCON53757.2021.9666555.
- [43] Altinoz, O. T., and H. Erdem. "Evaluation function comparison of particle swarm optimization for buck converter." *SPEEDAM 2010*. IEEE, 2010.
- [44] Sundareswaran, K., et al. "Buck-boost converter feedback controller design via evolutionary search." *International journal of electronics* 97.11 (2010): 1317-1327.
- [45] Sundareswaran, K., et al. "Robust controller identification for a boost type DC-DC converter using genetic algorithm." *2008 IEEE Region 10 and the third international Conference on Industrial and Information Systems*. IEEE, 2008.
- [46] Jaber, Aqeel S. "A novel tuning method of PID controller for a BLDC motor based on segmentation of firefly algorithm." *Indian Journal of Science and Technology* 10.6 (2017): 1-5.
- [47] Meher, Jayadev, and Arnab Gosh. "Comparative Study of DC/DC Bidirectional SEPIC Converter with Different Controllers." *2018 IEEE 8th Power India International Conference (PIICON)*. IEEE, 2018.
- [48] Komathi, C., and M. G. Umamaheswari. "Analysis and design of IMC-PI controller with faster set point tracking and disturbance rejection for interleaved DC-DC SEPIC converter-based power factor correction." *International Journal of Power Electronics* 13.1 (2021): 1-20.
- [49] Leoncini, Mauro, Salvatore Levantino, and Massimo Ghioni. "Design issues and performance analysis of CCM boost converters with RHP zero mitigation via inductor current sensing." *Journal of Power Electronics* 21.2 (2021): 285-295.
- [50] Hung, Ming-Fu, and Kuo-Hsiung Tseng. "Study on the corresponding relationship between dynamics system and system structural configurations—develop a universal analysis method for eliminating the RHP-zeros of system." *IEEE Transactions on Industrial Electronics* 65.7 (2017): 5774-5784.
- [51] Erickson, Robert W. "DC–DC power converters." *Wiley encyclopedia of electrical and electronics engineering* (2001).
- [52] Olalla, Carlos, et al. "Robust gain-scheduled control of switched-mode DC–DC converters." *IEEE Transactions on Power Electronics* 27.6 (2012): 3006-3019.
- [53] Hasaneen, B. M., and Adel A. Elbaset Mohammed. "Design and simulation of DC/DC boost converter." *2008 12th International Middle-East Power System Conference*. IEEE, 2008.
- [54] Mitchell, S. D., et al. "Applications and market analysis of dc-dc converters." *2008 International Conference on Electrical and Computer Engineering*. IEEE, 2008.
- [55] Hossain, M. Z., and N. A. Rahim. "Recent progress and development on power DC-DC converter topology, control, design and applications: A review." *Renewable and Sustainable Energy Reviews* 81 (2018): 205-230.
- [56] Reddy, B. Mallikarjuna, and Paulson Samuel. "A comparative analysis of non-isolated bi-directional dc-dc converters." *2016 IEEE 1st International Conference on Power Electronics, Intelligent Control and Energy Systems (ICPEICES)*. IEEE, 2016
- [57] Ardi, Hossein, Rouzbeh Reza Ahrabi, and Sajad Najafi Ravadanegh. "Non-isolated bidirectional DC–DC converter analysis and implementation." *IET Power Electronics* 7.12 (2014): 3033-3044
- [58] Gaboriault, Mark, and Andrew Notman. "A high efficiency, noninverting, buck-boost DC-DC converter." *Nineteenth Annual IEEE Applied Power Electronics Conference and Exposition, 2004. APEC'04. Vol. 3*. IEEE, 2004.

- [59] Ajami, Ali, Hossein Ardi, and Amir Farakhor. "Design, analysis and implementation of a buck–boost DC/DC converter." *IET Power Electronics* 7.12 (2014): 2902-2913.
- [60] Wang, Lanfei, et al. "Ground robot path planning based on simulated annealing genetic algorithm." *2018 International Conference on Cyber-Enabled Distributed Computing and Knowledge Discovery (CyberC)*. IEEE, 2018.
- [61] Milano, Marianna, et al. "SL-GLAlign: Improving the Local Alignment of Biological Networks through Simulated Annealing." *Proceedings of the 2018 ACM International Conference on Bioinformatics, Computational Biology, and Health Informatics*. 2018.
- [62] Cuk, Slobodan. "A new zero-ripple switching DC-to-DC converter and integrated magnetics." *IEEE Transactions on Magnetics* 19.2 (1983): 57-75.
- [63] Duran, E., et al. "A new application of the buck-boost-derived converters to obtain the IV curve of photovoltaic modules." *2007 IEEE Power Electronics Specialists Conference*. IEEE, 2007.
- [64] Duran, E., et al. "Comparative analysis of buck-boost converters used to obtain I–V characteristic curves of photovoltaic modules." *2008 IEEE Power Electronics Specialists Conference*. IEEE, 2008.
- [65] Azadeh Safari and Saad MEkhilef, "Simulation and Hardware Implementation of Incremental conductance MPPT with Direct control method Using Cuk Converter," *IEEE Transactions*.
- [66] Kavitha, A., G. Indira, and G. Uma. "Analysis and control of chaos in sepic dc-dc converter using sliding mode control." *2008 IEEE Industry Applications Society Annual Meeting*. IEEE, 2008.
- [67] Tian, Gao, et al. "High power factor LED power supply based on SEPIC converter." *Electronics Letters* 50.24 (2014): 1866-1868.
- [68] Kennedy, James, and Russell Eberhart. "Particle swarm optimization." *Proceedings of ICNN'95-international conference on neural networks*. Vol. 4. IEEE, 1995.
- [69] Poli, Riccardo, James Kennedy, and Tim Blackwell. "Particle swarm optimization." *Swarm intelligence* 1.1 (2007): 33-57.
- [70] Shi, Yuhui, and Russell C. Eberhart. "Empirical study of particle swarm optimization." *Proceedings of the 1999 congress on evolutionary computation-CEC99 (Cat. No. 99TH8406)*. Vol. 3. IEEE, 1999.
- [71] Bai, Qinghai. "Analysis of particle swarm optimization algorithm." *Computer and information science* 3.1 (2010): 180.
- [72] Banerjee, Chayan, and Ruchi Sawal. "PSO with dynamic acceleration coefficient based on mutiple constraint satisfaction: Implementing Fuzzy Inference System." *2014 International Conference on Advances in Electronics Computers and Communications*. IEEE, 2014.
- [73] Yang, Xin-She. "Swarm intelligence based algorithms: a critical analysis." *Evolutionary intelligence* 7.1 (2014): 17-28.
- [74] Sundareswaran, K., Kiran Kuruvinashetti, and P. S. Nayak. "Application of Particle Swarm Optimization for output voltage regulation of dual input buck-boost converter." *2014 International Conference on Green Computing Communication and Electrical Engineering (ICGCCEE)*. IEEE, 2014.
- [75] Dorigo, Marco, and Mauro Birattari. "Swarm intelligence." *Scholarpedia* 2.9 (2007): 1462.
- [76] Bonabeau, E.: Swarm Intelligence. In: O'Reilly Emerging Technology Conference (2003)
- [77] Osman, Ibrahim H., and Gilbert Laporte. "Metaheuristics: A bibliography." (1996): 511-623.
- [78] Blum, Christian, and Andrea Roli. "Metaheuristics in combinatorial optimization: Overview and conceptual comparison." *ACM computing surveys (CSUR)* 35.3 (2003): 268-308.
- [79] Yang, Xin-She, and Kingshi He. "Firefly algorithm: recent advances and applications." *International journal of swarm intelligence* 1.1 (2013): 36-50.
- [80] Johari, Nur Farahlina, et al. "Firefly algorithm for optimization problem." *Applied Mechanics and Materials*. Vol. 421. Trans Tech Publications Ltd, 2013.
- [81] Socha, Krzysztof, and Marco Dorigo. "Ant colony optimization for continuous domains." *European journal of operational research* 185.3 (2008): 1155-1173.
- [82] Dorigo, Marco, Mauro Birattari, and Thomas Stutzle. "Ant colony optimization." *IEEE computational intelligence magazine* 1.4 (2006): 28-39.

- [83] Chen, Zhiqiang, and Ronglong Wang. "GA and ACO-based hybrid approach for continuous optimization." *2015 International Conference on Modeling, Simulation and Applied Mathematics*. Atlantis Press. 2015.
- [84] Dorigo, Marco, Vittorio Maniezzo, and Alberto Coloni. "Ant system: optimization by a colony of cooperating agents." *IEEE Transactions on Systems, Man, and Cybernetics, Part B (Cybernetics)* 26.1 (1996): 29-41.
- [85] Roberts, Steve. "DC/DC book of knowledge." *Austria: RECOM Engineering GmbH & Co KG* (2015).
- [86] Miaja, Pablo F., Miguel Rodriguez, Alberto Rodriguez, and Javier Sebastian. "A linear assisted DC/DC converter for envelope tracking and envelope elimination and restoration applications." In *2010 IEEE Energy Conversion Congress and Exposition*, pp. 3825-3832. IEEE, 2010.
- [87] Chetty, P. R. K. "Current injected equivalent circuit approach to modeling switching dc-dc converters." *IEEE Transactions on Aerospace and Electronic Systems* 6 (1981): 802-808.
- [88] Liu, Kwang-Hwa, and Fred C. Lee. "Zero-voltage switching technique in DC/DC converters." In *1986 17th Annual IEEE Power Electronics Specialists Conference*, pp. 58-70. IEEE, 1986.
- [89] Kumar, J. Sai, and Tikeshwar Gajpal. "A Multi Input DC-DC Converter for Renewable Energy Applications." (2016).
- [90] Ortiz, G., J. Biela, D. Bortis, and J. W. Kolar. "1 Megawatt, 20 kHz, isolated, bidirectional 12kV to 1.2 kV DC-DC converter for renewable energy applications." In *Power Electronics Conference (IPEC), 2010 International*, pp. 3212-3219. IEEE, 2010.
- [91] Li, Wuhua, Xiaodong Lv, Yan Deng, Jun Liu, and Xiangning He. "A review of non-isolated high step-up DC/DC converters in renewable energy applications." In *Applied Power Electronics Conference and Exposition, 2009. APEC 2009. Twenty-Fourth Annual IEEE*, pp. 364-369. IEEE, 2009.
- [92] Koutroulis, Eftichios, and Kostas Kalaitzakis. "Design of a maximum power tracking system for wind-energy-conversion applications." *IEEE transactions on industrial electronics* 53, no. 2 (2006): 486-494.
- [93] Banerjee, Soumitro, and George C. Verghese. *Nonlinear phenomena in power electronics*. IEEE, 1999.
- [94] Tse, Chi Kong, and Mario Di Bernardo. "Complex behavior in switching power converters." *Proceedings of the IEEE* 90, no. 5 (2002): 768-781.
- [95] Hamill, David C., Jonathan HB Deane, and David J. Jefferies. "Modeling of chaotic DC-DC converters by iterated nonlinear mappings." *IEEE transactions on Power Electronics* 7, no. 1 (1992): 25-36.
- [96] A. H. R. Rosa, T. M. de Souza, L. M. F. Morais, and S. I. Seleme. "Adaptive and nonlinear control techniques applied to sepic converter in dc-dc, pfc, ccm and dcm modes using hil simulation." *Energies* 11, no. 3 (2018): 602.
- [97] Black, Harold S. "Stabilized feed-back amplifiers." *Proceedings of the IEEE* 87.2 (1999): 379-385.
- [98] Bennett, Stuart. "Development of the PID controller." *IEEE Control Systems Magazine* 13.6 (1993): 58-62.
- [99] Bennett, Stuart. "A brief history of automatic control." *IEEE Control Systems Magazine* 16.3 (1996): 17-25.
- [100] Kaliannan, Jagatheesan, Anand Baskaran, and Nilanjan Dey. "Automatic generation control of Thermal-Thermal-Hydro power systems with PID controller using ant colony optimization." *International Journal of Service Science, Management, Engineering, and Technology (IJSSMET)* 6.2 (2015): 18-34.
- [101] Rajesh, K. S., S. S. Dash, and Ragam Rajagopal. "Hybrid improved firefly-pattern search optimized fuzzy aided PID controller for automatic generation control of power systems with multi-type generations." *Swarm and evolutionary computation* 44 (2019): 200-211.
- [102] Hasanien, Hany M. "Whale optimisation algorithm for automatic generation control of interconnected modern power systems including renewable energy sources." *IET Generation, Transmission & Distribution* 12.3 (2017): 607-614.
- [103] Zhong, Jinghua. "PID controller tuning: A short tutorial." *Mechanical Engineering, Purdue University* (2006): 1-10.
- [104] Maroti, Pandav Kiran, et al. "Modified high voltage conversion inverting cuk DC-DC converter for renewable energy application." *2017 IEEE Southern Power Electronics Conference (SPEC)*. IEEE, 2017.

- [105] Emami, S. A., M. Bayati Poudeh, and S. Eshtehardiha. "Particle Swarm Optimization for improved performance of PID controller on Buck converter." *2008 IEEE International Conference on Mechatronics and Automation*. IEEE, 2008.
- [106] Sonmez, Yusuf, et al. "Improvement of buck converter performance using artificial bee colony optimized-pid controller." *Journal of Automation and Control Engineering* 3.4 (2015).